Review Article

A Review on the Toxicity and Properties of Organochlorine Pesticides, and Their Adsorption/Removal Studies from Aqueous Media Using Graphene-Based Sorbents

Aduloju Emmanuel Ibukun[1],* , **Muhammad Ariffuddin Bin Abd Hamid[2]**, **Ahmad Husaini Mohamed[2,3]**, **Nur Nadhirah Mohamad Zain[2]**, **Mohammad Anuar Kamaruddin[4]**, **Saw Hong Loh[5]**, **Sazlinda Kamaruzaman[6]**, **Noorfatimah Yahaya[2]**

[1]Department of Chemical and Biochemical sciences, School of Applied Science and Technology, The Federal Polytechnic Offa, P.M.B. 420, Kwara State, Nigeria
[2]Department of Toxicology, Advanced Medical and Dental Institute (AMDI), Universiti Sains Malaysia, 13200 Bertam Kepala Batas, Penang, Malaysia
[3]School of Chemistry and Environment, Faculty of Applied Sciences, Universiti Teknologi MARA, Cawangan Negeri Sembilan, Kampus Kuala Pilah, 72000 Kuala Pilah, Negeri Sembilan, Malaysia
[4]School of Industrial Technology, Universiti Sains Malaysia, Minden, Pulau Pinang, Malaysia
[5]Faculty of Science and Marine Environment, University Malaysia Terengganu, 21030, Kuala Terengganu, Terengganu, Malaysia
[6]Department of Chemistry, Faculty of Science, Universiti Putra Malaysia, 43400 UPM Serdang, Selangor Darul Ehsan, Malaysia

A B S T R A C T

Organochlorine pesticides (OCPs) have been extensively used in agriculture to boost crop yields, creating a significant and enduring global contaminant with adverse effects on the environment and human well-being. These pesticides are characterized by their bioaccumulative and persistent nature, capable of long-distance dispersion. To address this challenge, efforts are ongoing to develop advanced technologies for effectively removing OCPs from the environment, thereby mitigating their impact through appropriate treatment methods in soil and other environmental matrices. Specifically, extensive research has been conducted on the utilization of nanomaterials, including TiO_2, Fe_2O_3, graphene, and graphene oxide, as sorbents in sample preparation and degradation techniques. Graphene (G) and graphene oxide (GO) exhibit unique combination of outstanding characteristics derived from carbon materials (such as exceptional physical, chemical properties, mechanical, and electronic features), deep eutectic solvents (DES) (acting as a functionalization agent), and nanomaterials (including an ultrahigh surface area, abundant functional groups, and a nanometer-scale structure). This review focuses on the adsorption and degradation of OCPS and their metabolites using the remarkable attributes of a mixed graphene-based sorbent, deep eutectic solvents (DES) and MNPs. The combination of these materials, with features such as an expansive surface area (2630 m^2 g^{-1}), hydrophilicity, inherent adsorption sites on both sides for molecules, hydrophobicity, double-sided polyaromatic scaffold, adaptable surface modification, hydrogen-bonding, and extensive π-electron structure, positions them as excellent advanced adsorbents and efficient photocatalysts for Magnetic Solid Phase Extraction (MSPE) and Solid Phase Extraction (SPE). These characteristics make them suitable for extracting OCPs from different environmental matrices such as food, environment water, medicine, and biological samples.

*Corresponding Author: Aduloju Emmanuel Ibukun (dr.emmyjay@gmail.com)

Aduloju Emmanuel Ibukun: He obtained his B.Sc. in Industrial Chemistry (with Honors) from the University of Ado Ekiti in 2009. He pursued further studies and earned a Master of Technology in Chemistry from the Federal University of Technology Akure, Ondo State, Nigeria, in 2015. Subsequently, he achieved his Doctor of Philosophy (Ph.D.) in Environmental Chemistry from Universiti Sains Malaysia. Recently, Emmanuel serves as a Lecturer I at the Department of Biochemical and Chemical Sciences in The Federal Polytechnic Offa, Kwara State, Nigeria. His research interests span across various areas including ionic liquids, Deep Eutectic Solvents (DES), sample preparation, toxicology, wastewater treatment, extraction, and analytical separation studies. He has made substantial contributions to academia, boasting thirty research articles published in reputable international journals.

Muhammad Ariffuddin Abd Hamid: He obtained his B.Sc. in Chemistry from the University Malaysia Sarawak in 2021, followed by postgraduate studies culminating in a Master of Science in Analytical Chemistry. Presently, he serves as a Graduate Research Assistant at the Advanced Medical and Dental Institute, Universiti Sains Malaysia (USM). With a keen interest in developing sample preparation methods for identifying emerging pollutants in food and environmental matrices using analytical instruments, he brings valuable expertise to his role. Proficient in operating LCMS, GCMS, and qTOF systems, he has a proven track record of contributing to research initiatives. Notably, he held the position of President of the AMDI Student Association (ASA) for the 2022/2023 semester.

Ahmad Husaini Mohamed: He earned his B.Sc. in Chemistry (with Honors) from Universiti Malaysia Terengganu, followed by postgraduate studies leading to a Master of Science in Chemistry from Universiti Kebangsaan Malaysia, Bangi. He later attained his Doctor of Philosophy (Ph.D.) in Separation Chemistry from Universiti Sains Malaysia. Currently, he holds the position of Lecturer of Chemistry at the School of Chemistry and Environment, UiTM Negeri Sembilan, Kuala Pilah Campus. His research interests lie in Polysaccharides-based materials, ionic liquids, Deep Eutectic Solvents (DES), sample preparation, and analytical separation studies.

Nur Nadhirah Mohamad Zain: She has been a senior lecturer at the Department of Toxicology, USM since 2015. She obtained her Doctor of Philosophy (Ph.D.) in Analytical Chemistry with a specialization in separation science from the University of Malaya in 2015. Currently, her research is focused on the development of green materials based on deep eutectic solvents and supramolecular solvents which are trends in the field of the 12 Principles of Green Chemistry. She is particularly interested in their potential as alternative solvents/functional group materials, in extraction techniques for monitoring carcinogenic pollutants, pesticides, and pharmaceutical compounds in food and environmental matrices.

Mohammad Anuar Kamaruddin: He holds degrees in Environmental Engineering, including a BSc., MSc., and Ph.D., all from Universiti Sains Malaysia. His research interests encompass waste management, waste diversion, landfill technology, landfill leachate treatment, Environmental Impact Assessment (EIA), Environmental Management Plan (EMP), Environmental Monitoring Report (EMR), Environmental Audit, and Environmental Protection Works. He has actively participated in several international conferences organized by reputable bodies worldwide. Furthermore, Dr. Anuar is deeply committed to community empowerment through translational research, enabling effective communication with marginalized populations.

Saw Hong Loh: She is currently engaged at the Centre for Marine and Environmental Sciences (PPSMS), Universiti Malaysia Terengganu, situated in Kuala Terengganu, Terengganu, Malaysia. Her research focuses primarily on Analytical Chemistry, Chromatography, Applied Chemistry, and Physical Chemistry. With a concentration on Biochemistry and Analytical Chemistry, Dr. Loh Saw Hong has authored over seventy publications, which have collectively amassed over 1000 citations.

Sazlinda Kamaruzaman: She holds the position of Senior Lecturer in the Department of Chemistry, Faculty of Science, at UPM Universiti Teknologi Malaysia. She obtained her Doctor of Philosophy (Ph.D.) in Chemistry from Universiti Teknologi Malaysia in 2014, following her Bachelor of Science (Hons) in Pure Chemistry in 2010. Her research interests include Chromatography, Microextraction, Sample Preparation, and Environmental Chemistry. With over 70 publications to her credit, her work has garnered more than 1200 citations.

Noorfatimah Yahaya: She is an Associate Professor in the Department of Toxicology at the Advanced Medical and Dental Institute (AMDI) of Universiti Sains Malaysia. She earned her Ph.D. in Analytical Chemistry from Universiti Teknologi Malaysia in 2014, followed by M.Sc. in Chemical Instrumentation from Universiti Sains Malaysia in 2010 and a B.Sc. in Analytical and Environmental Chemistry from Universiti Malaysia Terengganu in 2009. She specializes in analytical chemistry, particularly in the field of separation science. Her research focuses on the development of green sample preparation and extraction techniques combined with chromatography/electrophoresis for analyzing emerging pollutants and important pharmaceutical compounds. With expertise in Liquid Chromatography, High-Performance Liquid Chromatography, Analytical Method Development, Sample Preparation, Chromatography, Mass Spectrometry, Chemical Analysis, and Food Chemistry.

Content

1. Introduction

The environment is frequently tainted by a variety of hazardous organic and inorganic pollutants that find their way into it. The toxicological concern arises from the bioavailability and non-biodegradability of these contaminants. A primary source of introducing these pollutants into the water system is the diverse set of industrial activities. Water, being a vital resource and an integral element in numerous human endeavors including food and beverage production, agrochemicals, pharmaceuticals, electronics, and household consumption, plays a pivotal role in sustaining life. Regrettably, the main contributors to water contamination are the discharges of contaminated water from these industries. Notably, the pollution of water resources with pesticide residues is a significant environmental apprehension, given that these toxic substances exhibit carcinogenic activity, posing risks to both the environment and human health even at very low concentrations. Agricultural waste, wastewater atmospheric deposition [1-3], industrial emission and waste, such as heavy metals, volatile organic chemicals, and toxic substances, is a major contributor to water contamination, with improper disposal and waste discharge being common causes. Pesticides, A pesticide is described as any product or combination of substances designed to prevent, eliminate, repel, or reduce any pest, such as mosquitoes, parasites, worms, herbicides, mice, and more [1,2].

The presence of inorganic pollutants, such as heavy metals, salts, and radioactive isotopes, further exacerbates water contamination, posing additional risks to water quality and aquatic ecosystems [3]. Therefore, the impact of industrial and agricultural activities on water contamination underscores the importance of effective waste management and pollution control measures to safeguard water resources and human well-being.

The World Health Organization (WHO) has reported that approximately a million people are affected by acute poisoning caused by pesticide exposure, with an annual death rate ranging from 0.4% to 1.9% [4,5]. In an effort to safeguard human well-being and preserve the environment from the adverse effects of these harmful chemicals, the European Union (EU) and the World Health Organization (WHO) have established Maximum Residual Limits (MRL) for pesticides in water, set at 0.1-0.5 µg/L.

These toxins cross boundaries and are transported from one location to another, accumulating in food and causing numerous significant health hazards and environmental impacts. Organochlorine pesticides are also classified in various countries worldwide by researchers with groups of harmful substances like short-chain chlorinated paraffins, persistent organic pollutants (POPs), and polybrominated diphenyl ethers (PBDEs) documented in human breast milk. These chemicals, known for their semi-volatile, toxic, and hydrophobic properties, exhibit resistance to environmental degradation. They can be transported by water and wind, among other media, to uncontaminated areas before settling. The group of POPs encompasses organochlorine pesticides (OCPs) such as aldrin, diphenyl trichloroethanes (DDTs), Dichlorodiphenyldichloroethylene (DDE), Dichlorodiphenyldichloroethane (DDD), Methoxychlor, heptachlor, endrin, and dieldrin, along with industrial chemicals, aromatic hydrocarbons, dibenzodioxins, and

dibenzofurans. Cyclodienes, such as endosulfan, endrin, dieldrin, and heptachlor, are commonly utilized as insecticides among organic pollutants. These substances have been identified for their high toxicity to aquatic life, demonstrating carcinogenic activity, low biodegradability, and significant bio-concentration in organisms across various trophic levels. The release of organic pollutants into wastewater has led to serious environmental issues [6]. Consequently, there is considerable interest in the removal of these synthetic organochlorine pollutants from the aqueous phase. Among various chemical and physical methods such as electrochemical oxidation, ion exchange supercritical oxidation, advanced oxidation processes [7], adsorption, and chemical precipitation, incineration, photochemical degradation [6], filtration chemical reduction [8,9], phytoremediation, bioremediation, biological processing [10] molten salt oxidation, and membrane nano-filtration, adsorption stands out as one of the most effective techniques employed for the eliminate or stabilize the concentration of pesticides and organic pollutants from wastewater and environmental media due to its simplicity in design, ease of operation, and convenience. This will also reduce on their extended persistence at application sites and their adverse impacts on non-target groups across the environment [11,12].

Engineered nanomaterials play a crucial role in tackling diverse environmental challenges, leveraging their exceptional physical and chemical properties that outshine those of other functional materials. Various methods such as thermal decomposition, solvothermal processes, microwave synthesis, sonochemistry, and biosynthesis techniques [13,14]. Magnetic Nanomaterials (MNMs) consist of nanometer-sized magnetic nanoparticles (MNPs) integrated into the magnetic fucntional sorbents. These include metal oxides such as Fe_3O_4 (NMPs), maghemite (γ-Fe_2O_3), nickel (Ni) [15], Au, CuO, $CoFe_2O_4$, iron (Fe), Ag, ZnO, MgO, $MnFe_2O_4$, ZrO_2, MnO_2, cobalt (Co), Al_2O_3, $MgFe_2O_4$, iron oxides (Fe_3O_4 and γ-Fe_2O_3), TiO_2, etc. They possess outstanding characteristics, including a high surface area, elevated magnetic moment, small particle size, straightforward synthesis methods, and cost-effective production processes [16].

However, these pristine MNPs, particularly those derived from Fe_3O_4, exhibit drawbacks such as the formation of assemblies through either aggregation or agglomeration. This phenomenon leads to reduced sensitivity and selectivity when targeting analytes in sample matrices [17,18]. To address these limitations, magnetic nanomaterial cores are subjected to functionalization or modification with a variety of substances, including deep eutectic solvents (DESs), polymers, metal oxides or sulfides, small organic compounds, proteins, carbon, and metals. Functionalized materials derived from graphene, benzenoid polymers, carbon nanotubes, metal-organic frameworks (MOFs), and calixarenes are characterized by a plethora of delocalized π-electron systems. These systems inherently enhance both π–π interactions and hydrophobic interactions with target analytes possessing benzene rings, such as pesticides. Among the myriad of nanostructures, graphene-based materials are particularly favored for their superior adsorption characteristics.

Graphene oxide nanoplates, composed of sp^2 carbon atoms arranged in a honeycomb plane structure, exhibit remarkable rigidity, high conductivity, and a giant specific surface area. These properties contribute to an outstanding adsorption capacity for organic pollutants from wastewater. However, a common issue faced by many nanomaterials is aggregation when used in a singular form, leading to a loss of their advantages. This limitation can be overcome by coating and/or doping these nanostructures into host materials, ionic liquids, and deep eutectic solvents (DES), preventing their dispersion or diffusion and preserving their functionality [14]. The Deep eutectic solvents (DES) are increasingly used to modify graphene oxide (GO) due to several advantageous properties such as ionicity, high tunability, low flammability, stability in air, and a broad liquid range [19-21]. They offer, making them a versatile and effective medium for graphene

modification. When compared to both organic solvents and ILs, DESs offer several green alternative advantages, such as straightforward production, cost-effectiveness, potential for industrialization, non-toxicity, biocompatibility, biodegradability, and sustainability [22]. DES has the ability to interact favorably with graphene oxide due to its functional groups. The hydrogen bond-forming capability of DES can facilitate effective interactions with the oxygen-containing functional groups on the graphene oxide surface.

While deep eutectic solvents (DES) have become a crucial tool in functionalizing composites and generating functional materials, their application in the synthesis of advanced materials for detecting pollutants and pesticides is still relatively new. DES gained prominence as a viable substitute for expensive organic solvents and ionic liquids (ILs), owing to its eco-friendly properties and cost-effective, sustainable analytical methods. Until January

12, 2023, a search on ScienceDirect using the terms "deep eutectic solvent functionalized magnetic oxide for extraction of organochlorine" yielded 88 publications from 2017 to 2023 (**Figure 1a**). While interest has surged over the years, particularly among researchers in Asia, Europe, North and South America, focusing on diverse fields (**Figure. 1b**), only around 3% of the publications pertain to material science, with a specific emphasis on pollutants (90 articles) (**Figure. 1c**).

DESs (Deep Eutectic Solvents) can be prepared using various methods such as heating-stirring, evaporating, freeze-drying, and grinding processes. Among these, heating-stirring is a commonly used approach, involving the mixing and stirring of hydrogen bond acceptors (HBAs) and hydrogen bond donors (HBDs) at a specific temperature (50-100 °C) until a homogeneous liquid is formed [23]. DES can be easily tailored by choosing different combinations of hydrogen bond donors and acceptors, allowing for the
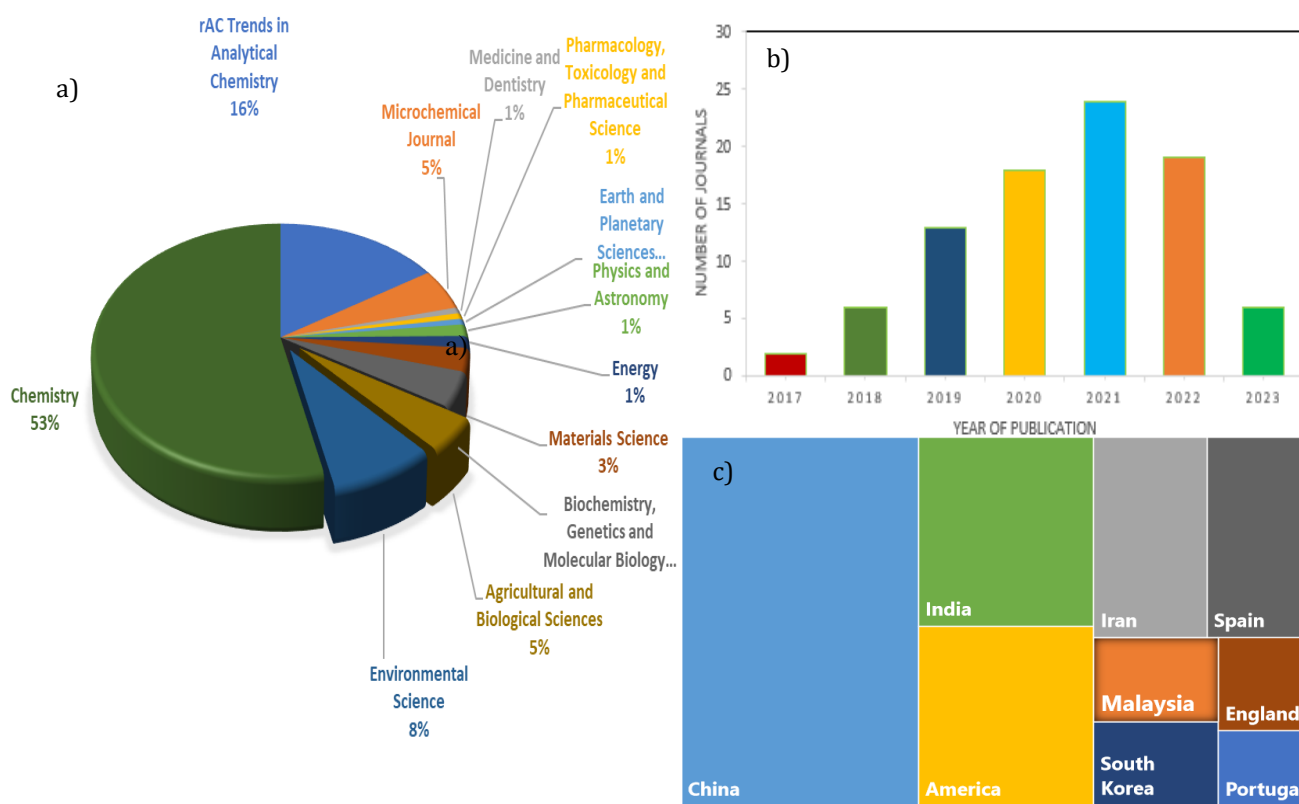
Figure 1. Analysis of publications with research topic related to DESs functionalized magnetic materials

tuning of their properties to suit specific applications. This versatility makes them adaptable to various chemical processes, including the modification of graphene oxide. In general, the use of deep eutectic solvents in modifying graphene oxide provides a combination of environmental sustainability, versatility, compatibility, and tunability, making them valuable in various applications involving graphene-based materials. These solvents can be categorized into five types based on the general formula Cat+X–ZY, where Cat+ represents a cation (e.g., ammonium, phosphonium, or sulfonium cation), X– is a Lewis base (typically a halide anion), Y is a Lewis or Brønsted acid, and Z indicates the number of Y molecules [24]. Type III DESs, which use Choline Chloride (ChCl) as an HBA, are particularly noteworthy due to their environmentally friendly nature, as they do not involve metal ions. ChCl is a cost-effective option for large-scale production, making ChCl-based DESs widely studied and utilized [25]. Additionally, non-ionic compounds like menthol and thymol have led to the development of Type V DESs, expanding the range of DES compositions [24]. The inclusion of graphene oxide in the ternary composite will further improve selectivity towards organic compounds. This enhancement is attributed to the presence of active sites and functional groups (such as OH, COOH, O–C double bond O), which significantly promote interactions with organic and aromatic molecules of pesticides [26]. Incorporating NMPs into the composite will enhance both selectivity and stability. Additionally, the pronounced magnetic properties of NMPs will simplify the collection and separation of adsorbent particles from purified wastewater, eliminating the necessity for a filtration process [27]. Thus, they serve as potential carriers of contaminants and facilitate their uptake by biota. This capability, commonly known as the Trojan horse effect, is linked to sorption events, particularly adsorption, wherein molecules adhere to the interface between fluid and solid phases [28].

DESs have also emerged as cutting-edge solvents for the functionalization of magnetic nanoparticles (MNPs) due to their exceptional physicochemical properties, thus their applications as adsorbents for both elemental analysis and organic compounds have expanded. The extraction efficiencies of magnetic graphene oxide (MGO), whether functionalized with or without DES, are influenced by various interactions, including electrostatic interaction, van der Waals forces, π–π donor/acceptor interactions, hydrophilic interactions, dipole–dipole electrostatic interactions, ion exchange, size exclusion, hydrogen bonding, and hydrophobic interactions. The extent of these interactions varies for both magnetic nanomaterials (MNMs) and magnetic graphene oxide (MGO), impacting their extraction performance, as observed, and reported by researchers.

In environmental samples, the analyte is often present at only trace concentrations, and the matrix is complicated. Sample preparation and pretreatment methods are, therefore, the most time-consuming and challenging steps in environmental analysis. The most common extraction techniques used in environmental analysis are classical solvent extraction or liquid–liquid extraction (LLE) [29-37], and solid-phase extraction (SPE). Both methods are time-consuming, labor-intensive, and tedious; however, they follow standard procedures and yield predictably accurate and precise results. Moreover, LLE requires a large amount of toxic and environmentally unfriendly organic solvent. Interestingly, due to the direct contact of the sample with the solid or liquid extraction phase, a separate cleanup step is often required to minimize sample matrix interferences.

In the past decades, miniaturization and the development of environmentally sound methods have become trends in analytical chemistry. Many microextraction techniques have been developed. Miniaturized variations of solvent extraction, such as liquid–liquid–liquid microextraction (LLLME), liquid-phase microextraction (LPME) [37], pressurized liquid extraction (PLE) [30], single drop microextraction (SDME)[31], fabric phase sorptive extraction (FPSE) [32], hollow-fiber LPME (HF-LPME), stir bar sorptive extraction (SBSE) [33], solvent bar microextraction

(SBME) [34] matrix solid-phase dispersion (MSPD) [35], dispersive liquid–liquid microextraction (DLLME) [36], QuEChERS method (acronymic name from quick, easy, cheap, effective, rugged and safe)[37], Magnetic solid-phase extraction (MSPE), thin film microextraction (TFME), microextraction in packed syringe (MEPS), solid phase microextraction (SPME) [37-40]) single-drop microextraction (SDME) [41], dispersive solid-phase extraction (DSPE) [42], solid-phase extraction (SPE) [43], and micro-solid phase extraction (μ-SPE) have also been employed for OCPs extraction.

Solid-phase extraction (SPE) stands out as a potent method for sample clean-up and pre-concentration, for the efficient extraction of target compounds from intricate matrices. However, the magnetic solid-phase extraction (MSPE), an innovative form of solid-phase extraction (SPE), has gained widespread acclaim since its exploration in 1999 by Šafaříková and Šafařík [44]. The magnetic solid-phase extraction (MSPE) method relies on magnetic or magnetized sorbents along with an external magnet for separation, requiring only a small quantity of eluent. The effectiveness and selectivity of the MSPE procedure are contingent upon the characteristics of the magnetic sorbents. In this methodology, magnetic adsorbents are directly dispersed into sample solutions, utilizing a dispersive extraction mode that significantly amplifies the contact area between adsorbents and analytes [45]. Consequently, the extraction efficiency of MSPE surpasses that of conventional SPE. Simultaneously, common SPE challenges associated with adsorbent packing, such as high pressure and packed bed clogging, can be circumvented [46]. A noteworthy feature of MSPE is its capacity to facilitate the separation of magnetic adsorbents from sample solutions using an external magnetic field, eliminating the need for traditional centrifugation or filtration and thereby simplifying the extraction process. In addition, magnetic adsorbents can be easily recycled and reused, contributing to both cost-effectiveness and environmental friendliness.

Graphene/graphene oxide (G/GO)-based magnetic nanocomposites have been extensively utilized in MSPE, thus they are recognized for their simplicity, and environmental friendliness, and adequate to mitigate the matrix effect and enhance the concentration of analytes before instrumental analysis. Given these findings, Graphene/graphene oxide (G/GO)-based magnetic nanocomposites have been extensively utilized in MSPE, thus the MSPE have demonstrated comprehensive advantages, including simplicity, accuracy, time and labor savings, environmental friendliness, and excellent extraction efficiency adequate to mitigate the matrix effect and enhance the concentration of analytes before instrumental analysis.

In the MSPE technique, magnetic adsorbents, typically comprising magnetic carriers and functionalities, play a crucial role as they directly impact extraction efficiency while simultaneously influencing the sensitivity and selectivity of the method [46]. To date, numerous magnetic adsorbents for MSPE have been documented in the literature, encompassing the direct utilization of magnetic nanoparticles (MNPs) following surface functionalization are most commonly employed in MSPE. This preference is attributed to their ease of synthesis, controllable magnetization, capacity to enhance adsorption selectivity, improve extraction efficiency, prevent self-aggregation, avoid core oxidation, exhibit superparamagnetism, and possess low toxicity. Among the various materials employed as adsorbents in magnetic solid-phase extraction (MSPE), graphene (G) stands out as a rapidly rising star. Graphene is a two-dimensional material consisting of single-/few-layer sheets composed of sp^2-hybridized carbon atoms arranged in a honeycomb lattice. It has gained prominence due to its exceptional mechanical strength, thermal, and electronic properties, along with an ultrahigh specific surface area (theoretical value 2630 m^2 g^{-1}) derived from both carbon materials and nanomaterials (including abundant functional groups, nanometer-scale structure, and ultrahigh surface area).

Generally, Graphene serves as a non-polar and hydrophobic adsorbent with a large delocalized π-electron system that facilitates a robust π–π stacking interaction with carbon-based ring structures. As a fundamental structural component of other carbon allotropes [47], Graphene (G) and graphene oxide (GO) are exceptional materials with numerous intrinsic unique structural and chemical properties that make them highly valuable in various scientific and engineering applications. These properties include good electrical conductivity, high Young's modulus, thermal conductivity, high intrinsic mobility, and ultrahigh theoretical specific surface area. Graphene, in particular, is considered an advanced sorbent for solid-phase extraction (SPE) and solid-phase microextraction (SPME) [48], especially for hydrophobic or aromatic compounds. On the contrary, GO, consisting of oxygenated G and layered sheets, has -OH, –CH(O)CH-, –C=O, –COOH groups on its surface and edge, making it highly polar and good at dispersing in water. Its stability as a colloidal suspension augments the sorption affinity for polar, hydrophobic [49], non-polar and low polar compounds (organochlorine pesticides), whereas the negatively charged surface under a pH higher than 3.9 enables the adsorption of positive ions or compounds [50] from environmental matrices.

However, both G and GO may suffer from irreversible aggregation, which can reduce the efficiency of analyte extraction and desorption. To address this, various functionalized G and GO materials have been developed for SPE, offering improved selectivity, high surface area, elasticity, chemical stability, flexibility, tensile strength, π-electron rich structure, and π-π interactions of graphene-based materials contribute to their excellent sorption performance in SPE applications and performance. GO sheets is chemically bonded to surfactants, silica [51] and chemically reduced to Graphene, providing sorbents for SPE. This innovative approach leverages G and GO in SPE applications. Subsequently, a variety of functionalized Graphene (G) and GO materials, incorporating functional polymers [52], nanomaterials [50], monomers [53], magnetic

nanoparticles (MNPs), Molecularly Imprinted Polymers (MIPs) [54], Covalent Organic Frameworks (COFs) [55,56], magnetic materials [56], ionic liquids (ILs) [57], aerogels [58], metal-organic frameworks (MOFs) [59], and Deep Eutectic solvent (DES) have been developed for enhanced SPE performance. In the solid-phase extraction (SPE), these substances act as highly efficient sorbents for selectively capturing and concentrating organochlorine pesticides from liquid samples.

Accurate quantification of these contaminants is essential for monitoring their residual levels in the environment. The majority of pesticides exhibit volatility and thermal stability. Particularly in the case of OCPs, these compounds are predominantly non-polar and readily undergo vaporization. As a result, a variety of methods, including enzyme-linked immunosorbent assay (ELISA) [4], biosensors [5], and chromatographic techniques such as liquid chromatography [6] or gas chromatography [60-64] coupled to different detectors such as electron-capture detection (ECD), nitrogen-phosphorus detection (NPD) and mass spectrometry (MS), are widely employed for the quantification of organochlorine pesticides (OCPs) across diverse matrices, as seen in **Table 4**. Gas chromatography–mass spectrometry (GC–MS) is particularly recommended due to its high selectivity and low detection limit [58]. The selected ion monitoring (SIM) mode of the MS detector further diminishes background noise [10]. To further increase confidence in confirmative analysis, a GC coupled with tandem MS is one of the suitable techniques [64].

This review evaluates the environmental remediation applications and sorption performance of graphene/graphene oxide (G/GO)-based materials in solid-phase extraction (SPE) and solid-phase microextraction (SPME), dispersive solid-phase extraction (DSPE), and magnetic solid-phase extraction (MSPE) in recent years. A comprehensive analysis is provided on the adsorption capacity, the influence of experimental conditions, potential adsorption

mechanisms, and structures of organochlorine pesticides (OCPs). Furthremore, the review incorporates a statistical analysis of the adsorption models concerning their fitting to experimental adsorption data and the adsorption process.

2. The Occurrence and Types of Organochlorine Pesticides

According to statistics on various pesticide usage data, approximately 40% of routinely employed pesticides fall under the category of organochlorine chemicals, underscoring their widespread utilization and indispensable role in environmental management [65]. Asia contributes to more than half of the global insecticide usage, with India ranking third after China and Turkey, holding the 12th position globally in pesticide usage. In 2018, India utilized over 58,160 tonnes of pesticides, while China, Japan, and the United States had consumption rates of about 13.07, 11.76, and 3.57 kg ha^{-1}, respectively [66].

Organochlorine pesticides (OCPs) find extensive application in developing countries due to their cost-effectiveness and essential role in insects and pest vectors control across various settings, including homes, fields, and the healthcare industry [67]. Notably posing as substantial environmental threat because of their heightened hazard levels, increased solubility, and stability within habitats. Organochlorine pesticides (OCPs) can infiltrate the aquatic system through various pathways, including spray drift, surface runoff, erosion, volatilization [68] from non-point sources, the discharge of industrial and sewage wastewater, wet/dry deposition, direct application, aerial spraying, careless disposal of empty containers and other mechanisms. Their persistence, toxicity, and bioaccumulation traits have raised concerns regarding their impact on the marine environment. Due to their relatively high octanol-water partition coefficient, most organochlorine pesticides (OCPs) exhibit low water solubility but have a propensity to accumulate in organisms, posing potential risks of bioaccumulation in the food chain (through both fatty and non-fatty products), accumulate

in aquatic organisms such as plankton and subsequently entering the food web and posing threats to ecosystems and public health [69, 70]. The transportation, dispersion, and ultimate effects of pesticides in marine systems are influenced by the chemicals' persistence under tropical conditions, as well as their bioaccumulation and biodegradation. The majority of OCPs have been listed in the Stockholm Convention since 2001. Despite efforts to control their use, the ubiquity, stability, volatility, resistance to degradation, and lipophilicity of OCPs have led to their accumulation in both natural environments and human tissues [71,72].

Given their persistent nature and potential health risks, reliable and accurate analytical procedures are essential to monitor OCP levels in environmental and clinical samples.

Various organochlorine pesticides have been employed, exhibiting differences in their chemical structures, toxicity mechanisms toward both intended and unintended species, and various other characteristics. Among the types of organochlorine pesticides are Dichlorodiphenyltrichloroethane (DDT), hexachlorobenzene, polychlorinated biphenyls, lindane, endosulfan, dieldrin, methoxychlor, chlordane, taxophene, and dicofol [73-76]. These substances vary widely in their chemical characteristics and impacts on the environment and living organisms. Researchers have also reported the degradation of reported levels of OCPs follows this pattern ∑HCHs > ∑endrins > ∑endosulfans > dieldrin > ∑heptachlors > ∑DDTs > ∑chlordanes > methoxychlor [77]. This can be attributed to the predominance of cement producing plant in the study areas, unlike agricultural farmstead, where DDTs have been continuously used.

2.1. Dichlorodiphenyltrichloroethane (DDT)

DDT is one of the most well-known organochlorine pesticides, gaining popularity for its effectiveness against insect pests, particularly in controlling mosquitoes that transmit diseases like malaria. The chemical

compound DDT (Dichlorodiphenyltrichloroethane) is composed of a mixture of aliphatic and aromatic groups [78], as presented in Table 1. Initially used since the 1940s in agriculture and healthcare to combat malaria, DDT faced global restrictions in 1972 due to its biomagnification and environmental persistence. India remains the sole country manufacturing DDT. Originally utilized during World War II to control parasite vectors, its enduring nature and ecological impact led to bans in some nations. DDT and its metabolite, dichlorodiphenyldichloroethylene (DDE), exhibit potent endocrine effects. Widely studied as a neurotoxic organochlorine insecticide, DDT is known for its carcinogenic and endocrine-disrupting properties, posing significant harm to humans and animals upon ingestion. Bacteria and fungi can degrade DDT to metabolites, such as dichlorodiphenyldichloroethylene (DDE) and dichlorodiphenyldichloroethane (DDD) and (p, p′-DDE + p, p′-DDD)/p, p′-DDT ratio that is greater/less than 1)), which are highly persistent and share similar chemical and physical properties. DDT and its breakdown products have been transported from warmer areas to the Arctic due to global distillation, accumulating in the food web. Research indicates that DDT exposure heightens the risk of breast cancer and negatively impacts metabolic, immunological, and neurological systems. Despite its six-decade use in eradicating plant pests and insect species, DDT has led to pesticide resistance in numerous insects. Unrestricted agricultural use has caused adverse environmental effects, including egg thinning and a decline in bird nestlings [79].

DDT undergoes dechlorination processes under different environmental conditions. Specifically, it is dechlorinated to DDE (dichlorodiphenyldichloroethylene) in aerobic conditions and reductively dechlorinated to DDD (dichlorodiphenyldichloroethane) under anaerobic conditions [80]. The DDE/DDD ratio serves as a valuable indicator to determine whether the degradation of parent DDT is taking place under aerobic or anaerobic conditions. If the ratio is less than 1, it signifies

a reductive dechlorination of the parent DDTs, thus implying the prevalence of microbial or chemical pathways in the degradation process [78].

2.2. Dichlorodiphenyldichloroethylene (DDE)

This is a DDT metabolite with the molecular formula $C_{14}H_8Cl_4$. It undergoes biomagnification in aquatic species, particularly fish, posing threats to human and wildlife health. Recent studies on Thunnus albacares and its prey found DDT levels in the range of 54.9-93.5 ng g^{-1} and 92.1–221.8 ng g^{-1}, respectively, indicating its persistence in the food web [80-82]. For example, in honey researchers have noted that the ratio of DDE + DDD to DDT was greater than 1 in all honey samples, thus confirming DDT has historical input in its formation. Furthermore, the report also infers that the DDE/DDD was less than 1 in 95% of the honey samples, thus suggesting that the predominant pathway for the degradation of parent DDT in honey involves reductive dechlorination to DDD under anaerobic conditions.

2.3. Aldrin

This is commonly used for controlling insects, worms, and larvae, posing a significant risk as an industrial and environmental contaminant. Its emergence as a major concern stems from past usage, and it tends to be prominently present in ecosystems [83]. Notably persistent, aldrin can be easily absorbed by organisms through food sources or direct contact. For instance, scientists detailed a preconcentration approach using the DLLME technique with N, N-diethanol ammonium chloride: pivalic acid deep eutectic solvent (DES) as the extraction medium. This method concentrated four organochlorine pesticides (aldrin, β–HCH, α–HCH, and dichlobenil) in cocoa samples. The ideal conditions of this technique were subsequently utilized for the analysis of cocoa samples, revealing the occurrence of aldrin and dichlobenil in specific [84]. In the environment and within living organisms, aldrin undergoes biotransformation, ultimately converting into

dieldrin. Despite being phased out, aldrin continues to linger, with environmental components often containing higher-than-permitted levels due to anthropogenic activities.

2.4. Endosulfan

Endosulfan is an insecticide and acaricide extensively used in agriculture since the 1950s, categorized as a cyclodiene organochlorine insecticide. India holds the title of the world's primary producer, consumer, and exporter of endosulfan, despite committing to discontinuing its use by 2017 [85]. Endosulfan is employed to manage insects in various products, including wool, coffee, cigarettes, small fruits and vegetables, cereals, and wood because it acts as a persistent pollutant. It comprises of two hazardous heteroatoms, α- and β-endosulfan which poses a significant risk due to its bioaccumulative nature. Scientific studies have documented that heightened exposure to endosulfan is associated with increased levels of proteins that promote atherosclerosis, especially in cases where there is an overexpression of Stromelysins, a member of the metalloproteinase family. In another experiment, Hassanpour and colleagues suggested utilizing liquid-liquid microextraction (LLME) assisted by switchable deep eutectic solvents (DESs) for extracting endosulfan and abamectin from water and fruit juice. Excessive exposure to endosulfan is undesirable due to its slow biodegradation, leading to its prolonged presence in the environment. Endosulfan and its metabolites can disrupt the endocrine system, impacting both humans and wildlife. Owing to its potential for biomagnification, extended durability, limited solubility, and neurotoxicity, endosulfan presents challenges as an agrochemical [86]. Hence, urgent attention from the scientific community is required for the swift elimination of endosulfan. It has faced international scrutiny due to its environmental persistence and toxicity concerns [87].

2.5. Dieldrin

Dieldrin is an organochlorine insecticide that was used in agriculture. It is known for its persistence in the environment and bioaccumulation in organisms. Dieldrin has been linked to declines in global raptor populations, although it does not cause eggshell thinning. Additionally, dieldrin has the potential to reduce neurotransmitters like serotonin and dopamine. Prolonged exposure to dieldrin can impede cognitive and motor skill development, resulting in heightened mortality rates due to accidents, disease, and starvation. This highly toxic pesticide has LD50 values ranging between 27 mg/kg to 381 mg/kg in various bird species. This class of organochlorine pesticides (OCPs), sensitive to sulfuric acid treatments, including endrin, endrin aldehyde, chlordecone, endosulfan I, endosulfan II, trans-heptachlor epoxide, and dicofol, can undergo complete sulfonation when exposed to concentrated sulfuric acid. Notably, dieldrin and endrin exhibit high sensitivity, degrading within a few minutes under this treatment. The other OCPs susceptible to acid-induced degradation will also undergo varying degrees of decomposition within an hour [88].

2.6. Methoxychlor

This organochlorine pesticide has been used to control pests in crops. It is less persistent than some other organochlorine pesticides (OCPs). In natural submerged environments, 1,1,1-trichloro-2,2-*bis*(4-methoxyphenyl)ethane has been reported to undergo dechlorination. Fuentes *et al.* conducted a study on the removal of three OCPs, such as lindane, chlordane, and methoxychlor, from wastewater using Streptomyces strains. The results indicated that Streptomyces sp. A5 exhibited the capability to eliminate 57.4% of lindane, 100.0% of chlordane, and 6.5% of methoxychlor. Methoxychlor exhibits remarkable persistence and a strong affinity for binding with environmental agents, as evidenced by its presence in Arctic samples, allowing for transport over long distances. Research indicates that methoxychlor demonstrates estrogenic activity, potentially impacting fertility and early pregnancy. Moreover, it seems to contribute to irregular cell development and the growth of breast cancer cells. In animals, the metabolite of

methoxychlor was observed to reduce testosterone production. Despite sunlight hastening its degradation, the resulting byproduct (methoxychlor olefin) is highly stable and degrades more slowly. The biodegradation of methoxychlor involves the loss of one chlorine atom along with demethylation [89].

2.7. Dicofol

Dicofol is an acaricide and insecticide utilized in agriculture, characterized by the chemical formula 2,2,2-trichloro-1,1-*bis*(4-chlorophenyl) ethanol, known for its poor degradability [90]. It exhibits endocrine-disrupting properties and is designated as a persistent organic pollutant in the Stockholm Convention [90,91]. It is widely employed in crops, cotton, fruits, and vegetables, and can be absorbed through inhalation, ingestion, and dermal exposure. Dicofol poses a moderate hazard to humans and is highly toxic to aquatic animals [92]. Dicofol has a bioconcentration factor (BCF) exceeding 5000 and significant environmental mobility, and is considered extremely harmful to aquatic life [93]. Dicofol contains impurities, majorly *o, p′*-DDT and *p, p′*-Cl-DDT (1, 2, 2, 2-tetrachloro-1, 1-*bis*-(4-chlorophenyl) ethane). However, during GC analysis, the latter breaks down thermally to *p, p′*-DDE leading to the elevated levels of DDE. This degradation into the organochlorine pesticide (OCP) DDT raises environmental and health concerns.

2.8. Toxaphene

This is a complex mixture of chlorinated terpenes, with molecular formula $C_{10}H_{10}C_{l8}$, consisting of 670 different compounds. It forms when camphene and chlorine gas react in the presence of ultraviolet light containing 67%–69% chlorine [94]. It was originally developed as an insecticide in the late 1940s, toxaphene is now used to control populations of predatory fish. It is produced worldwide in quantities of approximately 1.3 million tonnes. Analyses on wild aquatic animals have revealed that the organochlorine pesticide toxaphene poses an environmental hazard due to its persistence in soil and the atmosphere, frequent use, and

widespread distribution. Its impact on endocrine functions further adds to its environmental concerns [95].

2.9. Lindane

Lindane is an organochlorine insecticide used in agriculture and for controlling pests in wood and livestock. The gamma enantiomer of hexachlorocyclohexane, known as lindane. It is a highly persistent organic pollutant utilized for herbivorous pest control. Lindane is formed in different isomers during the photochemical chlorination of benzene using UV light. Commonly applied to fruits, vegetables, and coniferous forests and it serves to eliminate fungi on seeds [96]. With global consumption reaching 720,000 tonnes in 1995, lindane's stability and longevity in water make its removal challenging. Despite its historical use in crop protection and disease prevention, lindane is a neurotoxin disrupting human hormone function, potentially causing severe environmental concerns and health issues, including respiratory problems, convulsions, or excessive salivation. Its ecological impact is evident in its negative effects on biodiversity, organism communities, and biological traits [97]. Lindane's persistent and recalcitrant nature in aquatic environments raises global concerns due to its historical widespread use [98, 99]. From research, DDTs tend to be more predominant in soil samples, in contrast to the contamination pattern in honey samples, where noticeable transition from DDTs to lindane and α-endosulfan is revealed. This shift is likely attributed to variations in the uptake or degradation of OCPs in the honey samples [100].

2.10. Chlordane

Chlordane is a broad-spectrum organochlorine pesticide used for termite control and agricultural purposes. Chlordane is a persistent, non-systemic insecticide with contact and ingestion modes of action, and it also possesses fumigant properties. It is employed on land to combat formicidae, coleoptera, noctuidae larvae, saltatoria, subterranean termites

(including Coptotermes spp.), invertebrate animals, and various other insect pests. Additionally, it controls household insects, pests affecting humans and domestic animals, serves as a wood preservative, a protective treatment for underground cables, and helps reduce earthworm populations in lawns. Chlordane may be applied to soil, directly to foliage, or used as a seed treatment. Trans-Chlordan, a closely related compound, exhibits inhibitory effects on enzyme activities such as lipoxygenase, cyclooxygenase, and 5-lipoxygenase. Its chemical structure shares a common backbone with other compounds like chlordane and lindane." Others are two isomers of chlordane commercially available are cis-chlordane, and trans-nanochlordane. The three isomers are also sometimes referred to as α-, β-, and γ-chlordane, respectively [101].

2.11. Hexachlorobenzene

This organochlorine compound has been used as a fungicide and insecticide. HCB, or perchlorobenzene, is a fungicide used as a seed treatment to control fungal disease bunt. Introduced in 1945, it effectively kills fungi affecting food crops. HCB is a by-product of certain industrial chemicals and exists as an impurity in many pesticide formulations. In 1954 and 1959, individuals exposed to HCB developed various symptoms such as photosensitive skin lesions, colic, debilitation, porphyria turcica, etc. Moreover, HCB can be transmitted to infants through their mother's breast milk [96] This white crystalline solid is less soluble in water but sparingly soluble in organic solvents. Its highest solubility is in halogenated solvents like chloroform, esters, short-chain alcohols, and hydrocarbons. HCB is toxic and carcinogenic to humans, aquatic organisms, and animals. Chronic human exposure can lead to liver disease, skin lesions with discoloration, ulceration, photosensitivity, thyroid effects, bone effects, hair loss, embryo lethality, and teratogenic effects [96].

2.12. Polychlorinated biphenyls (PCBs)

Although not used as pesticides per se, PCBs were employed in various industrial applications, and electrical equipment. PCBs are pale-yellow viscous insulating liquids used in industry as dielectric and coolant fluids in capacitors and electric transformers, as well as additives in carbonless copy paper, paint, and plastics. They are toxic to some aquatic animals such as fish, causing spawning failures even at lower doses. Additionally, they lead to suppression of the immune system and reproductive failure in wild animals such as seals and mink. PCB exposure leads to various health effects, including mucous membranes, nausea, pigmentation of nails, fatigue, vomiting and swelling of the eyelids. In addition, the persistent presence of PCBs in mothers' bodies can lead to developmental delays and behavioral changes in children. Direct or indirect ingestion materials (PCB-contaminated food, such as rice oil) containing PCBs can trigger various dental and enamel abnormalities [102]. In addition, children may experience cavities, periodontitis, causing tooth infections and leading to shorter gums or tooth loss, while adults might develop discolored and inflamed gums. PCBs exhibit hydrophobic characteristics, low vapor pressure, limited water solubility, and high solubility in organic solvents, fats, and oils [103]. They possess dielectric constants with very high thermal conductivity and high flash points. They exhibit resistance to hydrolysis, acids, oxidation, bases, and temperature changes, PCBs find widespread use in various industries [103]. Through partial oxidation, they have the potential to generate highly toxic chemicals like dibenzodioxins and dibenzofurans. Additionally, PCBs can penetrate the skin, polyvinyl chloride (PVC), and latex, manifesting toxic effects. **Table 1** indicates the physicochemical properties of the selected OCPs pesticides used in this study.

3. The Degradation Process of Organochlorine Pesticides

3.1. 1,1,1-Trichloro-2,2-bis(p-chlorophenyl) ethane (DDT)

Bimetallic nanoparticles such as Ni/Fe and their oxides were discovered to efficiently degrade DDT in aqueous solution at alkaline

Table 1. Physicochemical properties of the OCPs and their respective ions for quantitative and qualitative analyses

| OCPs compound	Molecular structure	Molecular weight (g/mol)	Boiling point (ºC)	Log P	[a]Log K_{ow}	RT min	Range of Quant ion (m/z)	Confirm ion (m/z)	EFs
Dichlorodiphenyl-dichloroethylene (4,4 DDE)		318.02	403.45	6.51	5.50	14.984	409-426	412,416, 421	198
Heptachlor (HE)	Heptachlor	373.32	135 - 145	6.10	5.44	12.768	314-330	319, 322, 326	125
Dieldrin (HEOD)		380.93	330	5.40	5.48	14.594	398-402	399 402	130
Aldrin (HHDN)		364.90	145	5.40	5.52	13.373	342-354	344,348 ,351	506
Endosulfan	Endosulfan	406.93	480.7±45.0	4.67	3.83	15.403	426-438	429,434 ,439	491
Dichlorodiphenyl trichloroethane (4,4'-DDT)		345.49	440.74	6.36	5.44	16.053	448-467	458,461, 465	313
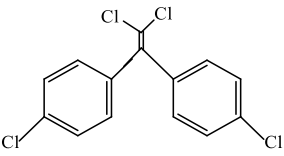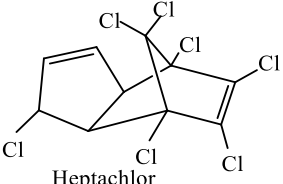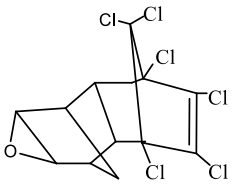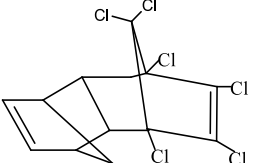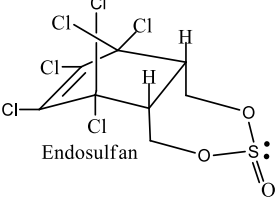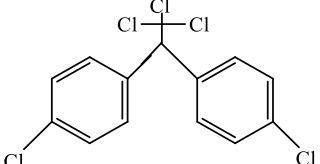
Table 1. Continued

OCPs compound	Molecular structure	Molecular weight (g/mol)	Boiling point (ºC)	Log P	[a]Log K$_{ow}$	RT min	Range of Quantion (m/z)	Confirmion (m/z)	EFs
Methoxychlor		345.65	346	5.40	5.08	16.795	486-498	487,493, 497	127
Dicofol		370.5	454.7±40.0	4.28	4.1		251.1		
Toxaphene		414.0	155	4.77	3-5		226		
Lindane		290.8	300	3.72	3.6		226		
Chlordane		409	275-325	6.16	3.5-4.6		373		
Hexachloro benzene		284.8	319	5.7	5.5 - 6.2		282-288		
PCBs		206- 538	275- 375	5.5 - 6.2	4 - 7				
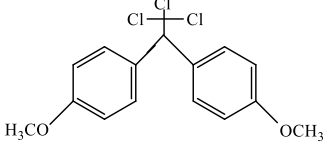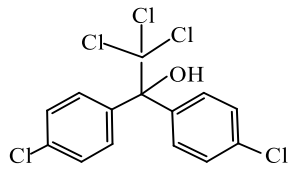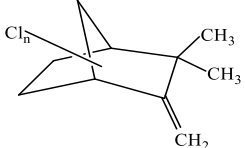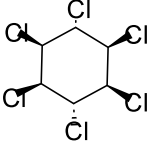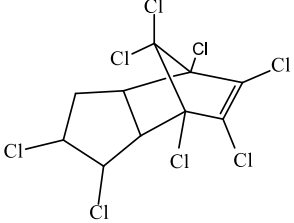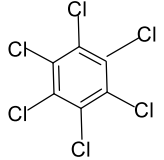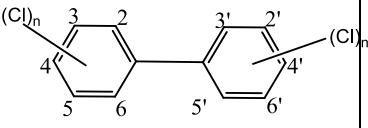
RT: Retention time
[a]Data are obtained from Syracuse Research Corporation's PHYSPROP database
Data of, boiling point and molecular weight were obtained from RSC Publishing Home:
http://www.chemspider.com
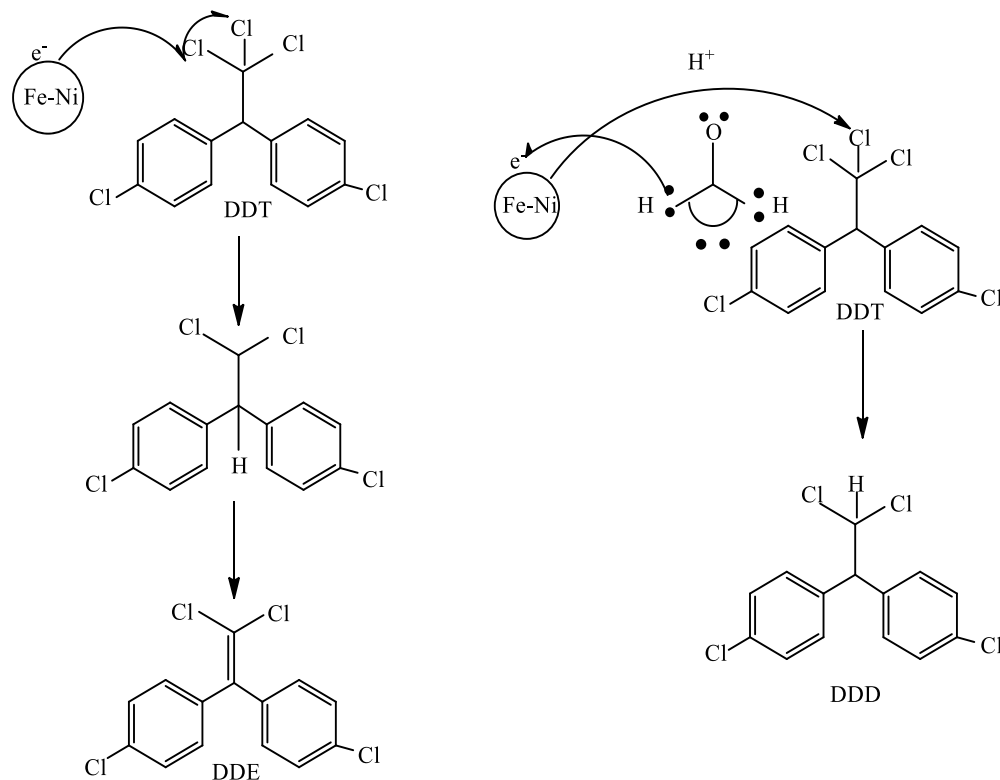
Scheme 1. Schematic diagram of DDT by bimetallic/metallic oxide nanoparticles

and weak acid conditions as shown in **Scheme 1**. Meanwhile, at acidic conditions, the nanometal particles promote the degradation of DDT by producing protons which help to generate hydrogen [104].

3.2. α-And β-endosulfan

The 6, 7, 8, 9, 10-hexachloro-1, 5, 5a, 6, 9, 9*a* hexahydro- 6, 9-methano-2, 3, 4-benzodioxathiepin-3-oxide is highly toxic in aqueous medium due to its low solubility [105]. It undergoes photolysis to yield endosulfandiol under UV, while in the soil, it forms Endosulfan sulfate, which is highly persistent and toxic when compared with the parent Endosulfan. It has two stereoisomers: α-Endosulfan and β-Endosulfan ($t_{1/2}$ = 60 days) and β ($t_{1/2}$ = 800 days), which are highly toxic to aquatic systems and animals due to low water solubility and can be degraded, as shown in **Scheme 2**. Researchers have confirmed the presence of this deleterious compound in ground and surface water and have degraded it by employing Ag-doped TiO$_2$ photocatalysts nanomaterial. Although the metabolite

Endosulfan sulfate, α- and β-Endosulfan are toxic and highly stable, they can be completely mineralized, as shown in **Scheme 2**, using *Aspergillusnige and Klebsiellaoxytoca* over a long period.

3.3. Methoxychlor

Methoxychlor is easily biodegraded by UV compared to the more stable and less degraded methoxychlor olefin, its by-product. The biodegradation and demethylation of methoxychlor results in the loss of one chlorine atom [104-106]. Researchers have reported different forms of methoxychlor ((4,4'-(2,2,2-trichloroethane-1,1-diyl)*bis*(methoxybenzene) degradation using TiO$_2$ under UV/O$_2$, dehydrogenation, dichlorination, and CN-replacement into 4,4'-(2-chloroethene-1,1-diyl)*bis* (methoxybenzene) and 4,4'-(ethene-1,1-diyl)*bis* (methoxybenzene) by catalytic reduction as depicted in **Scheme 3** [106]. Researchers have reported different forms of methoxychlor degradation using TiO$_2$ under UV/O$_2$, dehydrogenation, dichlorination, and CN-replacement into 4, 4'-(2-chloroethene-1,1-
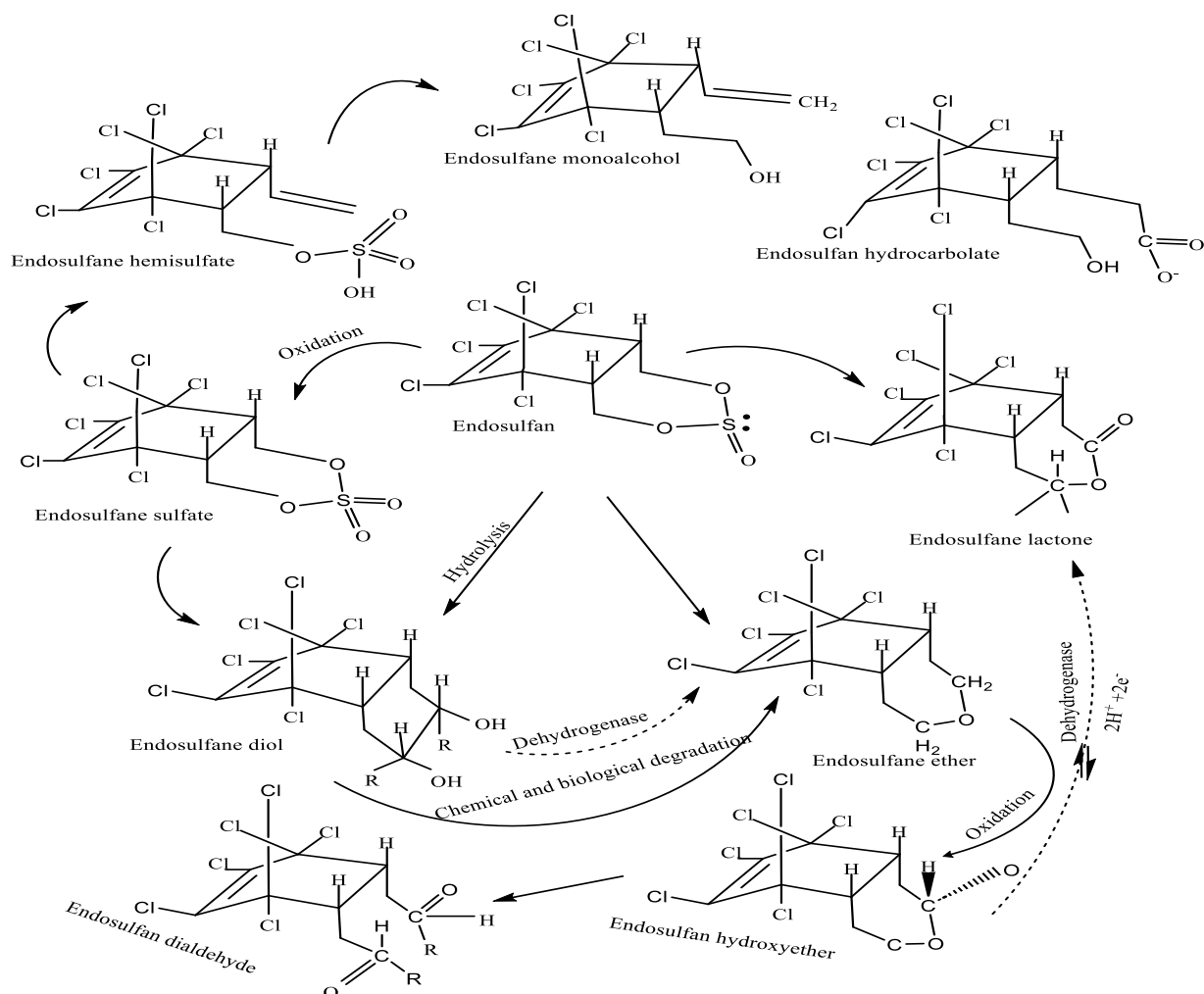
Scheme 2. Schematic structures of degradation of α,ß-Endosulfan

diyl) *bis* (methoxybenzene) and 4,4'-(ethene-1,1-diyl)*bis* (methoxybenzene) by catalytic reduction as shown in **Scheme 3**.

3.4. Aldrin and dieldrin

Researchers over the years, have proposed various methods including ion conversion, xenon lamp combustion, and microbial degradation for removing these chemicals from the environment. The microbial degradation process is economical, easy, convenient, and eco-friendly [107]. The molecular formula of aldrin is $C_{12}H_8C_{l6}$ and the nomenclature is 1,2,3,4,10,10-Hexachloro-1,4,4α,5,8,8α-hexahydro-1,4-*endo*, *exo*-5,8-dimethanonaphthalene, while Dieldrin's molecular formula is $C_{12}H_8C_{l6}O$ with nomenclature of 1,2,3,4,10,10-hexachloro-6,7-epoxy-1,4,4α,5,6,7,8,8α-octahydro-1,4-*endo*,

exo-5,8-dimethanonaphthalene[88-89]. A lot of microorganisms such as *Trichoderma viride*, *Cupriavidus* sp., *Burkholderia* sp., *Pleurotus ostreatus*, *Mucor racemosus*, *Pseudonocardia* sp., *Pseudomonas fluorescens*, have been used employed to degrade dieldrin/Aldrin under anaerobic microorganisms yielding the aldrin/dieldrin pathway.

The aldrin degradation pathways include reduction, hydroxylation, and oxidation of its major metabolite (dieldrin), while the dieldrin degradation pathway includes reduction, oxidation, hydrolysis, and hydroxylation, yielding dihydroxydieldrin and 9-hydroxydieldrin as major by-products. Other methods proposed, developed, and reported for the complete degradation of the aldrin/dieldrin pesticides include the use of vegetable waste via window composting and rotary drum, Na-montmorillonitte, activated carbon, and nano
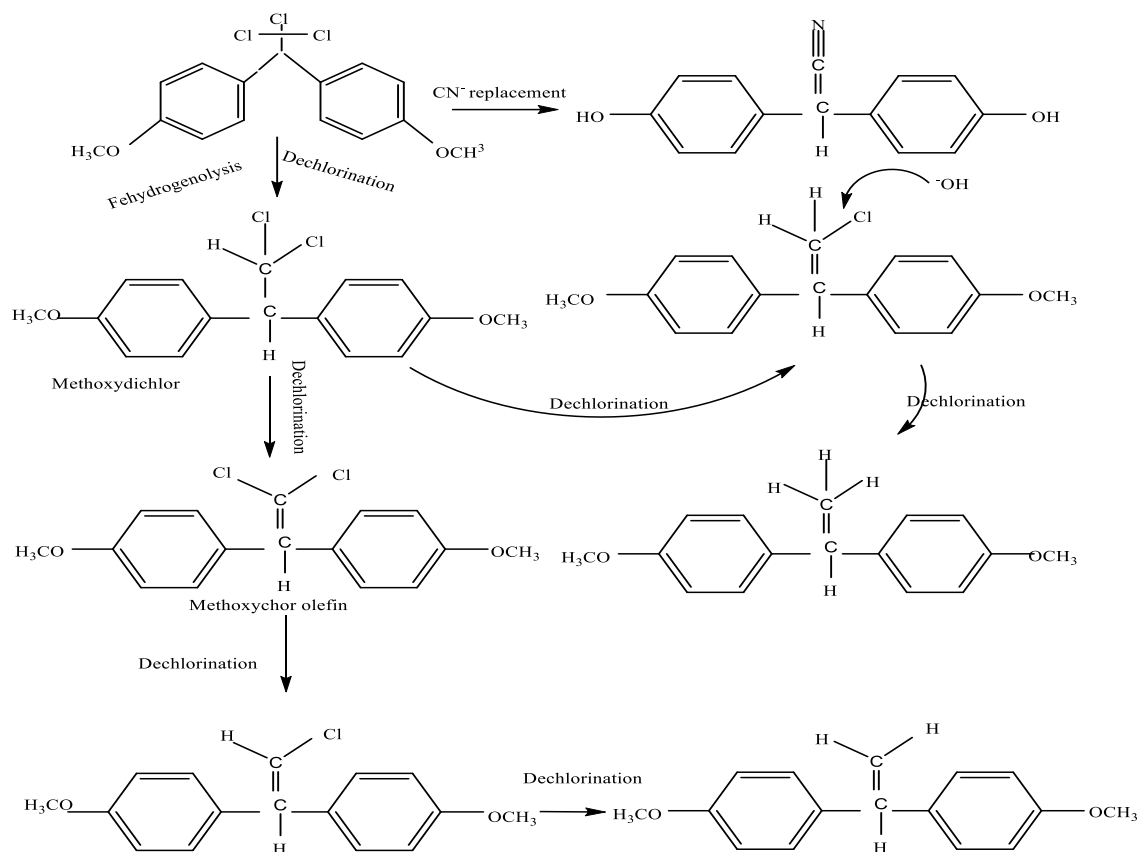
Scheme 3. Schematized reductive degradation pathway of methoxychlor

absorbent in different advanced oxidation processes- like Fenton in UV radiation. The presence and formation of 1-hydroxychlorodene and dieldrin metabolites confirm epoxidation, also, the oxidation of bridge carbon of aldrin contains methylene group, as shown in **Scheme 4** [91]. The complete degradation of aldrin in an aqueous medium into chlordane, dieldrin, and 12-hydroxy-dieldrin via bulk TiO_2 as photocatalyst. Although the use of nano-sized TiO_2 enhances the degradation efficiently.

3.5. Endrin

The 1,2,3,4,10,10-hexachloro-6,7-epoxy-1,4,4*a*,5,6,-7,8,8*a*-octahydro-1,4-*endo,endo*-5,8-dimethanonaphthalene is very stable in basic medium and can photodegrade into the epoxide of isodrin, correspondingly yielding endo-endo isomer of aldrin, endrin aldehyde, or delta-keto endrin, which can persist and bioaccumulate in soil with a normal half-life of up to 12 years. Endrin is very persistent because of its lipophilicity and chemical stability in the

sediment and soil environment; hence, high levels of endrin (above the maximum residue limit) have still been detected in recent years around the world. Recently, scientists have revealed from a survey that microorganisms like white rot fungi Phlebia brevispora and Phelibia lindtneri [108-111] and their secreted ligninolytic enzymes, including laccase, manganese, and lignin peroxidase, can bioremediate and degrade DDT and endrin in the soil, as shown in **Scheme 5**. This cost-effective approach can be used to degrade endrin from the soil, while other approaches, such as the use of acidified zinc and nano adsorbents in different forms, have also been explored and reported to degrade endrin [111].

3.6. Heptachlor

Its main ingredient includes ɣ-nonachlor, α- and ɣ- chlordane. In the human body, it can completely metabolize into oxychlordane, ɣ-nonachlor, and heptachlor epoxide. Microorganisms such as bacteria and fungi have been extensively utilized to degrade heptachlor
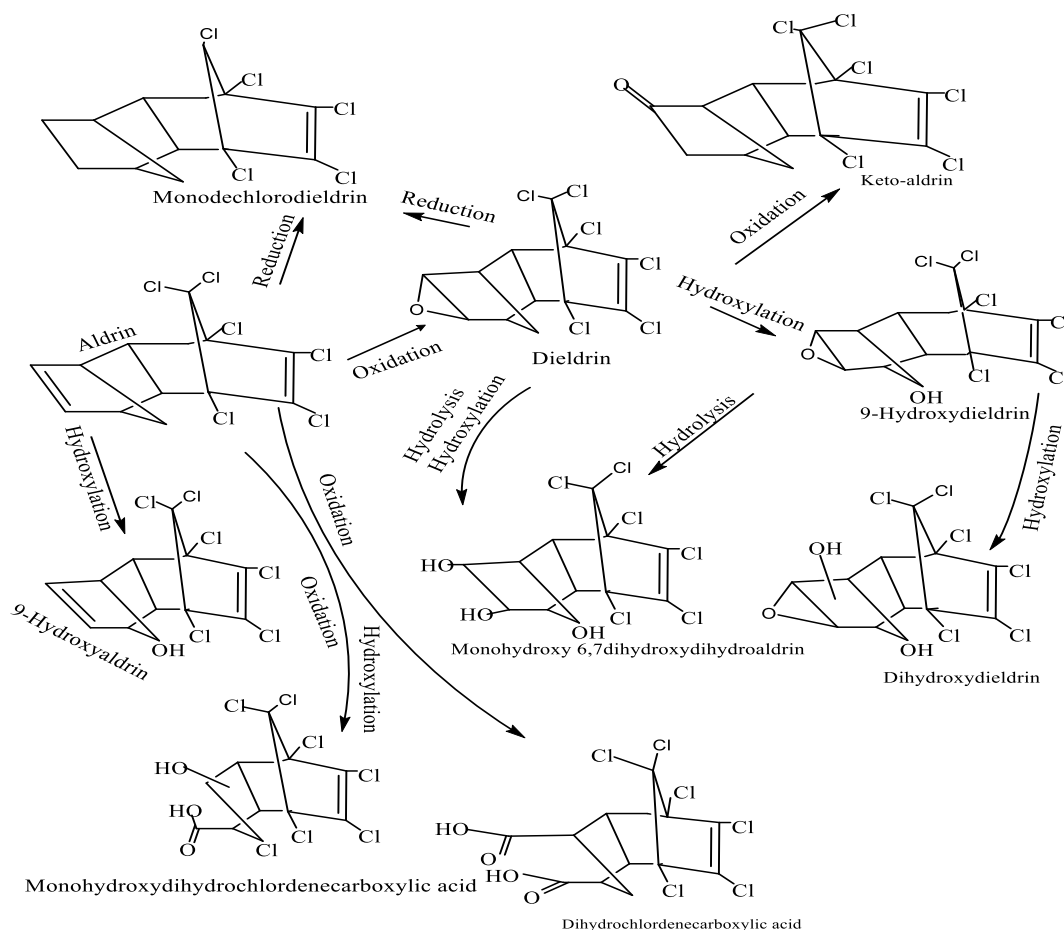
Scheme 4. Schematized microbial reductive degradation pathway of aldrin and dieldrin

as shown in **Scheme 6**. For example, biotic processes with different species of white rot fungi (genus *Phlebia*) have also been used to degrade heptachlor and its toxic metabolite heptachlor epoxide(~16%) in a range of 71–90% within 14 days of incubation under anaerobic conditions [97]. These white rot fungi (WRF) inocula can completely remove heptachlor via dechlorination in river sediments [112-114]. In another experiment, the fungal inoculum of Pleurotus ostreatus demonstrated an 89% elimination of heptachlor over 28 days, producing chlordene as the primary metabolite. Additionally, Pleurotus ostreatus exhibited a significant capacity to degrade heptachlor epoxide, with approximately 32% degradation observed, resulting in the formation of heptachlor diol. Encouraged by these results, Pleurotus ostreatus spent mushroom waste (SMW) was applied to artificially contaminated soil, leading

to a successful degradation of heptachlor (91%) and heptachlor epoxide (26%) over a 28-day period [115].

3.7. Dicofol

Dicofol is a miticide derived from DDT. The degradation of dicofol to Under alkaline conditions was catalyzed by hydroxide ions and induced by UV-light the degradation of dicofol to synthesize *p,p*-dichlorobenzophenone (DCBP) as represented in **Scheme 7** However, more effective outcomes were achieved using nanoparticles (TiO$_2$) compared to using UV light irradiation alone in an alkaline medium resulting in the complete degradation of dicofol in less than 2 hours. In another experiment, the photocatalytic degradation of dicofol, cyfluthrin, and fenvalerate was studied using boron and cerium co-doped nano titanium dioxide (B/Ce co-doped TiO$_2$) under light irradiation. The synthesis of B/Ce co-doped
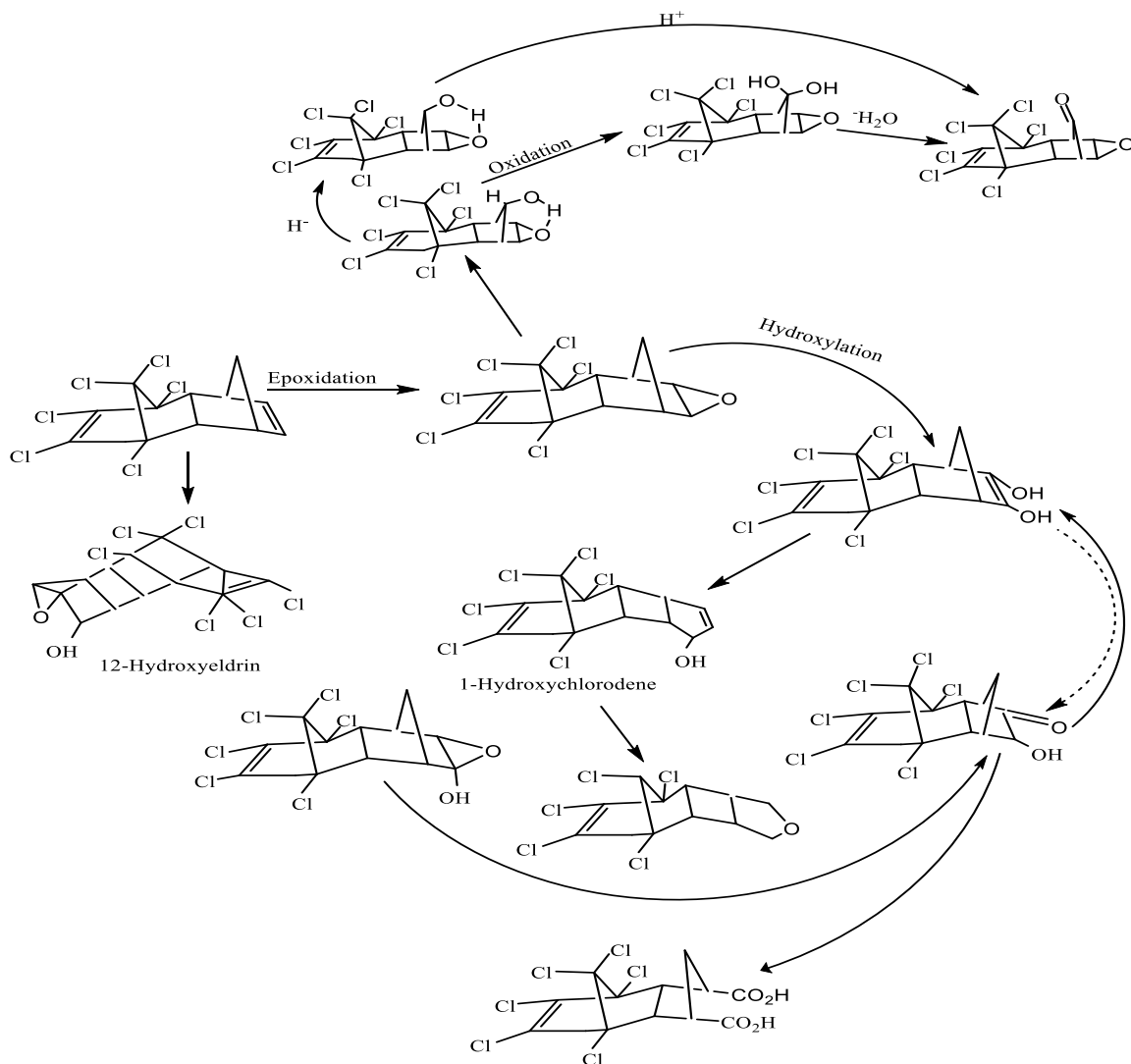
Scheme 5. Schematized proposed degradation pathway of endrin
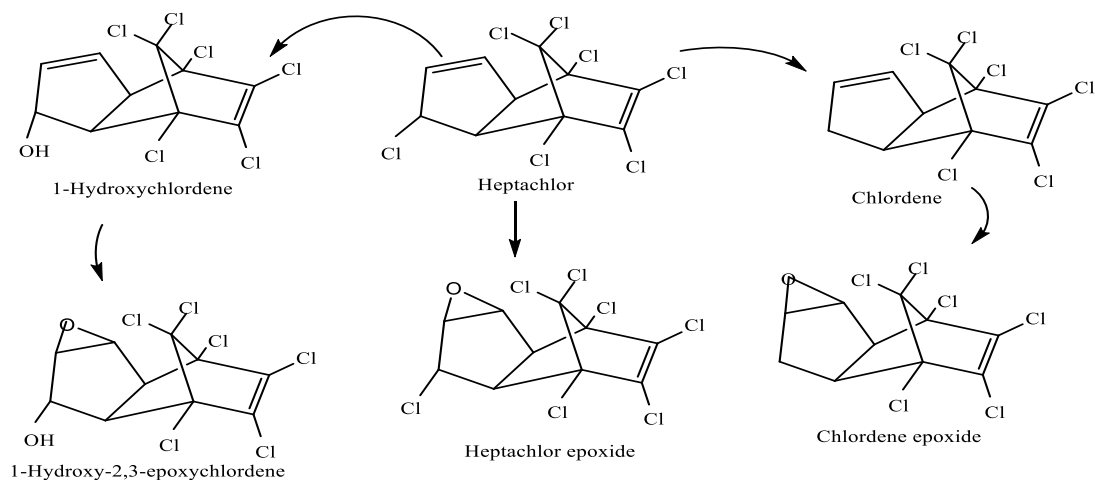
Scheme 6. Schematic pathway of Phlebia's complete metabolism of heptachlor
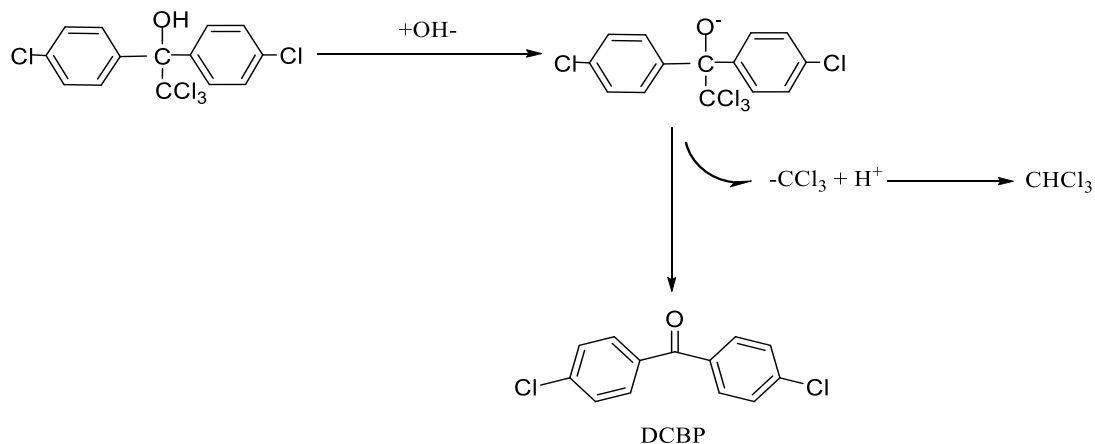
Scheme 7. Proposed dicofol degradation pathway induced by UV-light

TiO_2 involved a sol-gel technique with tetrabutyl titanate, boric acid, and cerous nitrate. The study revealed that B/Ce co-doped nano TiO_2 exhibited enhanced absorption in the 420 to 850 nm range compared to undoped TiO_2, resulting in higher photocatalytic activity as represented in **Scheme 7**. This increased activity was observed in the degradation of dicofol, cyfluthrin, and fenvalerate, surpassing both Ce-doped nano TiO_2 and pure nano TiO_2 under the same light conditions. The findings suggest the potential of B/Ce co-doped TiO_2 as an efficient photocatalyst for pesticide degradation under light irradiation [115].

3.8. Choldane

Chlordane is a complex mixture comprising more than 50 closely related chemicals including *trans*-chlordane and *cis*-chlordane which are (13.2%) and (11.3%) predominant components respectively in the technical mixture (EPA, 1990). Just like heptachlor in session 3.6, the microorganism degradation of chlordane using wood-rot fungi species such as Phlebia brevispora, Phlebia lindtneri GB 1027, and Phlebia aurea and three surfactants have been reported to effectively degrade at least 50% of trans-chlordane within 12 days through hydroxylation reactions, yielding 11 different metabolites, as shown in **Scheme 8**. These fungi are also capable of degrading other organochlorine pesticides, such as pentachlorophenol (PCP) [116]. At the end of 42 days of incubation, over 50% of trans-chlordane was degraded by the fungal

treatments in pure cultures. These fungi transformed trans-chlordane to at least eleven metabolites including a large amount of hydroxylated products such as 3-hydroxychlordane, chlordene chlorohydrin, heptachlor diol, monohydroxychlordene, and dihydroxychlordene. The use of bacterial strains whose interactions improve mycelial growth of the white-rot fungus Phlebia brevispora could also improve the degradation of chlordane [117-131].

4. Novel Sorbent and Methodologies for the Extraction and Determination of Organochlorine Pesticides (OCPS) from Environmental Matrices

In recent years, substantial attention has been devoted to the environmental remediation of organochlorine pesticides. A promising approach to address this concern involves employing graphene and graphene oxide (G/GO)-based materials in various extraction techniques, as provided in **Table 2**.

These methods have been proposed for the precise and sensitive monitoring of organochlorine pesticides (OCPs) across a broad spectrum of samples, as summarized in **Table 3**.

The common novel technologies and instruments are increasingly being employed for the analysis and detection of pesticide residues in complex matrices and plant-derived food items encompass chromatographic techniques, such as supercritical fluid
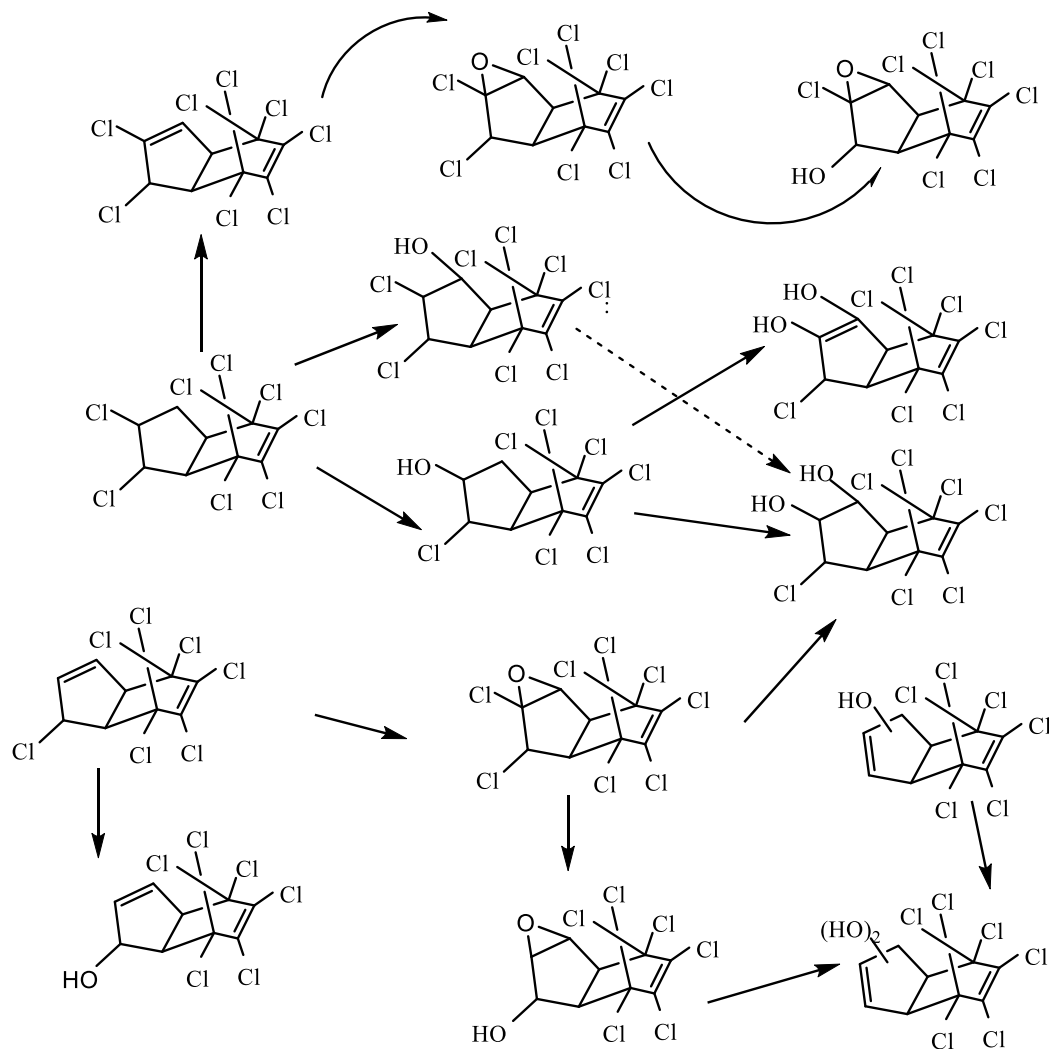
Scheme 8. Proposed schematized pathway for the degradation of *trans*-chlordane

chromatography [131], high-performance liquid chromatography[132], and gas chromatography[133], as shown in **Table 4**. Currently, chromatography methods combined with mass spectrometry are typical analytical techniques required prior sample pre-concentration to facilitate the analysis of trace amounts of pesticide residues. These methods are highly sensitive, enabling accurate detection and quantification of pesticide residues. Nevertheless, concerns persist regarding the long-term impact of pesticide residues on human health. As a result, there is a growing need for stringent monitoring and regulation of pesticide levels in food products. Various strategies, ranging from conventional extraction to sophisticated detection methods, are being employed to extract and detect pesticides in fruits and vegetables. Despite

advancements in detection technology, effective sample preparation procedures for pesticide residue measurement in cereals and feedstuffs are still required. The development of reliable and sensitive detection and extraction methods for pesticide residues is crucial for ensuring food safety and public health**.**

4.1. Factors affecting the adsorption of OCPS

Adsorption is the most commonly used efficient method for targeted analytes removal due to its effectiveness, cost-efficiency, ease of recycling, simplicity, and environmental friendliness. Adsorption methods can be divided into physical, chemical, and ion exchange adsorption based on adsorptive power. There are numerous chemical and physical methods for adsorption, but the adsorption of contaminants

Table 2. Advantages and disadvantages of novel extraction methods for the OCPS extraction

Extraction method	Advantage	Disadvantage
Solid-Phase Extraction (SPE)	• Lower solvent usage compared to traditional methods • Improved selectivity and sensitivity • Applicable to various sample types and sizes Reduced sample matrix interference	• Initial setup cost for equipment • Potential for sorbent saturation • Requires method optimization for different analytes and specialized equipment • Costly due to consumables May not be suitable for all pesticide classes
QuEChERS (Quick, easy, cheap, effective, rugged, and safe)	• Efficient for multi-residue analysis • Reduced solvent usage and extraction time • Compatible with a variety of pesticides • Fast, easy and do not need specific instruction. • Multiple extraction methods integrated • High sample throughput, • Improved detection accuracy	• Matrix effects may still be present and affect accuracy • Limited to certain sample matrices and pesticides • May require additional clean-up steps • Low enrichment factor • May require centrifugation • Single sample extraction • Long purification time • Low recovery rate • Large impact on human health
Liquid-phase microextraction (LPME)	• Effective for non-polar and polar analytes • Simple and cost effective • Can handle a wide range of sample matrices	• Limited solvent alternatives • Poor reproducibility • Time-consuming and labor-intensive • Requires large amounts of organic solvents • Potential for emulsion formation
Solid-phase micro extraction (SPME)	• Ease of preparation • Ease of handling • Eco-friendly • Versatile for various sample types • Applicable to volatile and semi-volatile compounds	• Fragile with limited shelf life Limited to smaller sample volumes • Potential for carryover between samples • Sensitivity can be affected by matrix effects
Stir bar sorptive extraction (SBSE)	• Good reproductivity and High extraction efficiency	• May require several desorption steps • Difficulty in removing stir bar
Ultrasound-Assisted Extraction (UAE)	• Enhanced extraction efficiency • Reduced extraction time • Applicable to various matrices	• Equipment cost and maintenance • Potential for sample degradation due to heat • Limited to small sample volumes
Pressurized liquid extraction (PLE)	• High extraction efficiency and speed • Reduced solvent usage • Automation capability	• Expensive instrumentation • Complexity in operation and method development • Limited to certain sample sizes
Microwave-assisted extraction (MAE)	• Rapid extraction process • Reduced solvent usage • Applicable to various sample types	• Equipment cost and maintenance • Potential for sample degradation due to heat • Limited to small sample volumes

Table 3. Various developed methods for the OCPs extraction

Pesticides	Environmental samples	The solid phase extraction technique	Adsorbent	Instrumental technique	Linearity range (ng/mL)	LOD (ng/mL, μg/kg,)	LOQs	Recoveries (%)	References
Pesticides	Honey	MSPE	β-CD/MrGO	GC-ECD	2 to 10,000 ng kg⁻¹	0.52–3.21 ng kg⁻¹	1.73–10.72 ng kg⁻¹	78.8–116.2%	[109]
Organochloride pesticide	Environmental water	DSPE	magnetic bucky gel/multiwalled carbon nanotube nanocomposite choline	GC-micro-ECD	0.5–2000 ng L⁻¹	0.04–0.27 ng L⁻¹	0.57–0.89 ng L⁻¹	80.73% to 120%	[113]
OCPs	Soil and water	QuEChERS	MGO	GC-MS	0.26–1.89	0.86–9.99	0.9931–0.9999	70.0–118.0	[114]
Organochlorine pesticides (18)	Water	DSPE	Fe₃O₄-MWCNTs-DES ChCl:urea = 1:2	GC-μ-ECD	0.00004–0.00027	0.0002–2	-	-	[115]
Organochlorine pesticide	Orange juices	MSPE	Fe₃O₄@SiO₂-G	GC/MS	1.0–200.0 ng m L⁻¹	0.01–0.05 ng m L⁻¹	-	73.8–105.4	[116]
Organochlorine pesticide	Tobacco	MSPE	Fe₃O₄@G	on-line GPC-GC-MS/MS	-	0.01275–3.150 ng g⁻¹	-	64–126	[112]
Organochlorine pesticide	Water	MSPE	Fe₃O₄@SiO₂-G	GC-μECD	1–100 pg mL⁻¹	0.12–0.28 pg m L⁻¹		80.8–106.3	[117]
Organochlorine pesticide	Water	MSPE	RGO/Fe₃O₄@Au	GC-MS	0.05 to 500 μg L⁻¹	0.4–4.1 ng L⁻¹		69–114	[118]
Organochlorine pesticides	Wastewater	SPME	CDs/RGO	GC–MS	0.05–2500	0.003–0.0051	0.01–0.0169		[119]
Organochlorine pesticide	Real and wastewater	SPME	Graphene	GC	10–1000	0.19–18.3	-		[120]

Table 3. Continued

Pesticides	Environmental samples	The solid phase extraction technique	Adsorbent	Instrumental technique	Linearity range (ng/mL)	LOD (ng/mL) µg/kg,	LOQS	Recoveries (%)	References
Organochlorine pesticides	Wastewater	SPME	Hierarchical graphene	GC-MS	10–20000	0.08–0.8	0.25–2.7		[121]
15 Organochlorine pesticides	Urine samples	SB-µ-SPE	(LDH-G) hybrid	GC-MS	1–200	0.22 and 1.38 ng m L^{-1}	-	-	[122]
16 organochlorine pesticides	Honey samples	MSPE	β-CD/MrGO)	GC–ECD	2–10,000 ng k g^{-1}	0.52–3.21 ng kg^{-1}	1.73–10.72 ng kg^{-1}	78.8% - 116.2%	[109]
Organochlorine pesticides	Apple juice	dSPE	rGO–ZnO	GC-MS	1.0–200.0 ng/ mL	0.011–0.053 ng/ mL.	-	78.1–105.8%	[111]

Note: *β-CD/MRGO): β-cyclodextrin/iron oxide reduced graphene oxide hybrid nanostructure; (LDH-G) hybrid : layered double hydroxide/graphene (LDH-G) hybrid;*
MA-HS-GNS: microwave assisted headspace novel graphene nanosheets; Fe3O4-MWCNTs-DES: DES magnetic bucky gel/multiwalled carbon nanotube nanocomposite

Table 4. Advantages and disadvantages of detection methods

Methods of analysis	Advantages	Disadvantages	Future prospects
Gas Chromatography (GC)	• Minimizes sample matrix interferences • High separation efficiency for volatile compounds • Well-established technique in pesticide analysis • Low detection limits • Excellent precision and reproducibility	• Extraction efficiency may vary with analyte types • Limited to volatile and thermally stable compounds • Requires derivatization for High equipment and maintenance costs some non-volatile compounds • Skilled personnel required for operation	• Integration with rapid detection technologies, improved sensitivity and selectivity
Liquid Chromatography (LC)	• Applicable to a wide range of pesticides • Suitable for polar and non-volatile compounds • Reduced derivatization requirements • Widely used in environmental analysis	• Limited applicability to polar compounds • Higher solvent usage compared to GC Equipment and maintenance costs • May have longer analysis times • Complex sample matrices may pose challenges	

Table 4. Continued

High-performance liquid chromatography (HPLC)	• High resolution and efficiency • Applicable to a broad range of compounds • Suitable for non-volatile compounds	• Expensive instrumentation and maintenance • Complexity in operation and method development	• Enhanced integration with rapid detection technologies, improved sensitivity and selectivity
Mass spectrometry (MS)	• High sensitivity and selectivity • Structural information available • Capability for multiple analyte detection	• Expensive equipment and maintenance • Requires skilled operators • Matrix interference	• Continued advancements in sensitivity and selectivity, integration with rapid detection technologies
Enzyme-linked immunosorbent assay (ELISA)	• Rapid results • Cost-effective • Suitable for high-throughput screening	• Limited to specific pesticides • Cross-reactivity issues • False positives or negatives	• Potential for improved specificity and sensitivity
Thin-layer chromatography (TLC)	• Simple and cost-effective • Quick results	• Lower sensitivity compared to other methods • Limited separation capability • Subjective interpretation	• Continued advancements in sensitivity and selectivity
Spectrophotometry methodology	• Ease of operation • Does not require sample preparation • Non-destructive	Prone to interference from external factors	Continued advancements in sensitivity and selectivity
Chromatography methodologies	• Require low samples • Precise separation	• Require skilled operator and handling • Not cost effective • Not environmentally friendly	• Continued commercialization • Potential for improved specificity and sensitivity
Rapid detection cards	• Rapid results, on-site screening capability	• Lack of specificity, • Poor sensitivity for some compounds	• Potential for improved integration with rapid detection technologies
Bioactive paper	• Low-cost platform, • Potential for on-site screening	• Limited to specific compounds, • may require validation	• Continued advancements in sensitivity and selectivity
Nanotechnology-based approaches	• Potential for improved sensitivity and selectivity	• Limited to specific compounds, • may require validation	• Continued focus on improving precision, selectivity, and sensitivity
Sample pretreatment techniques	• Improved precision, selectivity, and sensitivity	• Time-consuming, • potential for matrix effects	• Continued focus on reducing analysis duration
Multi-residue analysis	• Efficient for analyzing multiple compounds	• Potential for matrix effects, • time-consuming	• Continued commercialization • Potential for improved specificity and sensitivity

on solid surfaces emerges as a practical option. Adsorption, recognized for its effectiveness, cost-efficiency, recyclability, simplicity, and environmental friendliness, stands as the most employed method for the removal of targeted analytes. Adsorption methods can be categorized into physical, chemical, and ion exchange adsorption based on their adsorptive power [134]. The functional groups present in the adsorbent play a crucial role in chemical and physical interactions with dissolved xenobiotic compounds. The effectiveness of adsorption methods hinges on the properties and performance of the chosen adsorbent, with functions including the formation of ion bonds, covalent bonds, hydrophobic interactions, hydrogen bonds, and van der Waals forces. The rate of adsorption is influenced by factors such as pH, particle size, temperature, adsorbent concentration, stirring speed, surface area, and contact time. On soil, researcher have noted that the spatial distributions of OCPs in soil samples especially is influenced by parameters such as land use, soil pH, total organic carbon and point sources [135]. Therefore, in adsorption studies, experimentation with these factors is crucial for understanding their impact on the adsorption rate. Continuous efforts are made to identify adsorbents that are not only cost-effective but also efficient in adsorbing contaminants [136]

4.2. Adsorbent properties

The type and characteristics of the adsorbent used play a crucial role. The selection of a suitable sorbent nanomaterial, capable of exhibiting efficient affinity towards a wide range of target analytes with different polarities, is a crucial aspect of the experiment. The utilization of DES-functionalized graphene oxide and derivatives enables straightforward, sensitive, and cost-effective separation, preconcentration, and determination of inorganic and organic contaminants in complex environmental matrices. This approach can be adopted by laboratories for QA/QC of water, wastewater, and environmental samples.

4.2.1. Activation of sorbent

Activation is employed to enhance the adsorptive capacity of the adsorbent, aiming to increase the rate of adsorption. The ultimate goal is to expand the surface area of the adsorbent through mechanical, physical, or chemical methods [137]. A review indicates that treating the adsorbent with specific chemicals, termed activating agents, is effective in increasing the number of pores. Examples of such activating agents include hydrochloric acid, sodium hydroxide, nitric acid, sulfuric acid, zinc chloride, and more [137]. Physical activation primarily involves the use of heat and carbon dioxide as activation sources. While, chemical activation of the modified adsorbents exhibited superior packing density compared to physical activation.

4.2.2. Functionalization of graphene-based sorbent and MNPs with DES

DES-based materials exhibit excellent properties including fluidity, magnetism, stability, chromatographic compatibility, tunability, and reusability. These characteristics combined with the superior properties of DESs will create a synergistic effect to enhance their overall performance. The tunability of DES-based materials is attributed to their adjustable physicochemical properties which plays a crucial role in facilitating hydrogen bonding between molecules and is instrumental in extraction processes for detection technologies. In this scenario, GO/rGO modified sorbents with Deep eutectic solvent can attract OCPs and other contaminants through mechanisms involving hydrogen bonding, electrostatic forces, hydrophilic interactions, hydrophobic interactions, van der Waals forces, and π-π stackings with strong stability [138]. The presence of various functional groups, a high surface area, and accessible active binding sites in G/GO/rGO derivatives further influence or reinforce these interactions. In addition, the sorbent's ability to disperse properly in an aqueous medium is critical. Hydrophobicity of the sorbent may enhance floatation over the sample surface, leading to poor performance, while a sorbent with hydrophilic outer surfaces

and a hydrophilic inner core can serve the dual function of extraction and dispersion. Moreover, achieving an optimum ratio of magnetic support (MNPs) to sorbent is key to obtaining higher extraction efficiency. Other factors such as surface area, porosity, and surface chemistry impact the adsorption efficiency [138]. To fabricate an ideal or optimal sorbent material, suitable materials, binding methods, and properties, as illustrated in **Table 5** are selected for a stable composite with multiple active sites.

It is also vital to assess all sample preparation and pretreatment methods for its greenness after establishing any analytical method. AES, GAPI, AGREE, and ComplexGAPI are widely used GAC (Green Analytical Chemistry) metrics for this purpose. However, it is observed that many articles lack the evaluation of the green character of the proposed method. It is crucial for researchers to be attentive to this aspect, ensuring a thorough assessment, incorporating and aligning with the evaluations of principles of green chemistry to promote sustainable practices as well as enhance the overall understanding of the environmental impact of analytical within the scientific community.

Table 5. Summarized features between MNPs, GO, and mGO derivatives composites

Features	MNPs	GO	mGO and derivatives
Characteristics	• Possess magnetic properties. • Presence of hydroxy functional groups on the surface of the material • Particles are nano-sized • Uni-dimensional (oD) morphology	• Possess multiple functional groups such as carbonyl epoxy, carboxyl, and hydroxyl. • Nanosized particles possess large specific surface area. • Two-dimensional shaped morphology (2D) • Carbon structure is Sp^2 bonded	• Nanosized composites possess large specific surface areas, • Possess magnetic properties to ease separation and reuse, • Highly porous nanocomposites • Can exits in 2D or three (3D) dimensional morphology
Merits	• Can be used for analysis, and drug delivery. • High speed and ease of separation from solvent. • High elution, and adsorption capacity.	• Can be used for analysis, drug delivery, • Excellent dispersibility, physicochemical, mechanical, optical, thermal, and electrical properties • High elution and adsorption capacity • Possible selectivity for specific target analytes	• Can be used for analysis, drug delivery, • Excellent dispersibility and high nanocomposite stability, • Large surface area • Ease of solvent (elution or desorption) recovery • High speed and ease of separation from solvent. • High elution, adsorption capacity • Inclusion of more MNPs • Possible selectivity for specific target analytes
Demerits	• Tends to self-aggregate or agglomerate, • Less specific surface area. • Unstable dispersion • Non- selective for all analyte	Difficulty in recovering from solvent (elution or desorption)	Cannot be commercialized

4.2.3. Surface modification of graphene-based sorbent and MNPs with metals

Surface modification plays a crucial role in enhancing the adsorption process by introducing specific functional groups to the adsorbent. This modification influences the porous structure, surface chemistry, and improves the adsorbent's affinity for contaminants. Studies have demonstrated the positive impact of ligands like S−, N−, and Cl− on sorbents, increasing its capacity to adsorb any target analytes. Similarly, to enhance the adsorption capacity of organochlorine compounds on graphene-based sorbents, one could consider modifications that introduce functional groups with chlorine atoms or other groups known to interact with organochlorines such as Amino-functionalized graphene derivatives, Hydroxyl groups, oxygen-containing functional groups such as amino-functionalize. Overall, the presence of certain functional groups positively influences and improves the adsorption performance of the adsorbent.

4.2.4. Surface area of the sorbent

Surface area is an important aspect which governs the rate of adsorption. The structure of the adsorbent whether porous or finely divided materials will significantly impact adsorption rates. Various solid sorbents exhibit different adsorption rates under similar environmental conditions, thus emphasizing the importance of the adsorbent's structural characteristics. Also, the increase in the amount of sorbent enhances the availability of active binding sites and contact surface area. As the mass increases, the peak area correspondingly rises, facilitating mass transfer of the target analytes and resulting in increased extraction efficiency with contact time until equilibrium is achieved. Conversely, an elevated amount of sorbent exceeding the optimum level adversely affects the extraction of targeted analytes, impairs the sorbent's performance, and leads to inefficiency, dilution effects, and wastage. This can be attributed to poor dispersion, aggregation, or agglomeration of the sorbent particles within the optimum time frame [137].

4.2.5. Characterization of DES-functionalized graphene-based sorbent particles

The characterization of DES-functionalized graphene-based sorbent helps to investigate and understand the physical and chemical properties of the fabricated materials for achieving better analytical performance. These materials can be characterized based on their chemical composition, sorbent morphology, thermal, mechanical, and magnetic properties. The properties of magnetic graphene-based sorbents, including shape, crystal structure, granularity, magnetism, surface area, dispersion, multi-functionality, and agglomeration, were analyzed using various experimental techniques, such as: FTIR (Fourier Transform Infrared). FTIR is employed to determine the inherent functional moieties in the prepared adsorbent. It provides insights into structural information, such as changes in functionality and the type and nature of skeleton atoms through characteristic vibration spectra. The respective sharp peaks at varying absorption wavelengths ranging from 1100-1300 and 1400-1600 cm^{-1}, demonstrate a stretching vibration of an epoxy functionality in the magnetic GO. Also, absorption and the broad peak around the wavelength ranged from 1650-1750 and 3000–3400 cm^{-1}, respectively, further confirming and indicating the presence of carboxylic acids in the MGO, as shown in **Figure 2a**. Also, various data have shown that different batches of GO sheets can show a characteristic peak and bond vibration appearing at wavelength ∼3400 cm^{-1} ∼3434 cm^{-1}, reflecting the presence of O−H stretching vibration from −COOH and C−OH functionalities. In addition, peaks and bond vibration appearing at wavenumber 1747, 1700, 1637, 1624, 1403, 1235, and 1045 cm^{-1} are attributed to vibration stretching and bending vibrations of C=O, C=C, C−O−H, and C−O−C functionalities respectively. This also reveals the oxidation of graphite precursor by forming the GO phases. Concerning the Fe$_3$O$_4$/GO spectrum, two overall peaks and two specific bond vibrational modes belonging to GO and Fe$_3$O$_4$ phase appearing at the wavelength of 600 to 500 cm^{-1} (579 cm^{-1}) and 823 cm^{-1} primarily indicating the spinal

magnetic NP in tetrahedral bond O-M (Fe^{3+}-O^{2-}) and symmetric Fe–O–Fe stretching in octahedral bonds respectively and confirming the presence of different magnetic materials in the GO-based NPs [139] as presented in **Figure 2a**. The weakening intensity of the peak in the GO composite sample is a reflection and assertion of the direct dispersal of Fe_3O_4 NP into the GO layers and on its surface in the formed composite sample. In the successful modification of MGO NP with DES, the FTIR spectrum indicates the appearance of a broad vibration band ranged from 3000-3600 cm^{-1} (-OH), other peaks showing the successful synthesis of DES appeared at 2939 cm^{-1}, 2883 cm^{-1}, 1041 cm^{-1} indicating the appearance of CH_3, CH_2, and C-N respectively. Furthermore, the peaks appearing at 1071 cm^{-1}, 1226 cm^{-1}, 1739 cm^{-1}, and 3419 cm^{-1} indicate the presence of oxygen-based functionalities such as C-O-C, C-OH, and C=O stretching vibrations from COOH and O-H, respectively, as presented in **Figure 2**. The peaks appearing at 1645 cm^{-1} indicate the stretching vibrations of C=C existing in the Carbon skeletal network while the weakening of peaks located at 3419 cm^{-1} and 1739 cm^{-1} indicate the presence of O-H and C=O originating from the MGO and MGODES. Also, these same spectra present a peak at 582 cm^{-1} originating from Fe-O and confirming that Fe_3O_4 is present and another peak at 1033 cm^{-1} corresponding to C-N stretching vibration confirms the successful modification of MGO with DES.

Du *et al*., reported the spectra of Fe_3O_4, showing the presence of characteristic band at wavenumber 558, 1660, and 3225 cm^{-1} corresponding to the Fe-O vibration and indicating the presence of the hydroxyl functionalities conjugated on the surface of the Fe_3O_4 NP [140,141], as presented in **Figure 2** (**a-d**). This same characteristic iron band was clearly seen in position and intensity on FTIR spectra of the synthesized DES/GO-Fe_3O_4 nanocomposite implying the successful conjugation of GO and F_3O_4 NP after functionalization in DES reaction media [142-143], as presented in **Figure 2c**. In addition, the synthesized DES/GO-Fe_3O_4 nanohybrids FTIR spectra also indicate the predominant peaks at

wavenumber 947, 1217, 1472, 1696, 3192, and 3349 cm^{-1} originating from C-OH, C-N_+ stretching, scissoring band, CH_2, shifted N-H, N-H stretching of GO and DES as presented in 1b. This also confirms and attests to the utilization of ChCl: Urea DES for the conjugation and coupling of Fe_3O_4 and GO. Researchers have reported and provided clarity for each peak in the FTIR spectra of Fe_3O_4, GO, DES, DES/GO, and DES/GO-Fe_3O_4 nanocompound as presented in **Figure 2b**. The position and intensity of the band at wavenumber 3225 cm^{-1} on the spectra is assigned to O-H stretching vibrations originating from the hydroxyl functionalities [144]. The position and intensity of bands at wavenumber 1039, 1217,1619, and 1724cm^{-1} in the GO spectrum are indications of the presence of stretching vibrations for C=O, C=C, and C-OH and C-O, from carboxylic acid, unoxidized graphitic based nanocomposites functionalities, respectively [144,145]. The FTIR spectrum of ChCl:Urea DES confirms the presence of different visible and characteristic clear bands at wavenumber 787 cm^{-1}, 867 cm^{-1}, 1436 cm^{-1}, 1472 cm^{-1}, 1613 cm^{-1}, 1661 cm^{-1}, and 3323 cm^{-1} indicating the N-H, C-N^+, C-N, CH_2, N-H, C=O and -NH_2 bonds, respectively, the bonds originate from plane bending, scissoring stretching vibration from Urea, and symmetric stretching, vibration bending and stretching vibration from ChCl [140-146], as demonstrated in **Figure 2a**.

FESEM (Field Emission Scanning Electron Microscopy) is a surface imaging technique used to study the morphology of the prepared adsorbent. It generates signals illustrating the atomic composition and surface topography of the sample. However, limitations include the high cost of equipment and the requirement for dry, conductive materials.

XRD (X-ray Diffraction) is used to identify the phase of the sample, distinguishing between crystalline and non-crystalline materials. It determined the material purity and crystallinity of the prepared sorbent. Researchers have reported that from the XRD pattern of DES/GO-Fe_3O_4 nanohybrids, the original characteristic diffraction peaks of GO that were clearly seen
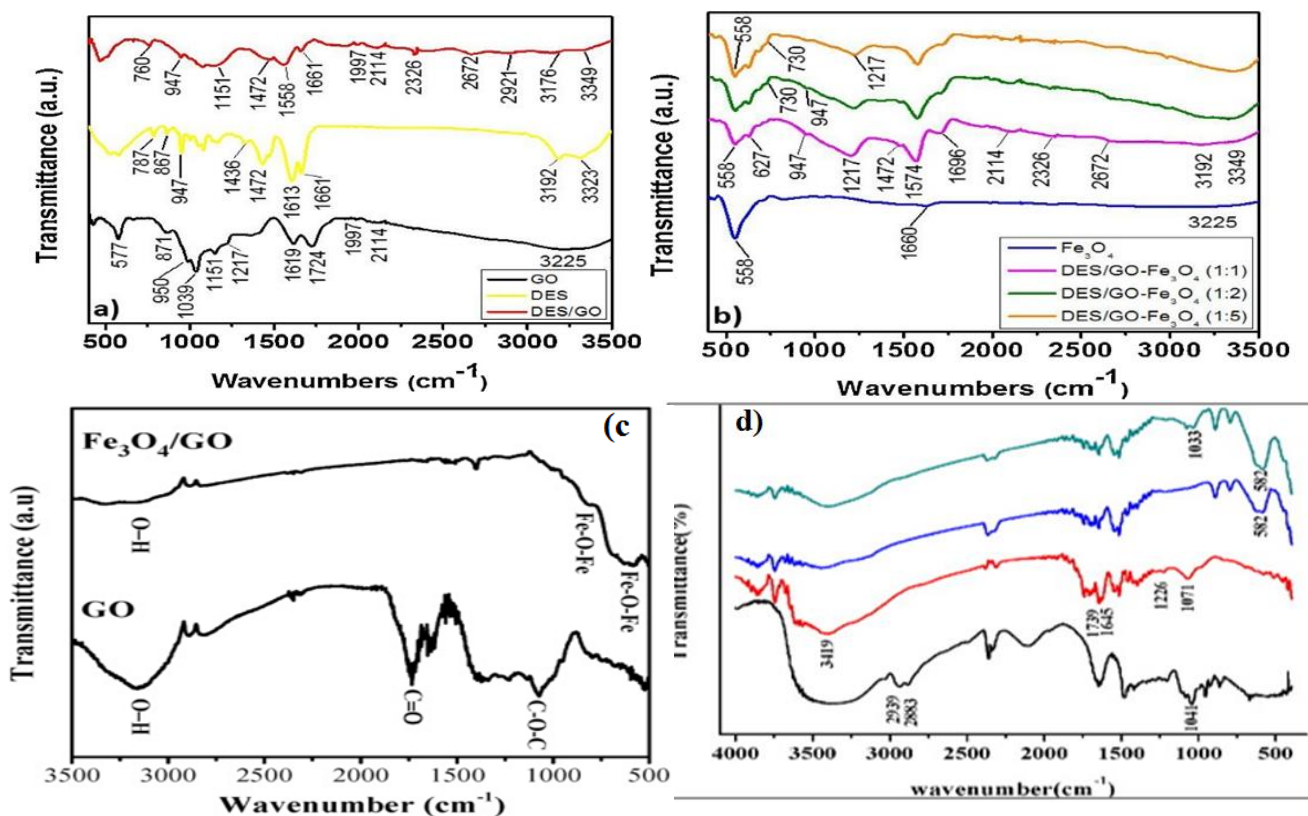
Figure 2. FTIR spectra of (a) DES, (b) GO, (c) MGO, and(d) Fe_3O_4@GO-DES

with intensities and position at (2θ) =10° in the GO samples disappeared in the pattern of DES/GO-Fe_3O_4 nanohybrids, being suppressed by iron nanoparticles. The functionalization of the GO with DES resulted in the shifting of this carbon characteristic peak to (2θ) =26°, confirming the reduction of the GO by DES as attested to by other reported experiments without further application of another reducing agent. Also, the DES/GO sheet agglomeration and restacking arising from the broadened peak (2θ) =26° The NMPs characteristic peaks were clearly seen in their intensities and position at (2θ) =30.4°, 35.7°,43.5°, 53.8°, 57.2°, 63.0°, 71.4°, 74.4°, and 79.1° for Fe_3O_4 NP sample composite. In the same vein, these characteristics' diffraction peaks were also observed and clearly seen in the DES/GO-Fe_3O_4 nanocomposite XRD spectrum, an indication of the successful synthesis, deposition, and conjugation of Fe_3O_4 NP on the GO-based nanocomposite sheets after functionalization with DES, as shown in **Figure 3a**. This confirms

the utilization of DES as a coupling reagent between Fe_3O_4 and GO NP for functionalization and surface modification in synthesizing DES/GO-Fe_3O_4 nanohybrids [147-155]. In another experiment, the XRD spectra pattern of Fe_3O_4@GO-DES shows a significant structural altercation from GO to Fe_3O_4@GO-DES, there was a conglomeration of significant sharp diffraction peak appearing at 10.12° and a wide diffraction vibration peak at 20.98°, as a result of the (0 0 2) plane originating from the GO and short-range order in the graphene layer-stacked sheets, as shown in **Figure 3 (a-c)**. Moreover, several primary diffraction peaks were observed appearing at 30.1°, 35.5°, 43.1°, 53.5°, 57.3° and 62.7 belonging to the (2 2 0), (3 1 1), (4 0 0), (4 2 2), (5 1 1) and (4 4 0) planes respectively for Fe_3O_4@GO and Fe_3O_4@GO-DES. It was also observed that a diffraction peak indicating the presence of GO was clearly sighted at 21.02°, as shown in **Figure 3b**. (a-c). The Fe_3O_4@GO-DES possesses magnetic properties bringing ease of magnetic separation.
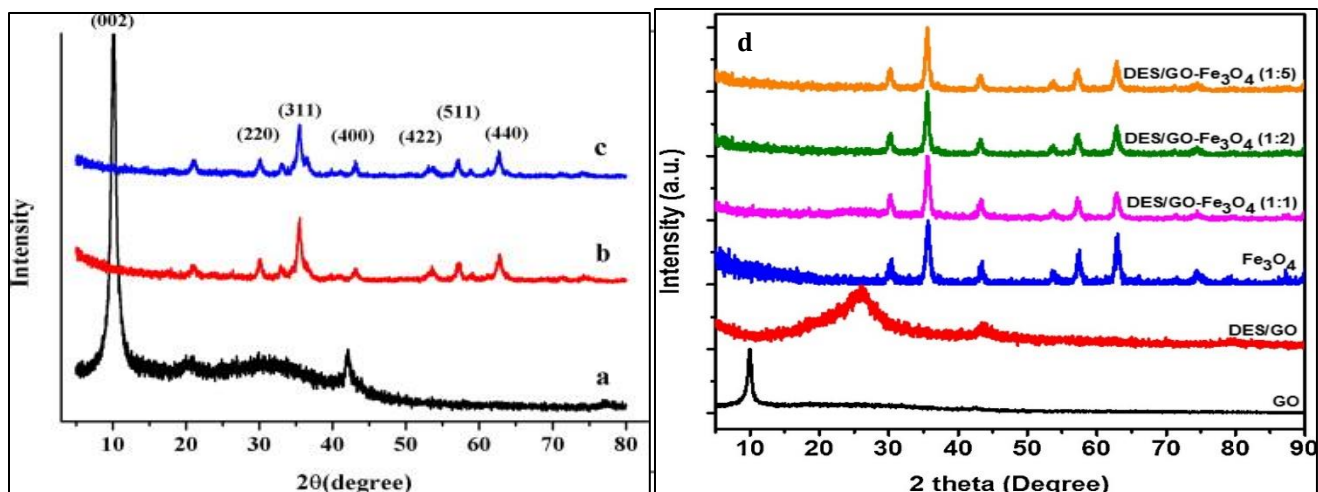
Figure 3. XRD image of (a), GO (b) Fe$_3$O$_4$@G, (c) Fe$_3$O$_4$@GO-DES patterns (d) spectra pattern of GO, DES/GO, Fe$_3$O$_4$, and DES/GO-Fe$_3$O$_4$ at different molar ration 1:1, 1:2, and 1:5[147]

TGA (Thermogravimetric Analysis) is a thermal analysis approach that measures the effects of temperature changes on the mass of the sorbent sample. It provides information on the composition and differential thermal stability of the prepared sorbent. The thermogravimetric analyzer, otherwise known as TGA Thermostep, can be used to evaluate various parameters such as ash, and moisture volatilities at specified pressure and temperature in a single examination. This approach can be utilized for the evaluation of more than 10 samples up to 5 g in mass at a very high-temperature range of 900-1000 °C. In this process, the installation and removal of the crucible lid are crucial and a unique feature that enables the concise evaluation of coal's volatile constituents (Nikitin, 2021). According to Fan *et al.*, MGO-

DES experiences about 2.7- 3.0% weight loss under experimental conditions at a temperature range 150-800 °C, the breaking down of DES occurred resulting to further weight loss of about 11.5%, indicating that the amount of DES conjugated on the basal planes and edges of the surface of the MGO nanoparticles was about 11.5%. This is more when compared to the weight loss exhibited by Fe$_3$O$_4$@GO under the same conditions, thus confirming the presence of the DES on the Fe$_3$O$_4$@GO particulate. Also, the performance, flexural modulus, thermal stability, and composite tensile of epoxy resin were enhanced with suitable addition of GO functionalized with fluorinated diol than that of pristine epoxy [148], as showed in **Figure 4**.
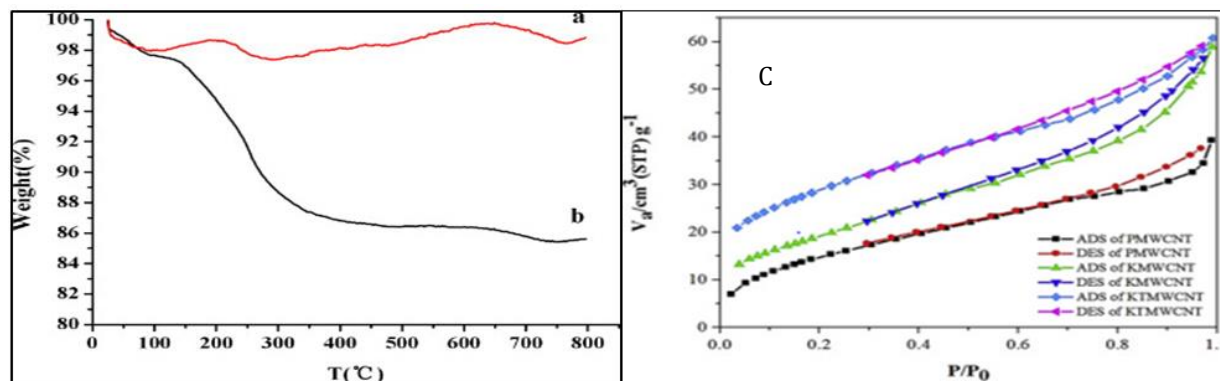
Figure 4. TGA curves of (a) Fe$_3$O$_4$NP@GO, (b) Fe$_3$O$_4$@GO-DES [136], (c) BET surface area of DES-modified and native PMWCNT, KMWCNT, and KTMWCN

Table 6. The BET surface area of some adsorbent, especially maximum surface areas $a_{s,max}$ increasing with each functionalization step

Adsorbent	BET surface area (m^2/g)	Total pore volume (cm^3/g)	Average pore diameter (Å)
PMWCNT	55.672	0.056	
KMWCNT	70.452	0.051	
KTMWCNT	103.18	0.049	
PChCl-CNTs	197.8	1.19	241.28
Pn,n-CNTs	169.7	1.27	300.9
P-CNTs	123.54	0.62	20.49

BET (Brunauer-Emmet-Teller) is utilized to evaluate the specific surface area of the prepared adsorbent, offering insights into its porosity and surface characteristics, using a cross-sectional area (16.3 Å) of nitrogen molecules. Generally, the De Boer method, also known as the t-plot is utilized to determine external surface area and microporous volume. This method involves analyzing the adsorption isotherm at low relative pressure values to distinguish between adsorption into the micropores (pores with a size < Å) and adsorption onto the external surface. A reference curve obtained for a non-porous solid is used for comparison to differentiate these adsorption processes. For example, **Table 6** summarizes the effect of surface area and pore diameter with increase in functionalization with DES. It may also be due to the removal of impurities on the surface of the sorbent by the used DESs.

VSM is used for measuring the magnetic characteristics of materials, specifically focusing on parameters like magnetic susceptibility, magnetization (ferromagnetic, antiferromagnetic, and paramagnetic properties), and magnetic hysteresis loops. Others include ICP-OES (Inductively Coupled Plasma Optical Emission Spectroscopy) which is used to determine elemental compositions of the prepared sorbent. XRF (X-ray Fluorescence) is utilized to assess the elemental compositions and evaluate optimal functionalization conditions. HRTEM (High-Resolution Transmission Electron Microscopy) offers direct imaging of the atomic structure of the sample, aiding in studying properties of sorbent nanomaterials, especially the size and arrangement of the framework network. AFM (Atomic Force Microscopy) is a scanning probe microscopy tool used for imaging surfaces at atomic scales. Energy-dispersive X-ray detector (EDX) combined with SEM enables the simultaneous collection of topographical and crystallographic data. Although, the Energy Dispersive X-ray Analysis (EDX) is a non-destructive technique used to identify the elemental composition of materials, enabling elemental and compositional analysis, elemental mapping of a sample, and image analysis. This approach can provide quantitative, qualitative, semi-quantitative, and spatial distribution of elements through mapping. X-rays are generated when a sample interacts with an electron beam, to assess the quantity of specific elements in the sample as well as its compositional maps. Additionally, EDX is used to measure multi-layer coating thickness of metallic coatings and analyze various alloys. These characterization techniques collectively provide a comprehensive understanding of the m-GO-DES sorbent, enabling optimization for analytical applications.

4.3. OCPs Concentration

The initial concentration of OCPs in the solution can affect removal efficiency. At low concentrations, the adsorption efficiency in MSPE is higher due to increased availability of binding sites on the sorbent material, facilitating a more effective adsorption process. Rapid attainment of equilibrium and saturation at low concentrations is advantageous, ensuring efficient utilization of the sorbent. Mass transfer of OCPs is often more favorable at lower concentrations, aided by a concentration gradient, enhancing movement from the sample matrix to the sorbent. Higher sensitivity at lower concentrations is crucial for accurate

detection in analytical methods, and MSPE's good adsorption efficiency at low concentrations enhances overall sensitivity. Lower initial concentrations pose a challenge to the sensitivity and detection limits of the analytical technique. Generally, higher concentrations might require longer contact times or higher adsorbent dosages.

4.4. pH of the solution

The pH of the solution influences the charge on both the adsorbent and OCP molecules, affecting their interaction. In any extraction experiment, the effect of pH on the sample is critical because it influences the charge and stability on the surface of the adsorbent and the charge on analytes [149]. For analytes with acidic and basic functionalities, the pH of the sample solution alters the available chemical species (*e.g.,* anions, cations, or neutral compounds), thus regulating the diffusion ratio of the target analytes to the binding sites (acceptor phase).

For example, the adsorption of pesticides on modified graphene oxide is greatly affected by the pH of the solution. The oxacyclopropane or oxirane group which is the main active site in all tested pesticides, is strained and easily affected by adjacent substituents acids and bases. In aqueous solution, the oxacyclopropane group maintains a positive charge ion, while the modified graphene oxide surface is negatively charged. Thus, the solution pH affects both the surface charge of the

modified graphene oxide and the degree of polarization of pesticide molecules. As the solution pH increases, the adsorption of pesticides on modified graphene oxide increases. The adsorption is an electrophilic attack of pesticide carbon [C+] on modified graphene oxide surface. In the presence of acid, there are two contrary actions; the first is the catalyzed ring breakage and a true positive charge on the carbon atom according to the following mechanism, as presented in **Scheme 9**.

In a basic solution, the hydroxide (OH) group of the base initiates an attack on the slightly positive carbon, leading to ring opening. This process results in the formation of a negatively charged ionized oxygen, represented as R-O–Na+, as illustrated in the mechanism as presented in **Scheme 10**.

The pH values of the sample solution can affect the dispersion and formation of the sorbent in the aqueous medium. Adsorption efficiency for neutral target compounds can increase with an increase in pH from 2.55 to 6.46 or leach the MNPs, while some low-polarity targeted analytes will be eluted at the optimum pH range of 6.56-7.12 (OCPs), affecting their desorption in the aqueous medium. Other compounds can achieve their optimum extraction efficiency at pH 8, and any pH > pKa may not be favorable. Hence, the optimum experimental pH should be evaluated, adopted, and maintained for subsequent experiments. Optimal pH conditions vary for different adsorbents and OCPs.
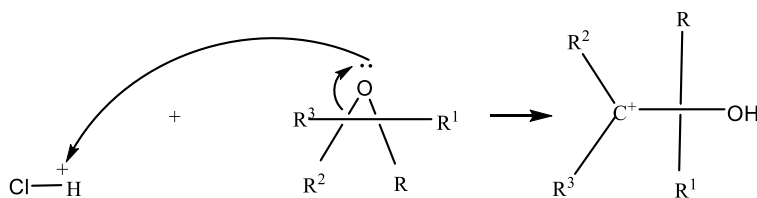
Scheme 9. Effect of pH on pesticide in acidic medium
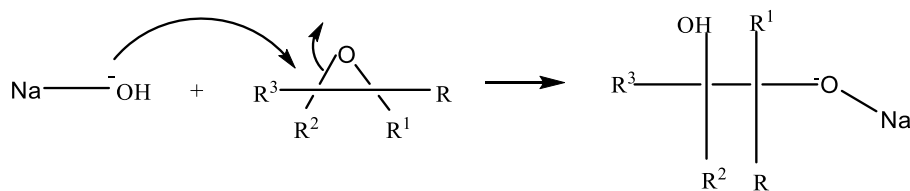
Scheme 10. Effect of pH on pesticide in basic medium

4.5. Temperature

Adsorption processes are often temperature-dependent. An increase in temperature significantly affects the adsorption process as adsorbate molecules are removed from the adsorbent due to the increased kinetic energy of the sorbents. Usually, elevated temperatures can enhance the diffusion rate of the analyte in the liquid sample matrix, while excessively high temperatures may reduce the partition coefficient of the analyte between the sorbent and the water sample [137]. The adsorption capability is adversely affected by temperature, and as the adsorption temperature increases, there is a decrease in adsorption capability. Temperature influences the thermodynamic parameters of adsorption, such as the equilibrium constant and free energy change. The adsorption equilibrium constantly decreases with increasing temperature, indicating a decrease in adsorption affinity. However, the free energy change of adsorption usually becomes more negative with higher temperatures, indicating that the process is more spontaneous. For example, the influence of temperature on the adsorption of OCPs was investigated in the range of 30-70 °C. The adsorption of most pesticides reached the highest value at 40 °C, and when the temperature continued to rise, the peak areas gradually decreased or no longer changed significantly. Thus, changes in temperature can influence the kinetics and thermodynamics of adsorption, impacting removal efficiency. Temperature has a negative effect on adsorption capability, with adsorption capability decreasing as the adsorption temperature increases. Therefore, adsorption is inversely proportional to temperature.

4.6. Contact time and choice of desorption solvent

The duration of contact between the adsorbent and the solution is crucial. Adequate contact time allows for sufficient adsorption, and this factor may vary based on the specific adsorbent and OCP combination. The exposure/contact time between the synthesized sorbent nanomaterial and the aqueous medium should sufficiently ensure the equilibrium of extraction. An increase in contact time enhances the peak area, resulting in increased extraction of the target analyte and improved extraction efficiency. The vortex time is consistently kept under 5 minutes while other variables remain constant. Immediately after reaching the optimum vortexing time, there is no further increase in extraction efficiency, signifying the attainment of extraction equilibrium. Any additional increment in extraction time will not enhance the extraction performance of the sorbent. Instead, there may be a decrease in extraction performance, attributed to the back diffusion of the target analytes [150].

The condition is assessed by fully immersing the sorbent in an appropriate desorption solvent (usually < 300 µL) for a specific duration with the aid of sonication. This process ensures strong elution of the target analytes present in the sorbent's pores. Sonication enhances extraction/desorption efficiency. Various types of green elution solvents, such as methanol, isopropanol, acetone, 1-propanol, acetonitrile, dichloromethane, and mixtures like acetone and acetonitrile, are essential for achieving higher efficiency, preconcentration factors, limits of detection (LOD), and dispersibility of the sorbent for extracting a wide range of pesticides. The LogP of these solvents is crucial for determining polarity, as it can increase the affinity of both hydrophilic and hydrophobic target analytes towards the desorption sorbent more than the sorbent material itself, making it vital to the process. Additionally, more polar solvents are suitable for eluting relatively polar or more polar analyte [150].

4.7. Ionic strength

The presence of ions in the solution can influence adsorption. This is also known as the salting-out effect. The addition of salt (NaCl, 0–5% w/v) with varying concentrations decreases the solubility of target analytes via the salting-out effect in the aqueous medium, thus increasing the extraction efficiency of the targeted analytes (OCPs). The enrichment

factor is based on the affinity of the target analytes (OCPs) with the synthesized extraction sorbent [151].

Conversely, a further increase in salt concentration (>8%) after the optimum concentration will increase the viscosity of the solution and impede the mass transfer of targeted analytes. However, it has also been reported of a decline in analyte recovery with the addition of 5% salt, whereas a remarkable increase was observed at 15% additional salt. This can also affect light and heavy pesticide molecules, especially those with increased aromatic rings and molecular weight. High ionic strength may compete with OCPs for adsorption sites, affecting the overall removal efficiency [151].

4.8. Matrix interference

The composition of the matrix in which OCPs are present can interfere with the adsorption process. The matrix effect must also be investigated because the analytical response of the targeted analytes can be altered by the co-elution and co-extraction of chemicals from the complex environmental matrices [152]. It was also observed that suppression and deterioration from interfering with multiple compounds can affect the ionization capability of the targeted analytes during separation. This can lead to poor limits of detection (LODs) for targeted analytes, rendering the results fallacious. MSPE has overcome several drawbacks associated with conventional extraction approaches, such as selectivity, sensitivity, complexity, and excessive solvent usage. Complex matrices, such as those found in natural waters or wastewater, may require additional treatment or modification of adsorption methods.

4.9. Presence of other ions

The presence of additional ions can significantly impact the adsorption process. Previous studies indicate that certain ions including sodium, potassium, calcium, aluminum, and magnesium, can adversely affect adsorption due to their ionic charges. Researchers have reported that monovalent ions have minimal influence on adsorption, whereas divalent ions attributed to their higher ionic strength, exhibit a notable impact. The pH of the environment plays a crucial role in determining the interaction between competing ions and contaminants. The specific ions hindering the adsorption process are pH-dependent [153]. In another experiments, Phosiri et al. proposed that silica-coated mixed iron hydroxides functionalized with deep eutectic solvent (MIH@SiO2@DES) utilize hydrophobic interaction, hydrogen bonding, and π–π interactions for the extraction of organochlorine pesticides (OCPs) [154].

4.10. Adsorbent regeneration

The ability to regenerate and reuse the adsorbent after every cycle of adsorption experiment is an important practical consideration. Regeneration of spent sorbent is key when considering sustainable industrial scale processes because it reduces overall time, workforce, the cost of production within the laboratory, scientific chemical properties, occupational and environmental hazards. Also, it ensures that sorbents use up their full potential before disposal into the immediate environment. For an ideal sorbent, there is an excellent display of regeneration and desorption potential as well as retaining a high amount of adsorption capacity [155]. This invariably increases the efficiency of sorbent and reduces the cost of the adsorption process. Although, it is evident that various sorbents exhibit different regenerative capabilities based on their compositions and synthetic routes. Hence, regeneration and desorption are critical factors to be evaluated in adsorption toward the significant decline in cost and commercialization of DES-modified magnetic graphene oxide sorbents. Generally, thermal treatment and desorption strategies are employed for the regeneration of sorbents. After adsorption from OCPs, the spent adsorption is separated from the contaminated solution, recycled, and eventually regenerated for the adsorption of these toxic chemicals. There are different conventional methods such

as magnetic and electric field, filed flow fractionation, centrifugation, and cross-flow filtration, which are suitable for separating spent adsorbents from solution. The separated spent adsorbents can be regenerated using different suitable desorption solvents (eluent agents). The choice of desorption solvents to be employed depends on the nature of both the sorbent and absorbate and target analytes (OCPs). Different solvents such as ethanol, methanol, isopropanol, acetone, 1-propanol, acetonitrile, and dichloromethane, including mixtures like acetone and acetonitrile are employed to regenerate the capacity of adsorbents efficiently. In the desorption process, it is crucial to choose solvents that do not react with the chemical functional groups, as well as ensuring the preservation of the adsorbents' texture [156]. The author clearly stated that the solvent used impacts negatively on hysteresis coefficient, emphasizing the need for compatibility and its influence on the reversibility of adsorption. The negative hysteresis was explained to be due to the sequestration of solutes in the organic carbon content and the entrapment of pollutants within the micro and mesopores of the adsorbent [157]. Adsorbents that can be easily regenerated without significant loss of efficiency are preferred.

5. Removal Studies and Adsorption Mechanisms

The removal and adsorption mechanisms of organochlorinated pesticides (OCPs) involve the interaction between the OCPs and adsorbent surfaces, which can be influenced by various physical and chemical properties. Adsorption process takes place via adhesion of particles from liquid phases onto the solid surface of adsorbents with the help of electrostatic attraction [158]. The capability of the adsorption process can be evaluated with the help of percentage removals i.e. RE (%) and sorption capacities i.e. q_m. In general, principal component analysis (PCA) supported the previous statements and affirmed that adsorption of OCPs on mGODES is influenced by different physico-chemical properties. Hence, selecting one key property to explain the

efficiency of OCPs adsorption proved difficult, as the affinity between OCPs and MGODES was found to be the result of a combination of several factors. These critical parameters include the presence of functional groups, strong variations in porosity of sorbent, surface charges, lipophilicity, complexation, ion exchange carbon content and chemical interaction between Metal ion(s) and inherent functional groups on the adsorbent surface to remove the metal ions from any aqueous media [9]. In addition, it is most likely that the degree of competition between different compounds in the environmental matrices for adsorption on sorbent (including OCPs and other matrix compounds), could influence the effective adsorption of OCPs. Also, increasing pH, the functional groups on the surface of the adsorbent gradually become de-protonated and negatively charged, amongst other several mechanisms creating a strong adsorption force resulting into formation of complexes between the metal cations and the anionic surface. Exchanging metal ions such as Ni^{2+} ions with ionized sites of the adsorbent results in adsorption of nickel ions on of sorbents oxidized surface. Therefore, the impact of these properties on the removal of pesticides is studied using various kinetic and isotherm models thus enhancing the understanding of the mechanism involved in removing the OCPs [159].

5.1. Adsorption thermodynamic studies

The relationship between adsorption capabilities and the physical-chemical properties of OCPs has been studied, emphasizing the adsorption kinetic and adsorption isotherm of OCPs. This highlights the importance of understanding the interaction between OCPs and adsorbents for effective removal. During the adsorption process, organochlorine pesticides (OCPs) are rapidly adsorbed onto the surface of mGO-DES due to the presence of numerous vacant surface sites and the heightened affinity of interacting functional moieties in the initial stage of adsorption. Subsequently, a repulsive force between OCP molecules on the solid-liquid phase hinders further occupation of the

remaining vacant surface binding sites. Adsorption reaches equilibrium when the outer surface of the mGO-DES sorbent becomes saturated [160].

The energy interactions between the adsorbent and the contaminant can be explained through thermodynamic modeling, offering insights into whether the mechanisms involved are chemical or physical. A change in enthalpy (ΔH_0) above 40 kJ/mol suggests a high probability of a chemical mechanism, while values below 40 kJ/mol indicate involvement of physical adsorption mechanisms [161]. Physical interactions are known to be weak interactions and prone to dissociation in water elution, but chemical interactions involve strong weak/bases/ionic solvents an indication of low probability of contaminant dissociation. Techniques like FTIR and XRD serve as identification pathways for the mechanistic behavior of adsorbent-sorbate interactions [162]. The feasibility of adsorption processes is evaluated by examining thermodynamic parameters that quantify energetic changes during adsorption using the Van't Hoff equation. These parameters, including standard enthalpy ($\Delta H°$), standard entropy ($\Delta S°$), and Gibbs free energy ($\Delta G°$), are instrumental in indicating the spontaneity of the adsorption mechanism and characterizing whether the adsorption processes are exothermic or endothermic. Over the years, researchers have employed or incorporated inadequate and wrong constants such as distribution coefficient K_d and L/g into the Van't Hoff equation to interpret the thermodynamic mechanism between graphene and Graphene oxide-based sorbents for aqueous sample, waste water, and contaminated waters treatment [163-172] yielding erroneous values, therefore thermodynamic parameters are expressed and calculated by **Equation** (**1-3**). Furthermore, evaluating the principles of chemical equilibrium ameliorate this, also thermodynamic equilibrium constant ought to be derived from isothermal studies.

$$\Delta G° = -RTlnK \tag{1}$$

where K represents the thermodynamic constant , R represent the ideal gas constant (8.314 J·mol⁻¹·K⁻¹), $\Delta G°$ represents Gibbs free energy change, $\Delta H°$ represent the change in standard enthalpy and, $\Delta S°$ represents standard entropy change.

$$lnk_c = \frac{\Delta S°}{R} - \frac{\Delta H°}{RT} \tag{2}$$

$Where, R$ represent gas constant $\left(\frac{8.314J}{K} - mol\right)$, T represents absolute temperature, and k_c represent equilibrium constant (dimensionless).

$$k_c = \frac{1000_{qe}}{C_e} \tag{3}$$

The value of $\Delta G°$ illustrates the spontaneity of the adsorption of the target analyte on the adsorbent, meanwhile, if the value falls between -2- and -80kJ/mol. It implies that both chemisorption and physisorption simultaneously occur in the adsorption process, but if the value range falls between -20 and 0 kJ/mol, it implies that the adsorption process occurred by physisorption only. The values for $\Delta G°$ and $\Delta H°$ were evaluated from the linear plot of ln k_c $against$ $\frac{1}{T}$ from **Equation 3**. If the values of $\Delta S°$ and $\Delta H°$ are positive, it implies the degree of randomness/ unpredictability of the adsorbent/solution interface and the adsorption of the target analyte is endothermic, respectively.

In the adsorption of some pesticides, a negative ΔH_0 implies an exothermic process and in most instances of such adsorption exhibit negative ΔG_0 which indicate the occurrence of spontaneous adsorption. For instance, researchers have reported the thermodynamic modeling of chlorpyrifos on sorbents at varied temperatures revealing a reduction in the rate of adsorption at elevated temperature (295 to 323 K), a negative ΔH_0 and an exothermic reaction [170]. Researchers have also reported adsorption of chlorpyrifos using nanoparticles sorbents by [171]. In this experiment, a ΔS_0 is negative suggests reduced disorder when the contaminant is adsorbed on the sorbent pores. Conversely, a positive ΔS_0 can indicates a higher rate of disorder [172]. Hence, the adsorption mechanism is identified as physical

if the ΔH_0 is less than 40 kJ/mol. Therefore, a negative ΔH_0 signifies favorable adsorption, while ΔS_0 determines whether the reaction is associative or dissociative that is when ΔS^o values is greater than 10 J/mol it is an indication of dissociative behavior while ΔS^o <10 J/mol represents associative behavior.

5.2. Adsorption isotherm and kinetics

A statistical analysis was conducted to identify the most effective isotherm models for describing the majority of adsorption processes involving organic pollutants in wastewater across various clay types. The isotherm model is graphically represented by a curve illustrating the connection between the adsorbate's quantity on the adsorbent, adsorbent, adsorbed species, and the concentration (in the case of liquids) or pressure (of the adsorbate in the case of gases) in a system at a consistent temperature. The shape of adsorption isotherms can vary, and the International Union of Pure and Applied Chemistry (IUPAC) has classified them into six types (I, II, III, IV, V, and VI) based on their characteristics. These different types represent distinct behaviors and can be observed in various adsorption processes [173]. The adsorption isotherm models are represented based on their shape in **Figure 5**.

Type I is a concave model on the x-axis (relative pressure), and it is reversible. This model is found in activated carbon and molecular zeolite [174]. Type II is also reversible, regular, and can be derived from non-porous adsorbents. For example, this adsorption model can be found in the adsorption of Nitrogen on silica gel [175]. Type III is a convex model on the relative pressure axis, and a common example of this model is the adsorption of water vapor on non-porous carbon [176]. Type IV is characterized by its hysteresis loop based on the resultant effect from capillary condensation ensuing in the mesopores of the sorbent and the limiting uptake over a high-pressure range. A typical example of this model is the adsorption of water or humid air on a few selected types of activated carbon [177,178] While, Type V isotherm model as described by literature defers from the type III model by its relatively weak interaction between the adsorbent and the adsorbate [179]. Although, this model is not very common, it does appear in specific porous adsorbent materials. A notable instance involves the adsorption of water on substances like carbon molecular sieve, graphene-based sorbent, or activated carbon fiber. On the other hand, type VI isotherm model is characterized by multilayer and stepwise adsorption processes that take place on a uniform nonporous surface, as represented in **Figure 5** [180]. This particular model is observed in the adsorption of inert gases on the planar surface of graphite.
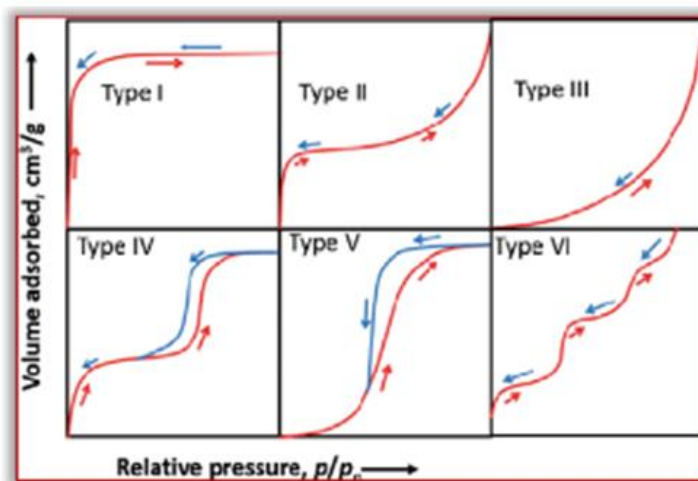
Figure 5. Schematic illustration of the IUPAC classification of adsorption isotherms

Several kinetic models are utilized to describe the interaction mechanism between adsorbent, and adsorbate, providing insights into the rate-determining step and the overall adsorption process. The pseudo-order kinetic model is commonly applied, indicating that chemical mechanisms play a significant role in the rate of adsorption. Specifically, the pseudo-first-order and pseudo-second-order models are frequently employed to elucidate the removal processes of pesticides, such as organochlorine pesticides (OCPs). The application of the pseudo-second-order kinetic model is often grounded in chemisorption, where the rate-limiting step involves valence forces through electron exchange or the sharing of electrons between the sorbate and the sorbent, rather than intramolecular diffusion (as expressed by Equation (20)). In recent studies, adsorption equilibrium data are commonly analyzed using the two-parameter Freundlich and Langmuir isotherm models [101]. The analysis findings revealed that the Langmuir model is predominantly utilized to fit experimental adsorption data, with approximately >80% of adsorption studies employing this model. While, the Freundlich model is the second most commonly applied, with a usage percentage of <60% in adsorption processes. The Freundlich model is applied to describe multilayer adsorption on non-uniform surfaces, emphasizing the effect of physisorption and diverse adsorption mechanisms. Conversely, the Langmuir model is used for finite identical adsorption sites, illustrating the impact of chemisorption on uniform surfaces and elucidating related adsorption mechanisms [181, 182]. The validity of an adsorption system is predicated on the plausibility and functions expressed from fundamental assumptions of the two prominent isotherm models.

Langmuir isotherm linear and nonlinear equations are attainable in **Equations** (**4**, **5**), respectively. Besides, the dimensionless Langmuir's isotherm constant (separation factor) expresses unfavorable adsorption when $R_L > 1$; favorable adsorption when $0 < R_L < 1$; irreversibility when $R_L = 0$; and linearity when $R_L = 1$ for all adsorbent-adsorbate systems as

expressed in **Equation (6)**. In the Langmuir model, if the values obtained for R^2 are higher, it implies that the adsorption process of the analytes of interest involves non-uniform and multilayer surfaces of the adsorbent[183] as shown in **Table 7**. It is factual, that in any adsorbent-adsorbate systems, the values of R will always fall within the range of 0-1 regardless of C_o values. The separation factor R is not a suitable parameter to evaluate the robustness of the adsorbate-adsorbent interaction, the favorability of the sorption process as well as the affinity of the sorbent toward the analyte of interest.

$$\frac{C_t}{q_e} = \frac{1}{q_m K_L}t + \frac{C_e}{q_m} \tag{4}$$

$$q_e = \frac{q_m K_L C_e}{1 + K_L C_e} \tag{5}$$

$$R_L = \frac{1}{1 + K_L C_o} \tag{6}$$

Where, K_L is the Langmuir isotherm constant (L/mg), C_e is the equilibrium concentration of adsorbate (mg/L), q_e is the adsorbed adsorbate per gram of the adsorbent at equilibrium (mg/g), q_{max} is the maximum adsorption capacity (mg/g), and C_o is the initial adsorbate concentration (mg/L).

Freundlich model adopts simultaneous solute adsorption on non-uniform sorbent surfaces, characterized by exponential distribution of sorption energy, as shown in **Table 7**. The Freundlich linear and non-linear model is given in **Equations** (**7**, **8**). An ideal sorbent material must fulfill more than one isotherm model depending on the nature of the sorbent material. Furthermore, if the values obtained for $\frac{1}{n}$ is between 0 and 1, the adsorption process using this model is said to be favorable. If the value is less than 1, it suggests the availability of multilayer and heterogeneous adsorption systems.

$$q_e = K_f C_e^{1/n} \tag{7}$$

$$\log q_e = \log K_f + \frac{1}{n}\log C_e \tag{8}$$

Where, q_e is the adsorption capacity or adsorbed adsorbate per gram at equilibrium (mg/g), K_f is Freundlich isothermal constant, and n is the intensity.

The Temkin isotherm model is built on strong electrostatic interactions and can be expressed in **Equation** (**9**) as:

$$q_e = \beta \ln K_T + \beta \ln C_e \tag{9}$$

Where, β comprises of $\frac{RT}{b_T} * K_T$ and K_T is the Temkin isotherm constant linked to the heat of adsorption and equilibrium binding energy.

The Temkin isotherm model examined how the concentration of the adsorbate alters the adsorption process when it is too low or too high. More also, the adsorbent active binding sites allow more adsorbate due to increased adsorbent-adsorbate interaction. Thus, the Temkin kinetic model proposes that all sorbents' active binding sites have uniform energies, so the Temkin constant (b_T) describes the variation of adsorption energy, and states whether the adsorption is endo-($b_T < 1$) or exothermic ($b_T > 1$).

The Dubinin-Radushkevich isotherm model (D-R) is employed to ascertain the nature of the adsorption process as either physisorption or chemisorption, as shown in **Table 7**. This can be expressed by **Equations** (**10**) and (**14**):

$$ln\, q_e = \ln q_m - \beta E^2 \tag{10}$$

Where, q_e is the adsorption capacity (mg/g), β is the adsorption energy constant, T is the temperature (K), R is the universal gas constant and, ε is the Polanyi potential, as expressed in **Equation** (**11**) is related to equilibrium concentration.

$$\varepsilon = RTln\left(\frac{C_s}{C}\right) \tag{11}$$

An adsorption process is said to be chemical adsorption (chemisorption) if the E_{cal} value ranges from 8-16 kJ/mol), while, the adsorption process is said to be Physisorption if the E_{cal} is less than 8 kJ/mol [184]

Also, The Dubinin-Radushkevich isotherm model is based on the adsorption potential

theory, as expressed I **Equation** (**12**). It assumes that the adsorption process is more linked to micropore volume filling than the multilayer (layer-layer) sorption experienced on the pore walls [185].

$$q_e = q_m e^{(\beta.\varepsilon^2)} \tag{12}$$

Where, C_s is the saturation concentration (mg/L), C is the bulk liquid concentration (mg/L), β is the Dubinin–Radushkevich isotherm constant (mol².kJ⁻². The value of β can be calculated as mean energy of sorption (E) according to **Equation** (**13**):

$$\varepsilon = RTln\left(1 + \frac{1}{C_e}\right)$$
$$E = \frac{1}{\sqrt{2\beta}} \tag{13}$$

The Halsey isotherm model is utilized to describe the layer-layer adsorption process [186], as expressed by **Equation** (**14**):

$$ln\, q_e = \left[\frac{1}{n}\ln K_H\right] - \frac{1}{n}\ln C_e \tag{14}$$

Where q_e is the adsorption capacity (mg/g), C_e is the equilibrium concentration and K_H is the Halsey isotherm model constant.

The plot of the linear graph of $ln\, q_e$ against $ln\, C_e$ reflects the degree of heteroporosity of the sorbents developed. The n value indicates whether the adsorption process is favorable, if it falls between 1 and 10, while, it is said to be a poor adsorption process if the n value is less than 1 [187].

The Toth isotherm model is a three-parameter equation utilized to describe the adsorption process on heterogenous surfaces as expressed by Equation 15. This empirical Langmuir-modified model is a monotonically enhanced expression that correctly several sub-monolayer systems; can be used to calculate excess adsorption [188]. In addition, the model overcomes the drawbacks of high and low ends pressure of Sips and Freundlich isotherms and is expressed as follows:

$$q_e = \frac{q_m C_e}{\left(\frac{1}{K_T} + C_t{}^{n_T}\right)^{\frac{1}{n_T}}} \tag{15}$$

Where, q_e is the adsorption capacity (mg/g), C_e is the equilibrium concentration, K_T is the Toth isotherm model constant (mgg^{-1}) and n_T is the Toth isotherm constant (mgg^{-1}).

When n = 1, the toth equation is reduced to Langmuir isotherm equation, hence, n characterizes the heterogeneity of the adsorption process. it can also be expressed in linear form as expressed in **Equation** (**16**):

$$\ln \frac{q_e^n}{q_m^n - q_e^n} = nlnK_L + nln\,C_e \qquad (16)$$

The Khan isotherm model is a three-parameter isotherm utilized for the adsorption of bi-adsorbate from pure dilute equation solutions, as shown in **Table 7**. Researchers have also used a non-linear approach to obtain this isotherm model. The khan isotherm is given by **Equation** (**17**):

$$q_e = \frac{q_{max}b_k C_e}{(1 + b_K C_e)^{a_K}} \qquad (17)$$

Where, q_e is the adsorption capacity (mg/g), q_{max} is the
Khan isotherm max adsorption capacity (mg/g), C_e is the equilibrium concentration and b_K is the Khan isotherm model constant (mg/g^{-1}) and a_K

Redlich-Peterson isotherm model is an empirical mix of Freundlich and Langmuir isotherms, hence the adsorption mechanism does not follow ideal monolayer adsorption, as shown in **Table 7**. The model is defined by the **Equation** (**18**):

$$q_e = \frac{K_{RP}C_e}{1 + a_{RP}C_e^t} = \ln\left(k_R \frac{C_e}{q_e} - 1\right) = g\ln C_e + ln\,a_R \qquad (18)$$

Where, q_e is the adsorption capacity (mg/g), C_e is the equilibrium concentration, K_{RP} is the R-P isotherm model constant (L/g^{-1}) and a_{RP} (mg/L), and g is dimensionless; lies between 0 and 1.

Sips isotherm model is a combination of Freundlich and Langmuir isotherms, capable of predicting adsorption on majorly heterogenous surfaces, thus eliminating the Freundlich drawback of increased adsorbent concentration; and expressed in **Equations** (**19-21**). This Sips isotherm depends on pH, concentration, and temperature. It also differs by non-linear and linear regression.

$$q_{e=}\left(\frac{q_e}{q_{max} - q_e}\right) = \frac{1}{n}\ln C_e + \ln k_S \qquad (19)$$

$$q_{e=}\frac{K_S C_e^{\beta s}}{1 - a_S C_e^{\beta s}} \qquad (20)$$

The linearized form is expressed as follows:

$$\beta_s \ln C_e = -\ln\left(\frac{K_S}{q_e}\right) + \ln(a_s) \qquad (21)$$

Where, q_e is the adsorption capacity (mg/g), C_e is the equilibrium concentration, K_s is the Sips isotherm model constant (Lg^{-1}), a_s is the Sips isotherm model constant (Lg^{-1}), and β_s is the Sips isotherm exponent.

The adsorption kinetic models are postulated to give information on the rate-determining step and the reaction mechanism, these models also help to determine the adsorption rate and equilibrium time. Also, they are used to determine the relationship and dependence of the adsorption capacity of the target analyte (adsorbate) relative to the adsorption time. In addition, they are employed to evaluate the rate and efficiency of the adsorption process [189-200].

To determine the suitability of an adsorption model to designated adsorption kinetics, the regularized standard deviation value (%) and relative error (%) are employed, as expressed in **Equations** (**22**) and (**23**).

$$\Delta q(\%) = \sqrt{\frac{((q_{exp} - q_{cal})/q_{exp})^2}{N-1}} * 100 \qquad (22)$$

$$Relative\ error\ (\%) = 100\left(\frac{q_{exp} - q_{cal}}{q_{exp}}\right) \qquad (23)$$

Where N is the number of data points, q_{exp} is the experimental adsorption capacity, (mg/g) and q_{cal} is the calculated adsorption capacity (mg/g).

Theoretically, the model is said to be suitable if the relative error and standard deviation values are lower [85].

Table 7. Adsorption process parameters for DES-functionalized graphene oxide nanomaterials used to remove/degrade different pollutants

Sorbent	Target analytes	Isotherm	Kinetics	q_{max} (mg/g)	Ref.
Magnetic ionic liquid/chitosan/graphene oxide	Cr(VI)	Langmuir	Pseudo second order	143.5	[201]
Graphene sheet with ferroferric oxide	Cd(II) Hg (II), Ni (II), Cr (VI) and Pb (II)	Freundlich	Pseudo second order	17.29-27.95	
NRG	2-MAQ	Freundlich		9.29	[202]
Magnetic graphene oxide	Cd(II)	Langmuir	Pseudo second order	51.55	[203]
RGO-βCD-ECH CS-PANI@GO RGO	2-CP phenol	Langmuir	Pseudo second order	674.155 602.41, 198.254	[204]
GO-Fe$_3$O$_4$/PRd	β-napthol, phenol	Freundlich	Pseudo second order	226.2 191	[205]
Magnetic graphene dolomite (DMG)	OCPs (DDT, DDE, DDD, Methoxychlor	Langmuir, Temkin, and Freundlich isotherms	Pseudo second order	10.06, 10.95, 10.64, and 10.22	[206]
Few-layered graphene nanosheets (GNs)	Chlorophenoxyacetic acid herbicides,	Langmuir adsorption isotherm	Pseudo-second-order		[207]

Table 7. Continued

Sorbent	Target analytes	Isotherm	Kinetics	q$_{max}$ (mg/g)	Ref.
GO	Naproxen	Langmuir, and Freundlich isotherms	pseudo-first-order and pseudo-second-order	196.01 19.09	[208]
THS-DES@M-GO	Mercury	Langmuir, and Freundlich isotherms	pseudo-second-order kinetic	215.1	[7]
ZMG-BA, ZMG-FA, and ZMG-PA	ephedrine (EPH), ketamine (KET), norketamine (NKET), and (AMP),	Langmuir, Freundlich, Temkin, and Dubinin-Radushkevich isotherm models	pseudo-second-order kinetic	732.110, 564.618, 636.518, 489.913 μg·g−1	[209]
EgLiCl-mGO	Indigotin blue dye (IBD), Pb(II) and Cd(II)	Langmuir isotherm	pseudo-second-order	95.4,111.11, 67.46 and 88.49	[210]
GO-IL	Sulfamethoxazole (SMZ), Carbamazepine (CBZ), and Ketoprofen (KET)	Freundlich, Redlich–Peterson, and Freundlich	second-order, Pseudo-first-order and Weber-Morris intraparticle diffusion	137.7, 11.2, 13.25, 14.8, and 14.5	[211]
GO@Fe$_3$O$_4$-DES FF	Ofloxacin (OFL) and sparfloxacin (SPR)	Freundlich and Halsey > Temkin > Dubinin-Radushkevich > Langmuir	pseudo second-order		[212]
reduced graphene oxide/ZIF-67 (MGZ) (LA/MGZ,	Methamphetamine (MAMP)	Langmuir, Freundlich models(b) and Dubinin-Radushkevich (D-R) model	pseudo-second-order model	674.490 2122.304 1550.220 1777.246	[213]

ABBREVIATIONS

THS: Ternary hydrosulphonyl-based DES;ZMG: magnetic GO/ZIF-67; LA:choline chloride-Levulinic acid (LA); UR:choline chloride-Urea (UR); EG- choline chloride-Ethylene glycol (EG);FF:ferrofluid (choline chloride-ethylene glycol DES; PA: choline chloride -Phenethyl Alcohol); BA:choline chloride -Butyric acid); FA- choline chloride -Formic Acid);UT: urea and tetramethylammonium chloride DES;AGO: amino-functionalized graphene oxide (AGO) aerogels; mGO:magnetic graphene oxide

The Elovich kinetic model is based on chemical adsorption and can be expressed and calculated by **Equation (24)**

$$q_t = \frac{1}{\beta}\ln(\alpha\beta) + \frac{1}{\beta}\ln t \qquad (24)$$

Where, α *repersent the adsorption rate*, β represents the activation energy and q_t represents the binding capacity.

The rate of diffusion at the early adsorption stage is calculated by the intraparticle diffusion kinetic model and expressed by **Equation (25)**

$$q_t = Kt^{\frac{1}{2}} + c \qquad (25)$$

Where, K represent the intraparticle diffusion rate constant, t represent constant time and, c is the intercept.
In theory, K is directly proportional to the thickness of boundary layers. The process of adsorption obeys the intraparticle diffusion if the $R^2 = 1$. Furthermore, if the intercept of the linear graph passes through the origin, the intraparticle diffusion of the target analytes (adsorbate) adsorption onto the adsorbent nanoparticles may be said to have obeyed the early stage of the adsorption process.

The external diffusion kinetic model is calculated by **Equation (26)**:
$$\ln\frac{C_t}{C_o} = -k_{ext}t \qquad (26)$$
Where,
C_t *represent the concentration of solute* in a liquid phase, t is the reaction time and, k_{ext} illustrates the diffusion rate constant. The intercepts for the linear graph may not pass through the origin which implies that the adsorption process involves external diffusion, although it may not be the rate-determining step.

BET isotherm model is calculated by **Equation (27)**:
$$\frac{x}{Q(1-x)} = \frac{1}{Q_m C} + \frac{c-1}{Q_m C} \qquad (27)$$
Where, relative pressure x= $\left(\frac{P}{P_o}\right)$, Q: amount of adsorbed adsorbate at x, Q_m: quantity of adsorbate required for monolayer coverage of

adsorbent and c: equilibrium constant for first adsorption layer.
Dual Langmuir model is calculated by **Equation (28)**:

$$q_e = \frac{q_{m,1}K_{L,1}C_{e,1}}{1+K_{L,1}C_{e,1}} + \frac{q_{m,2}K_{L,2}C_{e,2}}{1+K_{L,2}C_{e,2}}, \qquad (28)$$

Where, q_e: equilibrium capacity, $q_{m,1}, q_{m,2}$: maximum adsorption from two Langmuir models, $K_{L,2}, K_{L,1}$: Dual Langmuir constant, and C_e: equilibrium concentration.

Linear isotherms model is calculated by **Equation (29)**:

$$C_s = K_p\, C_e, \qquad (29)$$
$C_s = saturtion\ concentration\ (mg/L)$,

C_e: Equilibrum concentration (mg/L) and K_p Partition coefficient.

5.3. Reproductive risk assessment of Organochlorine Pesticide

The estimation of the mean daily intake (MDI) for Organochlorine Pesticide (OCP) residues involves the characterization of health hazard quotients (HQ) and hazard index (HI). It is crucial to highlight that, environmental matrices bee-derived products (such as like propolis, honey, honeybees, beeswax, royal jelly) serve not only as food but also as raw or intermediate materials for natural medications, supplements, additives, and in the preparation of cosmetics and pharmaceuticals. Thus, contribute to distinct pathways of human exposure to pesticide residues [202].

Estimation of the Mean Daily Intake (MDI) of Organochlorine Pesticide (OCP) residues.
The Mean Daily Intake (MDI) of Organochlorine Pesticide (OCP) residues in environmental samples was calculated using **Equation (30)**.
$$\text{MDI} = \frac{PS \times Q}{BW} \qquad (30)$$

Where, PS is the average concentration of OCP residues in environmental samples expressed in μg/kg, QQ is the amount of Environmental sample consumed by a person, and BW is the consumer's body weight. For example, based on the recommendations by the Food and

Agriculture Organization/World Health Organization (FAO/WHO), the average daily honey consumption is said to be 50 g of per person per day for adults, and 9-11 g per person per day for children [203,204]. This approach will help to quantify the potential exposure to OCP residues through honey consumption for different age groups.

5.3.1. Evaluation of the health hazard quotient (HQ) and the hazard index (HI)

The hazard quotient (HQ) can be determined using **Equation** (**31**):

$$HQ = \frac{MDI}{ARfD} \qquad (31)$$

Where, ARfD represents the acute reference dose of Organochlorine pesticides (OCP) residue, expressed in µg/kg/day [203]. It the concentrations of OCPS residues surpasses the ARfD is it deemed hazardous upon chronic exposure. The HQs are individually calculated for each pesticide congeners, while the summing up the individual HQs is estimated by Hazard Index (HI). Thus, HI is given [205] in **Equation** (**32**), thus providing a comprehensive assessment of the cumulative health risk associated with the exposure to multiple OCPs.

$$HI = HQ_1 + HQ_2 + HQ_3 + HQ_4 + HQ_5 \dots + HQ_n \qquad (32)$$

The calculated HI values greater than or equal to 1 indicate additive effects and high risk, while HI values less than 1 suggest low or negligible risks.

5.3.2. Human reproductive toxicity associated with pesticide residues "hang over" effect

Human reproductive toxicity associated with pesticide residues refers to the adverse effects these chemical substances may have on human reproductive health. Reproductive toxicity can manifest in various ways, affecting both male and female reproductive functions causing developmental toxicity in future generations.

Potential effects of pesticide residues on human reproductive health may include:

a. *Reproductive toxicity in woman such as fertility Issues:* Exposure to organochlorine (OCPs) insecticides has been linked to reduced fertility in women. It may affect ovulation, overall fertility rates, increasing serum levels of follicle-stimulating hormone and luteinizing hormones. Exposure to 2,4- dichlorophenoxy acetic acid (2,4-D) have also been linked to spontaneous abortion in women. In another study, a significant association between prostate cancer risk and exposure to DDT and lindane was discovered and reported for males with an odds ratio (OR) of 1.68 (95% CI: 1.04–2.70) for high exposure to DDT and an OR of 2.02 (95% CI: 1.15–3.55) for high exposure to lindane. Additionally, high serum levels of p,p′-DDE (mean: 13,700 ng/g lipid, 95% CI: 7000–26,800) in males were significantly linked to prostate cancer risks [206].

b. *Developmental effects:* Exposure to certain pesticides during pregnancy may lead to developmental issues in the fetus. This can include birth defects, low birth weight, and other adverse outcomes.

c. *Hormonal disruption:* Pesticides may interfere with the endocrine system, disrupting hormonal balance. This disruption can have implications for reproductive functions, including menstrual cycles and sperm production. This disruption to oxidative stress in various organisms has also been reported to be another side effect of pesticide residues (DDT, cyhalothrin, profenofos, imidacloprid, cypermethrin, diazinon, dimethoate, endosulfan, glyphosate, hexachlorocyclohexane, 2,4-dichlorophenoxyacetic acid, and zineb. Oxidative stress is characterized by an imbalance between reactive oxygen species (ROS) and the biological system's ability to counteract them, which can lead to damage in cellular components [207] Other residue (α endosulfan, β endosulfan and endosulfan sulfate)) can cause imbalances in sex sterol hormone synthesis, decreased antioxidant activities, induce testicular toxicity, testicular oxidative stress, sperm DNA fragmentation, imbalance in sex sterol hormone synthesis,

d. increase malondialdehyde content, increased lipid peroxidation and severe histopathological alterations in animals [208].

e. *Miscarriages and stillbirths:* Some studies suggest an association between pesticide exposure and an increased risk of miscarriages and stillbirths. Numerous studies have highlighted a substantial association between increased serum levels of DDE, DDD, and lindane and spontaneous abortion in women [209]. others have reposted that exposure to Endosulfan have resulted to endometrial degeneration, increased calcium ion levels leading to spontaneous abortions, disruption of normal muscular rhythm, causing infertility and reduced menstrual cycle.

f. *Genetic damage:* Pesticides may cause genetic mutations, potentially leading to hereditary health issues in offspring. The exposure to certain pesticides has been associated with adverse effects on spermatozoa and tubular differentiation. For instance, chlorpyrifos has been reported to induce immature sperm and DNA damage in sperm cells [210]. Similarly, cypermethrin exposure has been linked to necrosis, degeneration, decreased numbers of spermatogenic cells in some seminiferous tubules, and congested blood vessels in rat testes [211]. They can also stimulate spermatogonial germ cell apoptosis.

g. *Endocrine disruption:* Pesticides may act as endocrine disruptors, mimicking or blocking the effects of hormones in the body. This can result in reproductive disorders and disruptions to normal sexual development. Increasing evidence from human epidemiological studies has established significant associations between endometriosis and exposure to organochlorine chemicals. This endometriosis is a gynecological disease characterized by the presence of ectopic endometrial tissue, affecting lives, fertility, and healthcare of women in their reproductive years and having a significant impact on their healthcare costs [212].

h. *Neurological effects:* Pesticide exposure may also have neurological effects, potentially impacting the development of the nervous system in utero.

i. *Reproductive toxicity in man:* Although there are limited experimental studies existing on reproductive toxicity among humans, several epidemiological studies have been assessed to understand the effects of pesticides on various reproductive parameters. Currently, critical human exposure to pesticides may occur at the workplace, household, by accident and through the ambient environment. In rats, researchers have reported an observed increase in degenerate germ cells within the seminiferous tubules, indicating a deleterious effect on steroidogenesis, spermatogenesis and ultimately a complete failure of the sexual process. such pesticides include, carbendazim [213], carbofuran, chlorpyrifos, endosulfan [210].

i. Semen quality: The studies have revealed various adverse effects on male reproductive health, including reduced sperm concentration, motility, volume, total sperm count, and semen quality. Additionally, chronic occupational exposure to organophosphate, glyphosate, and carbamate pesticides was associated with damage to sperm chromatin, DNA fragmentation, and increased sperm DNA damage. Exposure to different organochlorine and pyrethroid pesticides also led to a deterioration in semen quality, lowered sperm count, and decreased semen volume and pH [214]

ii. Effect on testosterone: Studies have revealed various adverse effects on pesticides has linked to a decrease in testosterone levels in male reproductive health, resulting to alterations in follicle-stimulating hormone, reproductive hormone levels, prolactin, total testosterone, luteinizing hormone, free thyroxine. and thyroid-stimulating hormone, Additionally, these studies evaluated the deleterious effect of organochlorines (OCPs) insecticides, including γ- and δ-isomers of hexachlorocyclohexane (HCH), o,p′-DDT and p,p′-DDT isomers of dichlorodiphenyl-trichloroethane (DDT), its p,p′-DDE derivative, dieldrin, methoxychlor, chlorpyrifos acetamiprid[215], diazinon, permethrin, dimethoate [216], esfenvalerate, cypermethrin [217], and endosulfan [218] in relation with inhibition of testosterone biosynthesis in contaminated animals. Others have also reported that the exposure to

organochlorine pesticides can alter male hormone levels, including testosterone and estradiol [214].

It is important to note that the severity and nature of reproductive toxicity depend on factors such as the type of pesticide, the level and duration of exposure, and individual susceptibility. Regulatory agencies worldwide establish acceptable limits for pesticide residues in food and water to mitigate potential health risks. Regular monitoring and assessment of these residues help ensure that exposure levels remain within safe limits. Pregnant women are often advised to minimize exposure to pesticides and consume a diet with low pesticide residues to safeguard the health of both themselves, and their unborn children.

6. Conclusion

Unconventional agricultural practices, industrialization, and human activities have contributed to the emergence of pollutants (OCPs) that contaminate various environmental matrices (food, water, and soil), posing risks to the environment, biodiversity, and human health. Although numerous treatment processes exist for preconcentration, pretreatment, and degradation of these contaminants, each method has its inherent limitations and drawbacks. In recent times, a graphene-based approach has been utilized to address the drawbacks of other treatment methods towards developing new methods compatible with the principles of green analytical chemistry. This review discusses the properties, classification, synthesis, and functionalization methods to enhance their physical and chemical properties such as porosity, pore size, thermal stability, and chemical stability. In addition, this review paper focuses on the removal of OCPs pollutants from aqueous samples using DES-modified graphene oxide-based adsorbents, as well as emphases on the various isotherm models for maximum sorption capacity. Also, a comparative study of the removal mechanism of OCPs based on DES-modified graphene-based sorbents compared to conventional

approaches is presented. This low-cost, non-toxic DES-modified magnetic graphene oxide has shown good regeneration of the adsorbent, high enrichment factors, and ease of modification to allow different interactions with the OCPs in solid-phase extraction (SPE). Moreover, the interactive mechanism, regeneration, and reusability studies, adsorption kinetic and thermodynamic analysis between DES-modified graphene oxide-based adsorbents and adsorbate as well as the sorbent regeneration ability which suggests they can be effectively exploited effectiveness without any significant potential reduction, were also reviewed based on recently published work. This review also suggests that the DES functionalized magnetic graphene oxide is the best sorbent with excellent potential compared to other carbonaceous nanosorbent materials for the OCPs removal because of vigorous interactions mechanisms including hydrogen bonding, electrostatic interaction, hydrophobic interactions, electron donor-acceptor, π-π, and Van der Waals interaction. The impact of the modification also influences the selectivity, specificity, and efficiency of the sorbents, thereby increasing the versatility of their application in various fields and matrices. Also, the review outcome suggests possible degradation pathways for OCPs and shows encouraging prospects and the best fit for kinetic models; adsorption-desorption studies, competitive adsorption, and thermodynamic modeling were also explored. Moreover, we have identified more précised indicators for sorbate-sorbent adsorption process, thus reshaping future adsorption systems since adsorption stands out as a highly effective method for addressing pollutants in aqueous environments. Although, adsorption studies of pesticides using demonstrated fitting with pseudo-second-order kinetic models, Langmuir and Freundlich isotherms, other isotherms should also be employed to verify and completely understand the physisorption and chemisorption of the process. Data obtained from the kinetic profile, sorption behavior, reusability and magnetic properties are valuable insights for enhancing, implementing, and designing an effective clean-up for water treatment towards targeted

analytes. Meanwhile, challenges in the treatment of contaminated water and aqueous sample, and adsorbent ecotoxicity were also identified. Finally, further studies towards largescale commercialized production of this novel DES-modified magnetic graphene-based sorbent for the treatment of pollutants from real, contaminated aqueous samples should be explored, especially spent-sorbent disposal after multiple regeneration cycles. Priority should be given to reusable and biodegradable materials to design more novel analytical methods, to reduce the environmental impact of analytical procedures, sensitivity of methods, and enhancing precision of the methods for determining and monitoring OCPs. This will efficiently impact the analytical methodologies and uphold principles of green analytical chemistry and ensure public safety.

Disclosure Statement

No potential conflict of interest was reported by the authors.

Acknowledgments

Orcids

Aduloju Emmanuel Ibukun
https://orcid.org/0009-0009-5468-6283

References

[1]. A. Abdelfattah, S.S. Ali, H. Ramadan, E.I. El-Aswar, R. Eltawab, S.-H. Ho, T. Elsamahy, S. Li, M.M. El-Sheekh, M. Schagerl, Microalgae-based wastewater treatment: Mechanisms, challenges, recent advances, and future prospects, *Environmental Science and Ecotechnology*, **2023**, *13*, 100205. [Crossref], [Google Scholar], [Publisher]

[2]. A. Abdelfattah, M.A. Dar, H. Ramadan, E.I. El-Aswar, R. Eltawab, E. Abdelkarim, T. Elsamahy, M. Kornaros, S.S. Ali, L. Cheng, Exploring the potential of algae in the mitigation of plastic pollution in aquatic environments, Handbook of research on algae as a sustainable solution for food, energy, and the environment, *IGI Global*, **2022**, 501-523. [Crossref], [Google Scholar], [Publisher]

[3]. A. Mostafa, H. Shaaban, A. Alqarni, R. Al-Ansari, A. Alrashidi, F. Al-Sultan, M. Alsulaiman, F. Alsaif, O. Aga, Multi-class determination of pharmaceuticals as emerging contaminants in wastewater from Eastern Province, Saudi Arabia using eco-friendly SPE-UHPLC-MS/MS: occurrence, removal and environmental risk assessment, *Microchemical Journal*, **2023**, *187*, 108453. [Crossref], [Google Scholar], [Publisher]

[4]. M. Eddleston, Poisoning by pesticides, *Medicine*, **2024**, *48*, 214-217. [Crossref], [Google Scholar], [Publisher]

[5]. Y. Jia, Y. Wang, M. Yan, Q. Wang, H. Xu, X. Wang, H. Zhou, Y. Hao, M. Wang, Fabrication of iron oxide@ MOF-808 as a sorbent for magnetic solid phase extraction of benzoylurea insecticides in tea beverages and juice samples, *Journal of Chromatography A*, **2020**, *1615*, 460766. [Crossref], [Google Scholar], [Publisher]

[6]. X.O. Almirall, N.S. Yagüe, R. Gonzalez-Olmos, J. Díaz-Ferrero, Photochemical degradation of persistent organic pollutants (PCDD/FS, PCBS, PBDES, DDTS and HCB) in hexane and fish oil, *Chemosphere*, **2022**, *301*, 134587. [Crossref], [Google Scholar], [Publisher]

[7]. B. Kakavandi, S. Alavi, F. Ghanbari, M. Ahmadi, Bisphenol A degradation by peroxymonosulfate photo-activation coupled with carbon-based cobalt ferrite nanocomposite: performance, upgrading synergy and mechanistic pathway, *Chemosphere*, **2022**, *287*, 132024. [Crossref], [Google Scholar], [Publisher]

[8]. I.A. Saleh, N. Zouari, M.A. Al-Ghouti, Removal of pesticides from water and wastewater: Chemical, physical and biological treatment approaches, *Environmental*

Technology & Innovation, **2020**, *19*, 101026. [Crossref], [Google Scholar], [Publisher]

[9]. J. Chen, Y. Wang, X. Wei, P. Xu, W. Xu, R. Ni, J. Meng, Magnetic solid-phase extraction for the removal of mercury from water with ternary hydrosulphonyl-based deep eutectic solvent modified magnetic graphene oxide, *Talanta*, **2018**, *188*, 454-462. [Crossref], [Google Scholar], [Publisher]

[10]. X. Pan, F. Dong, J. Xu, X. Liu, Z. Chen, Y. Zheng, Stereoselective analysis of novel chiral fungicide pyrisoxazole in cucumber, tomato and soil under different application methods with supercritical fluid chromatography/tandem mass spectrometry, *Journal of Hazardous Materials*, **2016**, *311*, 115-124. [Crossref], [Google Scholar], [Publisher]

[11]. G.K. Sidhu, S. Singh, V. Kumar, D.S. Dhanjal, S. Datta, J. Singh, Toxicity, monitoring and biodegradation of organophosphate pesticides: a review, *Critical Reviews in Environmental Science and Technology*, **2019**, *49*, 1135-1187. [Crossref], [Google Scholar], [Publisher]

[12]. E. Morillo, J. Villaverde, Advanced technologies for the remediation of pesticide-contaminated soils, *Science of the Total Environment*, **2017**, *586*, 576-597. [Crossref], [Google Scholar], [Publisher]

[13]. E.I. El-Aswar, M.M. Zahran, M. El-Kemary, Optical and electrochemical studies of silver nanoparticles biosynthesized by Haplophyllum tuberculatum extract and their antibacterial activity in wastewater treatment, *Materials Research Express*, **2019**, *6*, 105016. [Crossref], [Google Scholar], [Publisher]

[14]. E.I. El-Aswar, S.E.-S. Gaber, M.M. Zahran, A.H. Abdelaleem, Characterization of biosynthesized silver nanoparticles by Haplophyllum tuberculatum plant extract under microwave irradiation and detecting their antibacterial activity against some wastewater microbes, *Desalination Water Treat*, **2020**, *195*, 275-285. [Crossref], [Google Scholar], [Publisher]

[15]. D. Wang, H. Duan, J. Lü, C. Lü, Fabrication of thermo-responsive polymer functionalized reduced graphene oxide@ Fe 3 O 4@ Au magnetic nanocomposites for enhanced catalytic applications, *Journal of Materials Chemistry A*, **2017**, *5*, 5088-5097. [Crossref], [Google Scholar], [Publisher]

[16]. M.N. Alves, M. Miró, M.C. Breadmore, M. Macka, Trends in analytical separations of magnetic (nano) particles, *TrAC Trends in Analytical Chemistry*, **2019**, *114*, 89-97. [Crossref], [Google Scholar], [Publisher]

[17]. A. Rios, M. Zougagh, Recent advances in magnetic nanomaterials for improving analytical processes, *TrAC Trends in Analytical Chemistry*, **2016**, *84*, 72-83. [Crossref], [Google Scholar], [Publisher]

[18]. L. Gutiérrez, L. De la Cueva, M. Moros, E. Mazarío, S. De Bernardo, J.M. De la Fuente, M.P. Morales, G. Salas, Aggregation effects on the magnetic properties of iron oxide colloids, *Nanotechnology*, **2019**, *30*, 112001. [Crossref], [Google Scholar], [Publisher]

[19]. A. Shishov, A. Pochivalov, L. Nugbienyo, V. Andruch, A. Bulatov, Deep eutectic solvents are not only effective extractants, *TrAC Trends in Analytical Chemistry*, **2020**, *129*, 115956. [Crossref], [Google Scholar], [Publisher]

[20]. G. Li, K.H. Row, Utilization of deep eutectic solvents in dispersive liquid-liquid micro-extraction, *TrAC Trends in Analytical Chemistry*, **2019**, *120*, 115651. [Crossref], [Google Scholar], [Publisher]

[21]. Z. Lin, Y. Zhang, Q. Zhao, A. Chen, B. Jiao, Ultrasound-assisted dispersive liquid-phase microextraction by solidifying L-menthol-decanoic acid hydrophobic deep eutectic solvents for detection of five fungicides in fruit juices and tea drinks, *Journal of Separation Science*, **2021**, *44*, 3870-3882. [Crossref], [Google Scholar], [Publisher]

[22]. F.M. Perna, P. Vitale, V. Capriati, Deep eutectic solvents and their applications as green solvents, *Current Opinion in Green and Sustainable Chemistry*, **2020**, *21*, 27-33. [Crossref], [Google Scholar], [Publisher]

[23]. A.M. Ramezani, R. Ahmadi, Y. Yamini, Homogeneous liquid-liquid microextraction

based on deep eutectic solvents, *TrAC Trends in Analytical Chemistry*, **2022**, *149*, 116566. [Crossref], [Google Scholar], [Publisher]

[24]. A.H. Panhwar, M. Tuzen, T.G. Kazi, Ultrasonic assisted dispersive liquid-liquid microextraction method based on deep eutectic solvent for speciation, preconcentration and determination of selenium species (IV) and (VI) in water and food samples, *Talanta*, **2017**, *175*, 352-358. [Crossref], [Google Scholar], [Publisher]

[25]. R.A. Zounr, M. Tuzen, M.Y. Khuhawar, Novel ultrasonic-assisted deep eutectic solvent-based dispersive liquid–liquid microextraction for determination of vanadium in food samples by electrothermal atomic absorption spectrometry: a multivariate study, *Applied Organometallic Chemistry*, **2018**, *32*, e4144. [Crossref], [Google Scholar], [Publisher]

[26]. X. Wang, M. Liu, F. Peng, X. Ding, Hydrophobic magnetic deep eutectic solvent: synthesis, properties, and application in DNA separation, *Journal of Chromatography A*, **2021**, *1659*, 462626. [Crossref], [Google Scholar], [Publisher]

[27]. B. Kakavandi, M. Jahangiri-rad, M. Rafiee, A.R. Esfahani, A.A. Babaei, Development of response surface methodology for optimization of phenol and p-chlorophenol adsorption on magnetic recoverable carbon, *Microporous and Mesoporous Materials*, **2016**, *231*, 192-206. [Crossref], [Google Scholar], [Publisher]

[28]. Y. Yu, W.Y. Mo, T. Luukkonen, Adsorption behaviour and interaction of organic micropollutants with nano and microplastics–a review, *Science of the Total Environment*, **2021**, *797*, 149140. [Crossref], [Google Scholar], [Publisher]

[29]. W.C. Tsai, S.D. Huang, Dispersive liquid–liquid microextraction with little solvent consumption combined with gas chromatography–mass spectrometry for the pretreatment of organochlorine pesticides in aqueous samples, *Journal of Chromatography A*, **2009**, *1216*, 5171-5175. [Crossref], [Google Scholar], [Publisher]

[30]. M. Mezcua, M. Repetti, A. Agüera, C. Ferrer, J. García-Reyes, A. Fernández-Alba, Determination of pesticides in milk-based infant formulas by pressurized liquid extraction followed by gas chromatography tandem mass spectrometry, *Analytical and Bioanalytical Chemistry*, **2007**, *389*, 1833-1840. [Crossref], [Google Scholar], [Publisher]

[31]. L. Zhao, H.K. Lee, Application of static liquid-phase microextraction to the analysis of organochlorine pesticides in water, *Journal of Chromatography A*, **2001**, *919*, 381-388. [Crossref], [Google Scholar], [Publisher]

[32]. R. Kaur, R. Kaur, S. Rani, A.K. Malik, A. Kabir, K.G. Furton, V.F. Samanidou, Rapid monitoring of organochlorine pesticide residues in various fruit juices and water samples using fabric phase sorptive extraction and gas chromatography-mass spectrometry, *Molecules*, **2019**, *24*, 1013. [Crossref], [Google Scholar], [Publisher]

[33]. P. Grossi, I.R. Olivares, D.R. de Freitas, F.M. Lancas, A novel HS-SBSE system coupled with gas chromatography and mass spectrometry for the analysis of organochlorine pesticides in water samples, *Journal of Separation Science*, **2008**, *31*, 3630-3637. [Crossref], [Google Scholar], [Publisher]

[34]. X. Jiang, H.K. Lee, Solvent bar microextraction, *Analytical Chemistry*, **2004**, *76*, 5591-5596. [Crossref], [Google Scholar], [Publisher]

[35]. J.-F. Focant, A. Sjödin, W.E. Turner, D.G. Patterson, Measurement of selected polybrominated diphenyl ethers, polybrominated and polychlorinated biphenyls, and organochlorine pesticides in human serum and milk using comprehensive two-dimensional gas chromatography isotope dilution time-of-flight mass spectrometry, *Analytical Chemistry*, **2004**, *76*, 6313-6320. [Crossref], [Google Scholar], [Publisher]

[36]. S.S. Caldas, F.P. Costa, E.G. Primel, Validation of method for determination of different classes of pesticides in aqueous samples by dispersive liquid–liquid microextraction with liquid chromatography–

tandem mass spectrometric detection, *Analytica Chimica Acta*, **2010**, *665*, 55-62. [Crossref], [Google Scholar], [Publisher]

[37]. M. Aguilera-Luiz, P. Plaza-Bolaños, R. Romero-González, J. Martínez Vidal, A.G. Frenich, Comparison of the efficiency of different extraction methods for the simultaneous determination of mycotoxins and pesticides in milk samples by ultra high-performance liquid chromatography-tandem mass spectrometry, *Analytical and Bioanalytical Chemistry*, **2011**, *399*, 2863-2875. [Crossref], [Google Scholar], [Publisher]

[38]. Q. Zhang, X. Cao, Z. Zhang, J. Yin, Preparation of magnetic flower-like molybdenum disulfide hybrid materials for the extraction of organophosphorus pesticides from environmental water samples, *Journal of Chromatography A*, **2020**, *1631*, 461583. [Crossref], [Google Scholar], [Publisher]

[39]. M. Shakourian, Y. Yamini, M. Safari, Facile magnetization of metal–organic framework TMU-6 for magnetic solid-phase extraction of organophosphorus pesticides in water and rice samples, *Talanta*, **2020**, *218*, 121139. [Crossref], [Google Scholar], [Publisher]

[40]. M. Saraji, B. Rezaei, M.K. Boroujeni, A.A.H. Bidgoli, Polypyrrole/sol–gel composite as a solid-phase microextraction fiber coating for the determination of organophosphorus pesticides in water and vegetable samples, *Journal of Chromatography A*, **2013**, *1279*, 20-26. [Crossref], [Google Scholar], [Publisher]

[41]. Q. Xiao, B. Hu, C. Yu, L. Xia, Z. Jiang, Optimization of a single-drop microextraction procedure for the determination of organophosphorus pesticides in water and fruit juice with gas chromatography-flame photometric detection, *Talanta*, **2006**, *69*, 848-855. [Crossref], [Google Scholar], [Publisher]

[42]. A. Salemi, R. Rasoolzadeh, M.M. Nejad, M. Vosough, Ultrasonic assisted headspace single drop micro-extraction and gas chromatography with nitrogen-phosphorus detector for determination of organophosphorus pesticides in soil, *Analytica Chimica Acta*, **2013**, *769*, 121-126. [Crossref], [Google Scholar], [Publisher]

[43]. S. Liu, L. Xie, J. Zheng, R. Jiang, F. Zhu, T. Luan, G. Ouyang, Mesoporous TiO2 nanoparticles for highly sensitive solid-phase microextraction of organochlorine pesticides, *Analytica Chimica Acta*, **2015**, *878*, 109-117. [Crossref], [Google Scholar], [Publisher]

[44]. S.E. Kepekci-Tekkeli, Z. Durmus, Magnetic solid phase extraction applications combined with analytical methods for determination of drugs in different matrices review, *Journal of the Chilean Chemical Society*, **2019**, *64*, 4448-4458. [Crossref], [Google Scholar], [Publisher]

[45]. C. Herrero-Latorre, J. Barciela-García, S. García-Martín, R. Peña-Crecente, J. Otárola-Jiménez, Magnetic solid-phase extraction using carbon nanotubes as sorbents: A review, *Analytica Chimica Acta*, **2015**, *892*, 10-26. [Crossref], [Google Scholar], [Publisher]

[46]. X. Liu, C. Wang, Q. Wu, Z. Wang, Metal-organic framework-templated synthesis of magnetic nanoporous carbon as an efficient absorbent for enrichment of phenylurea herbicides, *Analytica Chimica Acta*, **2015**, *870*, 67-74. [Crossref], [Google Scholar], [Publisher]

[47]. A. Mehdinia, N. Khodaee, A. Jabbari, Fabrication of graphene/Fe3O4@ polythiophene nanocomposite and its application in the magnetic solid-phase extraction of polycyclic aromatic hydrocarbons from environmental water samples, *Analytica Chimica Acta*, **2015**, *868*, 1-9. [Crossref], [Google Scholar], [Publisher]

[48]. X. Zang, Q. Chang, H. Li, X. Zhao, S. Zhang, C. Wang, Z. Wang, Construction of a ringent multi-shelled hollow MIL-88B as the solid-phase microextraction fiber coating for the extraction of organochlorine pesticides, *Separation and Purification Technology*, **2023**, *304*, 122350. [Crossref], [Google Scholar], [Publisher]

[49]. X.L. Chen, L.F. Ai, Y.Q. Cao, Q.X. Nian, Y.Q. Jia, Y.L. Hao, M.M. Wang, X.S. Wang, Rapid determination of sulfonamides in chicken muscle and milk using efficient graphene oxide-based monolith on-line solid-phase extraction coupled with liquid chromatography–tandem mass spectrometry, *Food Analytical Methods*,

2019, *12*, 271-281. [Crossref], [Google Scholar], [Publisher]

[50]. L. Guo, J. Wu, F. Xing, W. Liu, L. Hao, C. Wang, Q. Wu, Z. Wang, Graphene intercalated with carbon nanosphere: a novel solid-phase extraction sorbent for five carbamate pesticides, *Microchimica Acta*, **2020**, *187*, 1-10. [Crossref], [Google Scholar], [Publisher]

[51]. L. Zheng, F. Pi, Y. Wang, H. Xu, Y. Zhang, X. Sun, Photocatalytic degradation of Acephate, Omethoate, and Methyl parathion by Fe3O4@ SiO2@ mTiO2 nanomicrospheres, *Journal of Hazardous Materials*, **2016**, *315*, 11-22. [Crossref], [Google Scholar], [Publisher]

[52]. M. Farajvand, K. Farajzadeh, G. Faghani, Synthesis of graphene oxide/polyaniline nanocomposite for measuring cadmium (II) by solid phase extraction combined with dispersive liquid-liquid microextraction, *Materials Research Express*, **2018**, *5*, 075017. [Crossref], [Google Scholar], [Publisher]

[53]. X. Hou, S. Tang, X. Guo, L. Wang, X. Liu, X. Lu, Y. Guo, Preparation and application of guanidyl-functionalized graphene oxide-grafted silica for efficient extraction of acidic herbicides by Box-Behnken design, *Journal of Chromatography A*, **2018**, *1571*, 65-75. [Crossref], [Google Scholar], [Publisher]

[54]. R.T. Ma, W. Ha, J. Chen, Y.P. Shi, Highly dispersed magnetic molecularly imprinted nanoparticles with well-defined thin film for the selective extraction of glycoprotein, *Journal of Materials Chemistry B*, **2016**, *4*, 2620-2627. [Crossref], [Google Scholar], [Publisher]

[55]. A. Khodayari, S. Sohrabnezhad, S. Moinfar, A. Pourahmad, GNP/Al-MOF nanocomposite as an efficient fiber coating of headspace solid-phase micro-extraction for the determination of organophosphorus pesticides in food samples, *Microchimica Acta*, **2022**, *189*, 45. [Crossref], [Google Scholar], [Publisher]

[56]. Q. Lu, H. Guo, Y. Zhang, X. Tang, W. Lei, R. Qi, J. Chu, D. Li, Q. Zhao, Graphene oxide-Fe$_3$O$_4$ nanocomposite magnetic solid phase extraction followed by UHPLC-MS/MS for highly sensitive

determination of eight psychoactive drugs in urine samples, *Talanta*, **2020**, *206*, 120212. [Crossref], [Google Scholar], [Publisher]

[57]. S. Seidi, H. Abolhasani, Y. Razeghi, M. Shanehsaz, M. Manouchehri, Electrochemically deposition of ionic liquid modified graphene oxide for circulated headspace in-tube solid phase microextraction of naphthalene from honey samples followed by on-line liquid chromatography analysis, *Journal of Chromatography A*, **2020**, *1628*, 461486. [Crossref], [Google Scholar], [Publisher]

[58]. S. Peng, Y. Huang, S. Ouyang, J. Huang, Y. Shi, Y.-J. Tong, X. Zhao, N. Li, J. Zheng, J. Zheng, Efficient solid phase microextraction of organic pollutants based on graphene oxide/chitosan aerogel, *Analytica Chimica Acta*, **2022**, *1195*, 339462. [Crossref], [Google Scholar], [Publisher]

[59]. Y. Zhou, J. Xu, N. Lu, X. Wu, Y. Zhang, X. Hou, Development and application of metal-organic framework@ GA based on solid-phase extraction coupling with UPLC-MS/MS for the determination of five NSAIDs in water, *Talanta*, **2021**, *225*, 121846. [Crossref], [Google Scholar], [Publisher]

[60]. A.K. Sharma, Y. Sharma, p-toluene sulfonic acid doped polyaniline carbon nanotube composites: Synthesis via different routes and modified properties, *Journal of Electrochemical Science and Engineering*, **2013**, *3*, 47-56. [Crossref], [Google Scholar], [Publisher]

[61]. D.R. Rout, H.M. Jena, Synthesis of novel reduced graphene oxide decorated β-cyclodextrin epichlorohydrin composite and its application for Cr (VI) removal: Batch and fixed-bed studies, *Separation and Purification Technology*, **2021**, *278*, 119630. [Crossref], [Google Scholar], [Publisher]

[62]. A. Mariyam, J. Mittal, F. Sakina, R.T. Baker, A.K. Sharma, A. Mittal, Efficient batch and Fixed-Bed sequestration of a basic dye using a novel variant of ordered mesoporous carbon as adsorbent, *Arabian Journal of Chemistry*, **2021**, *14*, 103186. [Crossref], [Google Scholar], [Publisher]

[63]. G. Bhavya, S.A. Belorkar, R. Mythili, N. Geetha, H.S. Shetty, S.S. Udikeri, S. Jogaiah, Remediation of emerging environmental pollutants: a review based on advances in the uses of eco-friendly biofabricated nanomaterials, *Chemosphere*, **2021**, *275*, 129975. [Crossref], [Google Scholar], [Publisher]

[64]. S.W.C. Chung, B.L.S. Chen, Determination of organochlorine pesticide residues in fatty foods: A critical review on the analytical methods and their testing capabilities, J. Chromatogr. A. 1218 (2011) 5555–5567. https://doi.org/https://doi.org/10.1016/j.chroma.2011.06.066.

[65]. R. Jayaraj, P. Megha, P. Sreedev, Organochlorine pesticides, their toxic effects on living organisms and their fate in the environment, *Interdisciplinary Toxicology*, **2016**, *9*, 90-100. [Crossref], [Google Scholar], [Publisher]

[66]. Y. Zhou, J. Jing, R. Yu, Y. Zhao, Y. Gou, H. Tang, H. Zhang, Y. Huang, Distribution of pesticide residues in agricultural topsoil of the Huangshui catchment, Qinghai Tibet Plateau, *Environmental Science and Pollution Research*, **2023**, *30*, 7582-7592. [Crossref], [Google Scholar], [Publisher]

[67]. S.S. Caldas, C. Rombaldi, J.L. de Oliveira Arias, L.C. Marube, E.G. Primel, Multi-residue method for determination of 58 pesticides, pharmaceuticals and personal care products in water using solvent demulsification dispersive liquid–liquid microextraction combined with liquid chromatography-tandem mass spectrometry, *Talanta*, **2016**, *146*, 676-688. [Crossref], [Google Scholar], [Publisher]

[68]. P. Nayak, H. Solanki, Pesticides and Indian agriculture—A review, *International Journal of Research_Granthaalayah*, **2021**, *9*, 250-263. [Crossref], [Google Scholar], [Publisher]

[69]. Z. Liu, G. Zheng, Z. Liu, Organochlorine pesticides in surface water of Jiuxi Valley, China: distribution, source analysis, and risk evaluation, *Journal of Chemistry*, **2020**, *2020*, 1-8. [Crossref], [Google Scholar], [Publisher]

[70]. C. Chen, W. Zou, S. Chen, K. Zhang, L. Ma, Ecological and health risk assessment of organochlorine pesticides in an urbanized river network of Shanghai, China, *Environmental Sciences Europe*, **2020**, *32*, 1-14. [Crossref], [Google Scholar], [Publisher]

[71] C. Olisah, O.O. Okoh, A.I. Okoh, Occurrence of organochlorine pesticide residues in biological and environmental matrices in Africa: A two-decade review, *Heliyon*, **2020**, *6*. [Crossref], [Google Scholar], [Publisher]

[72]. S. Yao, J. Huang, H. Zhou, C. Cao, T. Ai, H. Xing, J. Sun, Levels, distribution and health risk assessment of organochlorine pesticides in agricultural soils from the pearl river delta of China, *International Journal of Environmental Research and Public Health*, **2022**, *19*, 13171. [Crossref], [Google Scholar], [Publisher]

[73]. J.H. Wang, C.P. Chang, C.C. Chang, C.M. Wang, C.F. Lin, J.W. Lin, W.L. Lin, H.J. Liao, C.Y. Kao, P.S. Fan, Analysis of persistent organochlorine pesticides in shellfish and their risk assessment from aquafarms in Taiwan, *Marine Pollution Bulletin*, **2021**, *172*, 112811. [Crossref], [Google Scholar], [Publisher]

[74]. X. Gong, L. Xu, S. Huang, X. Kou, S. Lin, G. Chen, G. Ouyang, Application of the NU-1000 coated SPME fiber on analysis of trace organochlorine pesticides in water, *Analytica Chimica Acta*, **2022**, *1218*, 339982. [Crossref], [Google Scholar], [Publisher]

[75]. E. Can-Güven, K. Gedik, P.B. Kurt-Karakuş, Organochlorine pesticides and polychlorinated biphenyls from a greenhouse area on the Mediterranean coast of Turkey: Distribution, air-soil exchange, enantiomeric signature, and source implications, *Atmospheric Pollution Research*, **2022**, *13*, 101263. [Crossref], [Google Scholar], [Publisher]

[76]. C.J. Martyniuk, A.C. Mehinto, N.D. Denslow, Organochlorine pesticides: Agrochemicals with potent endocrine-disrupting properties in fish, *Molecular and Cellular Endocrinology*, **2020**, *507*, 110764. [Crossref], [Google Scholar], [Publisher]

[77]. S.N. Ali, M. Baqar, M. Mumtaz, U. Ashraf, M.N. Anwar, A. Qadir, S.R. Ahmad, A.-S. Nizami, H. Jun, Organochlorine pesticides in the surrounding soils of POPs destruction facility: source fingerprinting, human health, and ecological risks assessment, *Environmental Science and Pollution Research*, **2020**, *27*, 7328-7340. [Crossref], [Google Scholar], [Publisher]

[78]. H. Tyagi, H. Chawla, H. Bhandari, S. Garg, Recent-enhancements in visible-light photocatalytic degradation of organochlorines pesticides: A review, *Materials Today: Proceedings*, **2022**, *49*, 3289-3305. [Crossref], [Google Scholar], [Publisher]

[79]. R. Kamata, F. Shiraishi, K. Nakamura, Avian eggshell thinning caused by transovarian exposure to o, p′-DDT: changes in histology and calcium-binding protein production in the oviduct uterus, *The Journal of Toxicological Sciences*, **2020**, *45*, 131-136. [Crossref], [Google Scholar], [Publisher]

[80]. J. Ma, L. Pan, X. Yang, X. Liu, S. Tao, L. Zhao, X. Qin, Z. Sun, H. Hou, Y. Zhou, DDT, DDD, and DDE in soil of Xiangfen County, China: residues, sources, spatial distribution, and health risks, *Chemosphere*, **2016**, *163*, 578-583. [Crossref], [Google Scholar], [Publisher]

[81]. M. Baqar, Y. Sadef, S.R. Ahmad, A. Mahmood, J. Li, G. Zhang, Organochlorine pesticides across the tributaries of River Ravi, Pakistan: Human health risk assessment through dermal exposure, ecological risks, source fingerprints and spatio-temporal distribution, *Science of the Total Environment*, **2018**, *618*, 291-305. [Crossref], [Google Scholar], [Publisher]

[82]. R.X. Sun, Y. Sun, X.D. Xie, B.Z. Yang, L.Y. Cao, S. Luo, Y.Y. Wang, B.X. Mai, Bioaccumulation and human health risk assessment of DDT and its metabolites (DDTs) in yellowfin tuna (Thunnus albacares) and their prey from the South China Sea, *Marine Pollution Bulletin*, **2020**, *158*, 111396. [Crossref], [Google Scholar], [Publisher]

[83]. R.C. Jhamtani, S. Shukla, P. Sivaperumal, M. Dahiya, R. Agarwal, Impact of co-exposure of aldrin and titanium dioxide nanoparticles at

biochemical and molecular levels in Zebrafish, *Environmental Toxicology and Pharmacology*, **2018**, *58*, 141-155. [Crossref], [Google Scholar], [Publisher]

[84]. A. Mardani, M.R. Afshar Mogaddam, M.A. Farajzadeh, A. Mohebbi, M. Nemati, M. Torbati, A three-phase solvent extraction system combined with deep eutectic solvent-based dispersive liquid–liquid microextraction for extraction of some organochlorine pesticides in cocoa samples prior to gas chromatography with electron capture detection, *Journal of Separation Science*, **2020**, *43*, 3674-3682. [Crossref], [Google Scholar], [Publisher]

[85]. K. Ghosh, B. Chatterjee, A.G. Jayaprasad, S.R. Kanade, The persistent organochlorine pesticide endosulfan modulates multiple epigenetic regulators with oncogenic potential in MCF-7 cells, *Science of the Total Environment*, **2018**, *624*, 1612-1622. [Crossref], [Google Scholar], [Publisher]

[86]. A. Ahmad, M. Shahid, S. Khalid, H. Zaffar, T. Naqvi, A. Pervez, M. Bilal, M.A. Ali, G. Abbas, W. Nasim, Residues of endosulfan in cotton growing area of Vehari, Pakistan: an assessment of knowledge and awareness of pesticide use and health risks, *Environmental Science and Pollution Research*, **2019**, *26*, 20079-20091. [Crossref], [Google Scholar], [Publisher]

[87]. M. Hassanpour, M. Shamsipur, N. Babajani, F. Shiri, B. Hashemi, N. Fattahi, pH-responsive deep eutectic solvents applied in the extraction of abamectin and endosulfan from water and fruit juice samples: a comparative study, *Microchemical Journal*, **2023**, *187*, 108391. [Crossref], [Google Scholar], [Publisher]

[88]. K. Padayachee, C. Reynolds, R. Mateo, A. Amar, A global review of the temporal and spatial patterns of DDT and dieldrin monitoring in raptors, *Science of The Total Environment*, **2023**, *858*, 159734. [Crossref], [Google Scholar], [Publisher]

[89]. M.S. Fuentes, P.E. Sineli, S. Pons, A.d.M. de LeBlanc, C.S. Benimeli, R.T. Hill, S.A. Cuozzo, Study of the removal of a pesticides mixture by a Streptomyces strain and their effect on the

cytotoxicity of treated systems, *Journal of Environmental Chemical Engineering*, **2018**, *6*, 6836-6843. [Crossref], [Google Scholar], [Publisher]

[90]. H. Zhai, Z. Liang, Z. Chen, H. Wang, Z. Liu, Z. Su, Q. Zhou, Simultaneous detection of metronidazole and chloramphenicol by differential pulse stripping voltammetry using a silver nanoparticles/sulfonate functionalized graphene modified glassy carbon electrode, *Electrochimica Acta*, **2015**, *171*, 105-113. [Crossref], [Google Scholar], [Publisher]

[91]. D. Panda, S. Manickam, Hydrodynamic cavitation assisted degradation of persistent endocrine-disrupting organochlorine pesticide Dicofol: Optimization of operating parameters and investigations on the mechanism of intensification, *Ultrasonics Sonochemistry*, **2019**, *51*, 526-532. [Crossref], [Google Scholar], [Publisher]

[92]. P. Gulipalli, T. Punugoti, P. Nikhil, V.R. Poiba, M. Vangalapati, Synthesis and characterization of Ni/Zn dually doped on multiwalled carbon nanotubes and its application for the degradation of dicofol, *Materials Today: Proceedings*, **2021**, *44*, 2760-2766. [Crossref], [Google Scholar], [Publisher]

[93]. P. Debabrata, M. Sivakumar, Sonochemical degradation of endocrine-disrupting organochlorine pesticide Dicofol: Investigations on the transformation pathways of dechlorination and the influencing operating parameters, *Chemosphere*, **2018**, *204*, 101-108. [Crossref], [Google Scholar], [Publisher]

[94]. V. Perez-Rodriguez, N. Wu, A. de la Cova, J. Schmidt, N.D. Denslow, C.J. Martyniuk, The organochlorine pesticide toxaphene reduces non-mitochondrial respiration and induces heat shock protein 70 expression in early-staged zebrafish (Danio rerio), *Comparative Biochemistry and Physiology Part C: Toxicology & Pharmacology*, **2020**, *228*, 108669. [Crossref], [Google Scholar], [Publisher]

[95]. Y.Y. Yang, G.S. Toor, C.F. Williams, Pharmaceuticals and organochlorine pesticides in sediments of an urban river in Florida, USA, *Journal of Soils and Sediments*, **2015**, *15*, 993-1004. [Crossref], [Google Scholar], [Publisher]

[96]. M. Grgić, S. Maletić, J. Beljin, M.K. Isakovski, S. Rončević, A. Tubić, J. Agbaba, Lindane and hexachlorobenzene sequestration and detoxification in contaminated sediment amended with carbon-rich sorbents, *Chemosphere*, **2019**, *220*, 1033-1040. [Crossref], [Google Scholar], [Publisher]

[97]. E.E. Raimondo, J.D. Aparicio, G.E. Briceño, M.S. Fuentes, C.S. Benimeli, Lindane bioremediation in soils of different textural classes by an Actinobacteria consortium, *Journal of Soil Science and Plant Nutrition*, **2019**, *19*, 29-41. [Crossref], [Google Scholar], [Publisher]

[98]. D. Kumar, R. Pannu, Perspectives of lindane (γ-hexachlorocyclohexane) biodegradation from the environment: a review, *Bioresources and Bioprocessing*, **2018**, *5*, 1-18. [Crossref], [Google Scholar], [Publisher]

[99]. S.I. Grondona, M. Gonzalez, D.E. Martínez, H.E. Massone, K.S.B. Miglioranza, Assessment of organochlorine pesticides in phreatic aquifer of Pampean Region, Argentina, *Bulletin of Environmental Contamination and Toxicology*, **2019**, *102*, 544-549. [Crossref], [Google Scholar], [Publisher]

[100] F. Gierer, S. Vaughan, M. Slater, H.M. Thompson, J.S. Elmore, R.D. Girling, A review of the factors that influence pesticide residues in pollen and nectar: Future research requirements for optimising the estimation of pollinator exposure, *Environmental Pollution*, **2019**, *249*, 236-247. [Crossref], [Google Scholar], [Publisher]

[101]. F.A. Martins, J.K. Daré, M.P. Freitas, Theoretical study of fluorinated bioisosteres of organochlorine compounds as effective and eco-friendly pesticides, *Ecotoxicology and Environmental Safety*, **2020**, *199*, 110679. [Crossref], [Google Scholar], [Publisher]

[102]. C. Sonne, U. Siebert, K. Gonnsen, J.P. Desforges, I. Eulaers, S. Persson, A. Roos, B.-M. Bäcklin, K. Kauhala, M.T. Olsen, Health effects from contaminant exposure in Baltic Sea birds

and marine mammals: A review, *Environment International*, **2020**, *139*, 105725. [Crossref], [Google Scholar], [Publisher]

[103]. A.V.B. Reddy, M. Moniruzzaman, T.M. Aminabhavi, Polychlorinated biphenyls (PCBs) in the environment: Recent updates on sampling, pretreatment, cleanup technologies and their analysis, *Chemical Engineering Journal*, **2019**, *358*, 1186-1207. [Crossref], [Google Scholar], [Publisher]

[104]. Y.S. El-Temsah, A. Sevcu, K. Bobcikova, M. Cernik, E.J. Joner, DDT degradation efficiency and ecotoxicological effects of two types of nano-sized zero-valent iron (nZVI) in water and soil, *Chemosphere*, **2016**, *144*, 2221-2228. [Crossref], [Google Scholar], [Publisher]

[105]. K. Jayaprabha, K. Suresh, Endosulfan contamination in water: a review on to an efficient method for its removal, *Journal of Chemistry Science*, **2016**, *6*, 182-191. [Crossref], [Google Scholar], [Publisher]

[106]. C.M. McGuire, A.M. Hansen, J.A. Karty, D.G. Peters, Catalytic reduction of 4, 4′-(2, 2, 2-trichloroethane-1, 1-diyl) bis (methoxybenzene)(methoxychlor) with nickel (I) salen electrogenerated at reticulated vitreous carbon cathodes, *Journal of Electroanalytical Chemistry*, **2016**, *772*, 66-72. [Crossref], [Google Scholar], [Publisher]

[107]. S. Pang, Z. Lin, J. Li, Y. Zhang, S. Mishra, P. Bhatt, S. Chen, Microbial degradation of aldrin and dieldrin: Mechanisms and Biochemical Pathways, *Frontiers in Microbiology*, **2022**, *13*, 713375. [Crossref], [Google Scholar], [Publisher]

[108]. B.L. Blaylock, Aldrin, Encyclopedia of Toxicology (Second Edition), **2005**, 15–17. [Crossref], [Publisher]

[109]. B.L. Blaylock, Aldrin, Encyclopedia of Toxicology (Second Edition), **2005**, 66–68. [Crossref], [Publisher]

[110]. E.R. Bandala, S. Gelover, M.T. Leal, C. Arancibia-Bulnes, A. Jimenez, C.A. Estrada, Solar photocatalytic degradation of Aldrin, *Catalysis Today*, **2002**, *76*, 189-199. [Crossref], [Google Scholar], [Publisher]

[111]. P. Xiao, T. Mori, R. Kondo, Biotransformation of the organochlorine pesticide trans-chlordane by wood-rot fungi, *New biotechnology*, **2011**, *29*, 107-115. [Crossref], [Google Scholar], [Publisher]

[112]. P. Xiao, T. Mori, I. Kamei, R. Kondo, Metabolism of organochlorine pesticide heptachlor and its metabolite heptachlor epoxide by white rot fungi, belonging to genus Phlebia, *FEMS Microbiology Letters*, **2011**, *314*, 140-146. [Crossref], [Google Scholar], [Publisher]

[113]. J. Miles, C. Tu, C. Harris, Metabolism of heptachlor and its degradation products by soil microorganisms, *Journal of Economic Entomology*, **1969**, *62*, 1334-1338. [Crossref], [Google Scholar], [Publisher]

[114]. T.C. Chiu, J.H. Yen, T.L. Liu, Y.S. Wang, Anaerobic degradation of the organochlorine pesticides DDT and heptachlor in river sediment of Taiwan, *Bulletin of Environmental Contamination & Toxicology*, **2004**, *72*. [Crossref], [Google Scholar], [Publisher]

[115]. A.S. Purnomo, S.R. Putra, K. Shimizu, R. Kondo, Biodegradation of heptachlor and heptachlor epoxide-contaminated soils by white-rot fungal inocula, *Environmental Science and Pollution Research*, **2014**, *21*, 11305-11312. [Crossref], [Google Scholar], [Publisher]

[116]. H.j. Zhao, R.J. Wu, X.C. Wang, Y.m. An, W.X. Zhao, F. Ma, Heterojunction of BiPO4/BiOBr photocatalysts for Rhodamine B dye degradation under visible LED light irradiation, *Journal of the Chinese Chemical Society*, **2020**, *67*, 1016-1023. [Crossref], [Google Scholar], [Publisher]

[117]. P.F. Xiao, T.X. You, Y.Z. Song, S. Ying, J.Q. Wang, Influence of Surfactants on Biodegradation of Chlordane by Wood-Rotting Fungus, *Applied Mechanics and Materials*, **2013**, *361*, 908-911. [Crossref], [Google Scholar], [Publisher]

[118]. S. Mahpishanian, H. Sereshti, One-step green synthesis of β-cyclodextrin/iron oxide-reduced graphene oxide nanocomposite with high supramolecular recognition capability:

Application for vortex-assisted magnetic solid phase extraction of organochlorine pesticides residue from honey samples, *Journal of Chromatography A*, **2017**, *1485*, 32-43. [Crossref], [Google Scholar], [Publisher]

[119]. S.M. Yousefi, F. Shemirani, S.A. Ghorbanian, Deep eutectic solvent magnetic bucky gels in developing dispersive solid phase extraction: Application for ultra trace analysis of organochlorine pesticides by GC-micro ECD using a large-volume injection technique, *Talanta*, **2017**, *168*, 73-81. [Crossref], [Google Scholar], [Publisher]

[120]. Z. Cheng, F. Dong, J. Xu, X. Liu, X. Wu, Z. Chen, X. Pan, Y. Zheng, Atmospheric pressure gas chromatography quadrupole-time-of-flight mass spectrometry for simultaneous determination of fifteen organochlorine pesticides in soil and water, *Journal of Chromatography A*, **2016**, *1435*, 115-124. [Crossref], [Google Scholar], [Publisher]

[121]. S.M. Yousefi, F. Shemirani, S.A. Ghorbanian, Deep eutectic solvent magnetic bucky gels in developing dispersive solid phase extraction: Application for ultra trace analysis of organochlorine pesticides by GC-micro ECD using a large-volume injection technique, *Talanta*, **2017**, *168*, 73-81. [Crossref], [Google Scholar], [Publisher] تکراری ۱۱۹

[122]. T. Sun, J. Yang, L. Li, X. Wang, X. Li, Y. Jin, Preparation of graphene sheets with covalently bonded Fe_3O_4 for magnetic solid-phase extraction applied to organochlorine pesticides in orange juice, *Chromatographia*, **2016**, *79*, 345-353. [Crossref], [Google Scholar], [Publisher]

[123]. Y.B. Luo, X. Li, X.Y. Jiang, B.D. Cai, F.P. Zhu, H.F. Zhang, Z.G. Chen, Y.Q. Pang, Y.Q. Feng, Magnetic graphene as modified quick, easy, cheap, effective, rugged and safe adsorbent for the determination of organochlorine pesticide residues in tobacco, *Journal of Chromatography A*, **2015**, *1406*, 1-9. [Crossref], [Google Scholar], [Publisher]

[124]. H.R. Nodeh, W.A.W. Ibrahim, M.A. Kamboh, M.M. Sanagi, Dispersive graphene-based silica coated magnetic nanoparticles as a new adsorbent for preconcentration of chlorinated pesticides from environmental water, *RSC Advances*, **2015**, *5*, 76424-76434. [Crossref], [Google Scholar], [Publisher]

[125]. A. Mehdinia, S. Rouhani, S. Mozaffari, Microwave-assisted synthesis of reduced graphene oxide decorated with magnetite and gold nanoparticles, and its application to solid-phase extraction of organochlorine pesticides, *Microchimica Acta*, **2016**, *183*, 1177-1185. [Crossref], [Google Scholar], [Publisher]

[126]. S. Xu, H. Liu, C. Chen, S. Feng, J. Fan, Ultrasound-assisted one-step reduction and self-assembly of carbon dots-reduced graphene oxide: Mechanism investigation and solid phase microextraction of ultra-trace organochlorine pesticides, *Chemical Engineering Journal*, **2023**, *451*, 138569. [Crossref], [Google Scholar], [Publisher]

[127]. Y. Ke, F. Zhu, F. Zeng, T. Luan, C. Su, G. Ouyang, Preparation of graphene-coated solid-phase microextraction fiber and its application on organochlorine pesticides determination, *Journal of Chromatography A*, **2013**, *1300*, 187-192. [Crossref], [Google Scholar], [Publisher]

[128]. F. Wang, S. Liu, H. Yang, J. Zheng, J. Qiu, J. Xu, Y. Tong, F. Zhu, G. Ouyang, Hierarchical Graphene coating for highly sensitive solid phase microextraction of organochlorine pesticides, *Talanta*, **2016**, *160*, 217-224. [Crossref], [Google Scholar], [Publisher]

[129]. M. Sajid, C. Basheer, M. Daud, A. Alsharaa, Evaluation of layered double hydroxide/graphene hybrid as a sorbent in membrane-protected stir-bar supported micro-solid-phase extraction for determination of organochlorine pesticides in urine samples, *Journal of Chromatography A*, **2017**, *1489*, 1-8. [Crossref], [Google Scholar], [Publisher]

[130]. T. Sun, H. Sun, F. Zhao, Dispersive solid-phase extraction for the determination of trace organochlorine pesticides in apple juices using reduced graphene oxide coated with ZnO nanocomposites as sorbent, *Journal of separation science*, **2017**, *40*, 3725-3733. [Crossref], [Google Scholar], [Publisher]

[131]. V. Cutillas, F. Jesús, C. Ferrer, A.R. Fernández-Alba, Overcoming difficulties in the evaluation of captan and folpet residues by supercritical fluid chromatography coupled to mass spectrometry, *Talanta*, **2021**, *223*, 121714. [Crossref], [Google Scholar], [Publisher]

[132]. J. Ran, L. Zhang, J. Yao, S. Wang, P. Liang, N. Dong, Cucurbit [7] uril as a matrix solid-phase dispersion for the extraction of quaternary ammonium pesticides from vegetables and their determination using HPLC–UV, *Food Chemistry*, **2021**, *350*, 129236. [Crossref], [Google Scholar], [Publisher]

[133]. I. Boneva, S. Yaneva, D. Danalev, Development and validation of method for determination of organophosphorus pesticides traces in liver sample by GC-MS/MS-ion trap, *Acta Chromatographica*, **2021**, *33*, 188-194. [Crossref], [Google Scholar], [Publisher]

[134]. G. Liu, L. Li, X. Huang, S. Zheng, X. Xu, Z. Liu, Y. Zhang, J. Wang, H. Lin, D. Xu, Adsorption and removal of organophosphorus pesticides from environmental water and soil samples by using magnetic multi-walled carbon nanotubes@ organic framework ZIF-8, *Journal of Materials Science*, **2018**, *53*, 10772-10783. [Crossref], [Google Scholar], [Publisher]

[135]. Y.L. G Wang T Wang, X Zhang, J Han, W Luo, Y Shi, J Li, W Jiao, Factors influencing the spatial distribution of organochlorine pesticides in soils surrounding chemical industrial parks, J. Environ. Qual. 37 (2008) 1–8. https://doi.org/10.2134/jeq2007.0084.

[136]. S. Álvarez-Torrellas, A. Rodríguez, G. Ovejero, J.M. Gómez, J. García, Removal of caffeine from pharmaceutical wastewater by adsorption: influence of NOM, textural and chemical properties of the adsorbent, *Environmental Technology*, **2016**, *37*, 1618-1630. [Crossref], [Google Scholar], [Publisher]

[137]. R. Xie, Y. Jin, Y. Chen, W. Jiang, The importance of surface functional groups in the adsorption of copper onto walnut shell derived activated carbon, *Water Science and Technology*, **2017**, *76*, 3022-3034. [Crossref], [Google Scholar], [Publisher]

[138]. G. Hotová, V. Slovák, T. Zelenka, R. Maršálek, A. Parchaňská, The role of the oxygen functional groups in adsorption of copper (II) on carbon surface, *Science of the Total Environment*, **2020**, *711*, 135436. [Crossref], [Google Scholar], [Publisher]

[139]. L.P. Lingamdinne, J.R. Koduru, R.R. Karri, A comprehensive review of applications of magnetic graphene oxide based nanocomposites for sustainable water purification, *Journal of Environmental Management*, **2019**, *231*, 622-634. [Crossref], [Google Scholar], [Publisher]

[140]. C. Du, B. Zhao, X.B. Chen, N. Birbilis, H. Yang, Effect of water presence on choline chloride-2urea ionic liquid and coating platings from the hydrated ionic liquid, *Scientific Reports*, **2016**, *6*, 29225. [Crossref], [Google Scholar], [Publisher]

[141]. K. Yang, H. Peng, Y. Wen, N. Li, Re-examination of characteristic FTIR spectrum of secondary layer in bilayer oleic acid-coated Fe3O4 nanoparticles, *Applied Surface Science*, **2010**, *256*, 3093-3097. [Crossref], [Google Scholar], [Publisher]

[142]. N. Mehrabi, A. Masud, M. Afolabi, J. Hwang, G.A.C. Ortiz, N. Aich, Magnetic graphene oxide-nano zero valent iron (GO–nZVI) nanohybrids synthesized using biocompatible cross-linkers for methylene blue removal, *RSC Advances*, **2019**, *9*, 963-973. [Crossref], [Google Scholar], [Publisher]

[143]. Y. Huang, Y. Wang, Q. Pan, Y. Wang, X. Ding, K. Xu, N. Li, Q. Wen, Magnetic graphene oxide modified with choline chloride-based deep eutectic solvent for the solid-phase extraction of protein, *Analytica Chimica Acta*, **2015**, *877*, 90-99. [Crossref], [Google Scholar], [Publisher]

[144]. C. Caliman, A. Mesquita, D. Cipriano, J. Freitas, A. Cotta, W. Macedo, A. Porto, One-pot synthesis of amine-functionalized graphene oxide by microwave-assisted reactions: an outstanding alternative for supporting materials in supercapacitors, *RSC Advances*, **2018**, *8*, 6136-6145. [Crossref], [Google Scholar], [Publisher]

[145]. N. Alzate-Carvajal, D.A. Acevedo-Guzmán, V. Meza-Laguna, M.H. Farías, L.A. Pérez-Rey, E. Abarca-Morales, V.A. García-Ramírez, V.A. Basiuk, E.V. Basiuk, One-step nondestructive functionalization of graphene oxide paper with amines, *RSC Advances*, **2018**, *8*, 15253-15265. [Crossref], [Google Scholar], [Publisher]

[146]. N. Mehrabi, U.F.A. Haq, M.T. Reza, N. Aich, Application of deep eutectic solvent for conjugation of magnetic nanoparticles onto graphene oxide for lead (II) and methylene blue removal, *Journal of Environmental Chemical Engineering*, **2020**, *8*, 104222. [Crossref], [Google Scholar], [Publisher]

[147]. Y. Huang, Y. Wang, Q. Pan, Y. Wang, X. Ding, K. Xu, N. Li, Q. Wen, Magnetic graphene oxide modified with choline chloride-based deep eutectic solvent for the solid-phase extraction of protein, *Analytica chimica acta*, **2015**, *877*, 90-99. [Crossref], [Google Scholar], [Publisher]

[148]. B. Fan, S. Zhu, H. Ding, Y. Bai, Y. Luo, P. Di, Influence of MgO whisker addition on microstructures and mechanical properties of WC-MgO composite, *Materials Chemistry and Physics*, **2019**, *238*, 121907. [Crossref], [Google Scholar], [Publisher]

[149]. Y. Zhou, D. Chang, J. Chang, Preparation of nano-structured pig bone hydroxyapatite for high-efficiency adsorption of Pb2+ from aqueous solution, *International Journal of Applied Ceramic Technology*, **2017**, *14*, 1125-1133. [Crossref], [Google Scholar], [Publisher]

[150]. N. Manousi, G.A. Zachariadis, Recent advances in the extraction of polycyclic aromatic hydrocarbons from environmental samples, *Molecules*, **2020**, *25*, 2182. [Crossref], [Google Scholar], [Publisher]

[151]. M. Yazdanpanah, S. Nojavan, Micro-solid phase extraction of some polycyclic aromatic hydrocarbons from environmental water samples using magnetic β-cyclodextrin-carbon nano-tube composite as a sorbent, *Journal of Chromatography A*, **2019**, *1585*, 34-45. [Crossref], [Google Scholar], [Publisher]

[152]. M.N.L. Suseela, M.K. Viswanadh, A.K. Mehata, V. Priya, A. Setia, A.K. Malik, P. Gokul, J. Selvin, M.S. Muthu, Advances in solid-phase extraction techniques: Role of nanosorbents for the enrichment of antibiotics for analytical quantification, *Journal of Chromatography A*, **2023**, *1695*, 463937. [Crossref], [Google Scholar], [Publisher]

[153]. N. Tiadi, M. Mohanty, C. Mohanty, H.P. H. Panda, Studies on adsorption behavior of an industrial waste for removal of chromium from aqueous solution, *South African Journal of Chemical Engineering*, **2017**, *23*, 132-138. [Crossref], [Google Scholar], [Publisher]

[154]. J. Huang, S. Cao, Z. Liu, J. Tian, C. Xi, Z. Chen, High-efficiency removal of methcathinone from water using a novel DES modified magnetic biochar nanocomposite, *Journal of Environmental Chemical Engineering*, **2022**, *10*, 108456. [Crossref], [Google Scholar], [Publisher]

[155]. W. Peng, H. Li, Y. Liu, S. Song, A review on heavy metal ions adsorption from water by graphene oxide and its composites, *Journal of Molecular Liquids*, **2017**, *230*, 496-504. [Crossref], [Google Scholar], [Publisher]

[156]. G. Prasannamedha, P.S. Kumar, V. Shankar, Facile route for synthesis of Fe0/Fe3C/γ-Fe2O3 carbon composite using hydrothermal carbonization of sugarcane bagasse and its use as effective adsorbent for sulfamethoxazole removal, *Chemosphere*, **2022**, *289*, 133214. [Crossref], [Google Scholar], [Publisher]

[157]. A. Mandal, N. Singh, T. Purakayastha, Characterization of pesticide sorption behaviour of slow pyrolysis biochars as low cost adsorbent for atrazine and imidacloprid removal, *Science of the Total Environment*, **2017**, *577*, 376-385. [Crossref], [Google Scholar], [Publisher]

[158]. J.O. Ighalo, C.A. Igwegbe, A.G. Adeniyi, C.A. Adeyanju, S. Ogunniyi, Mitigation of Metronidazole (Flagyl) pollution in aqueous media by adsorption: A review, *Environmental Technology Reviews*, **2020**, *9*, 137-148. [Crossref], [Google Scholar], [Publisher]

[159]. A. Marican, E.F. Durán-Lara, A review on pesticide removal through different processes, *Environmental Science and Pollution Research*, **2018**, *25*, 2051-2064. [Crossref], [Google Scholar], [Publisher]

[160]. L. Zhou, S. Pan, X. Chen, Y. Zhao, B. Zou, M. Jin, Kinetics and thermodynamics studies of pentachlorophenol adsorption on covalently functionalized Fe3O4@ SiO2–MWCNTs core–shell magnetic microspheres, *Chemical Engineering Journal*, **2014**, *257*, 10-19. [Crossref], [Google Scholar], [Publisher]

[161]. L. Hevira, J.O. Ighalo, H. Aziz, R. Zein, Terminalia catappa shell as low-cost biosorbent for the removal of methylene blue from aqueous solutions, *Journal of Industrial and Engineering Chemistry*, **2021**, *97*, 188-199. [Crossref], [Google Scholar], [Publisher]

[162]. M. Bergaoui, A. Nakhli, Y. Benguerba, M. Khalfaoui, A. Erto, F.E. Soetaredjo, S. Ismadji, B. Ernst, Novel insights into the adsorption mechanism of methylene blue onto organo-bentonite: Adsorption isotherms modeling and molecular simulation, *Journal of Molecular Liquids*, **2018**, *272*, 697-707. [Crossref], [Google Scholar], [Publisher]

[163]. L. Cui, Y. Wang, L. Gao, L. Hu, L. Yan, Q. Wei, B. Du, EDTA functionalized magnetic graphene oxide for removal of Pb (II), Hg (II) and Cu (II) in water treatment: adsorption mechanism and separation property, *Chemical Engineering Journal*, **2015**, *281*, 1-10. [Crossref], [Google Scholar], [Publisher]

[164]. K. Dai, G. Liu, W. Xu, Z. Deng, Y. Wu, C. Zhao, Z. Zhang, Judicious fabrication of bifunctionalized graphene oxide/MnFe2O4 magnetic nanohybrids for enhanced removal of Pb (II) from water, *Journal of Colloid and Interface Science*, **2020**, *579*, 815-822. [Crossref], [Google Scholar], [Publisher]

[165]. Z. He, M. Qin, C. Han, X. Bai, Y. Wu, D. Yao, Y. Zheng, Pectin/graphene oxide aerogel with bamboo-like structure for enhanced dyes adsorption, *Colloids and surfaces A: Physicochemical and Engineering Aspects*, **2022**, *652*, 129837. [Crossref], [Google Scholar], [Publisher]

[166]. W. Yang, M. Cao, Study on the difference in adsorption performance of graphene oxide and carboxylated graphene oxide for Cu (II), Pb (II) respectively and mechanism analysis, *Diamond and Related Materials*, **2022**, *129*, 109332. [Crossref], [Google Scholar], [Publisher]

[167]. A. Paton-Carrero, J. Valverde, E. Garcia-Alvarez, M. Lavin-Lopez, A. Romero, Influence of the oxidizing agent in the synthesis of graphite oxide, *Journal of Materials Science*, **2020**, *55*, 2333-2342. [Crossref], [Google Scholar], [Publisher]

[168]. R.K.S. Rathour, H. Singh, J. Bhattacharya, A. Mukherjee, Sand coated with graphene oxide-PVA matrix for aqueous Pb2+ adsorption: Insights from optimization and modeling of batch and continuous flow studies, *Surfaces and Interfaces*, **2022**, *32*, 102115. [Crossref], [Google Scholar], [Publisher]

[169]. M.J. Lima, M.K. Sasaki, O.R. Marinho, T.A. Freitas, R.C. Faria, B.F. Reis, F.R. Rocha, Spot test for fast determination of hydrogen peroxide as a milk adulterant by smartphone-based digital image colorimetry, *Microchemical Journal*, **2020**, *157*, 105042. [Crossref], [Google Scholar], [Publisher]

[170]. O. Ogunlalu, I.P. Oyekunle, K.O. Iwuozor, A.D. Aderibigbe, E.C. Emenike, Trends in the mitigation of heavy metal ions from aqueous solutions using unmodified and chemically-modified agricultural waste adsorbents, *Current Research in Green and Sustainable Chemistry*, **2021**, *4*, 100188. [Crossref], [Google Scholar], [Publisher]

[171]. H.M. Hamadeen, E.A. Elkhatib, M.E. Badawy, S.A. Abdelgaleil, Novel low cost nanoparticles for enhanced removal of chlorpyrifos from wastewater: sorption kinetics, and mechanistic studies, *Arabian Journal of Chemistry*, **2021**, *14*, 102981. [Crossref], [Google Scholar], [Publisher]

[172]. H. Esfandian, A. Samadi-Maybodi, M. Parvini, B. Khoshandam, Development of a novel method for the removal of diazinon pesticide from aqueous solution and modeling by artificial neural networks (ANN), *Journal of*

Industrial and Engineering Chemistry, **2016**, *35*, 295-308. [Crossref], [Google Scholar], [Publisher]

[173]. K.S. Sing, Reporting physisorption data for gas/solid systems with special reference to the determination of surface area and porosity (Recommendations 1984), *Pure and Applied Chemistry*, **1985**, *57*, 603-619. [Crossref], [Google Scholar], [Publisher]

[174]. L. Hauchhum, P. Mahanta, Carbon dioxide adsorption on zeolites and activated carbon by pressure swing adsorption in a fixed bed, *International Journal of Energy and Environmental Engineering*, **2014**, *5*, 349-356. [Crossref], [Google Scholar], [Publisher]

[175]. M. Sultan, T. Miyazaki, S. Koyama, Optimization of adsorption isotherm types for desiccant air-conditioning applications, *Renewable Energy*, **2018**, *121*, 441-450. [Crossref], [Google Scholar], [Publisher]

[176]. P. Carrott, Adsorption of water vapor by non-porous carbons, *Carbon*, **1992**, *30*, 201-205. [Crossref], [Google Scholar], [Publisher]

[177]. C. Buttersack, Modeling of type IV and V sigmoidal adsorption isotherms, *Physical Chemistry Chemical Physics*, **2019**, *21*, 5614-5626. [Crossref], [Google Scholar], [Publisher]

[178]. G. Wang, N. Li, X. Xing, Y. Sun, Z. Zhang, Z. Hao, Gaseous adsorption of hexamethyldisiloxane on carbons: Isotherms, isosteric heats and kinetics, *Chemosphere*, **2020**, *247*, 125862. [Crossref], [Google Scholar], [Publisher]

[179]. V.J. Inglezakis, S.G. Poulopoulos, H. Kazemian, Insights into the S-shaped sorption isotherms and their dimensionless forms, *Microporous and Mesoporous Materials*, **2018**, *272*, 166-176. [Crossref], [Google Scholar], [Publisher]

[180]. M.A. Al-Ghouti, D.A. Da'ana, Guidelines for the use and interpretation of adsorption isotherm models: A review, *Journal of Hazardous Materials*, **2020**, *393*, 122383. [Crossref], [Google Scholar], [Publisher]

[181]. M. Nurhadi, R. Kusumawardani, I. Widiyowati, H. Nur, Utilization of fish bone as adsorbent of Fe^{3+} ion by controllable removal of its carbonaceous component, *Journal of Physics: Conference Series, IOP Publishing*, **2018**, 012031. [Crossref], [Google Scholar], [Publisher]

[182]. L. Tang, J. Yu, Y. Pang, G. Zeng, Y. Deng, J. Wang, X. Ren, S. Ye, B. Peng, H. Feng, Sustainable efficient adsorbent: alkali-acid modified magnetic biochar derived from sewage sludge for aqueous organic contaminant removal, *Chemical Engineering Journal*, **2018**, *336*, 160-169. [Crossref], [Google Scholar], [Publisher]

[183]. T. Wang, S. Ai, Y. Zhou, Z. Luo, C. Dai, Y. Yang, J. Zhang, H. Huang, S. Luo, L. Luo, Adsorption of agricultural wastewater contaminated with antibiotics, pesticides and toxic metals by functionalized magnetic nanoparticles, *Journal of Environmental Chemical Engineering*, **2018**, *6*, 6468-6478. [Crossref], [Google Scholar], [Publisher]

[184]. R. Asadi, H. Abdollahi, M. Gharabaghi, Z. Boroumand, Effective removal of Zn (II) ions from aqueous solution by the magnetic $MnFe_2O_4$ and $CoFe_2O_4$ spinel ferrite nanoparticles with focuses on synthesis, characterization, adsorption, and desorption, *Advanced Powder Technology*, **2020**, *31*, 1480-1489. [Crossref], [Google Scholar], [Publisher]

[185]. Q. Hu, Z. Zhang, Application of Dubinin–Radushkevich isotherm model at the solid/solution interface: A theoretical analysis, *Journal of Molecular Liquids*, **2019**, *277*, 646-648. [Crossref], [Google Scholar], [Publisher]

[186]. M.A. El-Nemr, U.O. Aigbe, M.A. Hassaan, K.E. Ukhurebor, S. Ragab, R.B. Onyancha, O.A. Osibote, A. El Nemr, The use of biochar-NH_2 produced from watermelon peels as a natural adsorbent for the removal of Cu (II) ion from water, *Biomass Conversion and Biorefinery*, **2022**, 1-17. [Crossref], [Google Scholar], [Publisher]

[187] R. Khakpour, H. Tahermansouri, Synthesis, characterization and study of sorption parameters of multi-walled carbon

nanotubes/chitosan nanocomposite for the removal of picric acid from aqueous solutions, *International Journal of Biological Macromolecules*, **2018**, *109*, 598-610. [Crossref], [Google Scholar], [Publisher]

[188]. V. Kumar, P. Saharan, A.K. Sharma, A. Umar, I. Kaushal, A. Mittal, Y. Al-Hadeethi, B. Rashad, Silver doped manganese oxide-carbon nanotube nanocomposite for enhanced dye-sequestration: Isotherm studies and RSM modelling approach, *Ceramics International*, **2020**, *46*, 10309-10319. [Crossref], [Google Scholar], [Publisher]

[189]. Y. Wang, A. Li, C. Cui, Remediation of heavy metal-contaminated soils by electrokinetic technology: Mechanisms and applicability, *Chemosphere*, **2021**, *265*, 129071. [Crossref], [Google Scholar], [Publisher]

[190]. L. Li, C. Luo, X. Li, H. Duan, X. Wang, Preparation of magnetic ionic liquid/chitosan/graphene oxide composite and application for water treatment, *International Journal of Biological Macromolecules*, **2014**, *66*, 172-178. [Crossref], [Google Scholar], [Publisher]

[191]. M. Song, H. Sun, J. Yu, Y. Wang, M. Li, M. Liu, G. Zhao, Enzyme-free molecularly imprinted and graphene-functionalized photoelectrochemical sensor platform for pollutants, *ACS Applied Materials & Interfaces*, **2021**, *13*, 37212-37222. [Crossref], [Google Scholar], [Publisher]

[192]. J.H. Deng, X.R. Zhang, G.M. Zeng, J.L. Gong, Q.Y. Niu, J. Liang, Simultaneous removal of Cd (II) and ionic dyes from aqueous solution using magnetic graphene oxide nanocomposite as an adsorbent, *Chemical Engineering Journal*, **2013**, *226*, 189-200. [Crossref], [Google Scholar], [Publisher]

[193]. D.R. Rout, H.M. Jena, Enhanced Cr (VI) adsorption using ZnO decorated graphene composite: Batch and continuous studies, *Journal of the Taiwan Institute of Chemical Engineers*, **2022**, *140*, 104534. [Crossref], [Google Scholar], [Publisher]

[194]. N. Parvin, A. Babapoor, A. Nematollahzadeh, S.M. Mousavi, Removal of phenol and β-naphthol from aqueous solution by decorated graphene oxide with magnetic iron for modified polyrhodanine as nanocomposite adsorbents: Kinetic, equilibrium and thermodynamic studies, *Reactive and Functional Polymers*, **2020**, *156*, 104718. [Crossref], [Google Scholar], [Publisher]

[195]. M.M. Sanad, S.E. Gaber, E.I. El-Aswar, M.M. Farahat, Graphene-magnetite functionalized diatomite for efficient removal of organochlorine pesticides from aquatic environment, *Journal of Environmental Management*, **2023**, *330*, 117145. [Crossref], [Google Scholar], [Publisher]

[196]. M.K.M. Nodeh, N. Kanani, E.B. Abadi, H. Sereshti, A. Barghi, S. Rezania, Equilibrium and kinetics studies of naproxen adsorption onto novel magnetic graphene oxide functionalized with hybrid glycidoxy-amino propyl silane, *Environmental Challenges*, **2021**, *4*, 100106. [Crossref], [Google Scholar], [Publisher]

[197]. Y. Liu, S. Cao, Z. Liu, D. Wu, M. Luo, Z. Chen, Adsorption of amphetamine on deep eutectic solvents functionalized graphene oxide/metal-organic framework nanocomposite: Elucidation of hydrogen bonding and DFT studies, *Chemosphere*, **2023**, *323*, 138276. [Crossref], [Google Scholar], [Publisher]

[198]. M. Hejazikhah, P. Jamshidi, Modification of Magnetic Graphene Oxide by an Earth-Friendly Deep Eutectic Solvent to Preconcentrate Ultratrac Amounts of Pb (II) and Cd (II) in Legume Samples, *Applied Sciences*, **2023**, *13*, 5702. [Crossref], [Google Scholar], [Publisher]

[199]. I.A. Lawal, M.M. Lawal, S.O. Akpotu, H.K. Okoro, M. Klink, P. Ndungu, Noncovalent graphene oxide functionalized with ionic liquid: theoretical, isotherm, kinetics, and regeneration studies on the adsorption of pharmaceuticals, *Industrial & Engineering Chemistry Research*, **2020**, *59*, 4945-4957. [Crossref], [Google Scholar], [Publisher]

[200]. R.E.A. Mohammad, A.A. Elbashir, J. Karim, N. Yahaya, N.Y. Rahim, M. Miskam, Development of deep eutectic solvents based ferrofluid for liquid phase microextraction of ofloxacin and sparfloxacin in water samples, *Microchemical Journal*, **2022**, *181*, 107806. [Crossref], [Google Scholar], [Publisher]

[201]. S. Cao, F. Song, Z. Liu, H. Su, J. Tian, J. You, Z. Chen, Experimental and theoretical investigation on enhanced selective recognition of methamphetamine by customized adsorbent, *Journal of Environmental Chemical Engineering*, **2023**, *11*, 109927. [Crossref], [Google Scholar], [Publisher]

[202]. D. Sgargi, B. Adam, L.T. Budnik, G. Dinelli, H.R. Moldovan, M.J. Perry, P.T. Scheepers, V. Schlünssen, J.P. Teixeira, D. Mandrioli, Protocol for a systematic review and meta-analysis of human exposure to pesticide residues in honey and other bees' products, *Environmental Research*, **2020**, *186*, 109470. [Crossref], [Google Scholar], [Publisher]

[203]. Y. El-Nahhal, Pesticide residues in honey and their potential reproductive toxicity, *Science of the Total Environment*, **2020**, *741*, 139953. [Crossref], [Google Scholar], [Publisher]

[204]. O. Wilmart, A. Legrève, M.-L. Scippo, W. Reybroeck, B. Urbain, D.C. de Graaf, W. Steurbaut, P. Delahaut, P. Gustin, B.K. Nguyen, Residues in beeswax: a health risk for the consumer of honey and beeswax?, *Journal of Agricultural and Food Chemistry*, **2016**, *64*, 8425-8434. [Crossref], [Google Scholar], [Publisher]

[205]. V. Bommuraj, Y. Chen, H. Klein, R. Sperling, S. Barel, J.A. Shimshoni, Pesticide and trace element residues in honey and beeswax combs from Israel in association with human risk assessment and honey adulteration, *Food Chemistry*, **2019**, *299*, 125123. [Crossref], [Google Scholar], [Publisher]

[206]. N. Pi, S.E. Chia, C.N. Ong, B.C. Kelly, Associations of serum organohalogen levels and prostate cancer risk: Results from a case–control study in Singapore, *Chemosphere*, **2016**,

144, 1505-1512. [Crossref], [Google Scholar], [Publisher]

[207]. E.A. Nantia, A.S. Kada, F.P. Manfo, N.N. Tangu, K.M. Mbifung, D.H. Mbouobda, A. Kenfack, Parastar insecticide induced changes in reproductive parameters and testicular oxidative stress biomarkers in Wistar male rats, *Toxicology and Industrial Health*, **2018**, *34*, 499-506. [Crossref], [Google Scholar], [Publisher]

[208]. I.A. Adedara, O. Owoeye, B.O. Ajayi, I.O. Awogbindin, J.B. Rocha, E.O. Farombi, Diphenyl diselenide abrogates chlorpyrifos-induced hypothalamic-pituitary-testicular axis impairment in rats, *Biochemical and Biophysical Research Communications*, **2018**, *503*, 171-176. [Crossref], [Google Scholar], [Publisher]

[209]. A. Pandey, S.P. Jaiswar, N.G. Ansari, S. Deo, P. Sankhwar, S. Pant, S. Upadhyay, Pesticide risk and recurrent pregnancy loss in females of subhumid region of India, *Nigerian Medical Journal*, **2020**, *61*, 55-59. [Crossref], [Google Scholar], [Publisher]

[210]. M. Babazadeh, G. Najafi, Effect of chlorpyrifos on sperm characteristics and testicular tissue changes in adult male rats, Veterinary Research Forum, Faculty of Veterinary Medicine, Urmia University, Urmia, Iran, **2017**, 319. [Crossref], [Google Scholar], [Publisher]

[211]. E.A. Alaa-Eldin, D.A. El-Shafei, N.S. Abouhashem, Individual and combined effect of chlorpyrifos and cypermethrin on reproductive system of adult male albino rats, *Environmental Science and Pollution Research*, **2017**, *24*, 1532-1543. [Crossref], [Google Scholar], [Publisher]

[212]. G. Cano-Sancho, S. Ploteau, K. Matta, E. Adoamnei, G.B. Louis, J. Mendiola, E. Darai, J. Squifflet, B. Le Bizec, J.-P. Antignac, Human epidemiological evidence about the associations between exposure to organochlorine chemicals and endometriosis: Systematic review and meta-analysis, *Environment International*, **2019**, *123*, 209-223. [Crossref], [Google Scholar], [Publisher]

[213]. M. Salihu, B. Ajayi, I. Adedara, D. De Souza, J. Rocha, E. Farombi, 6-Gingerol-rich

fraction from Zingiber officinale ameliorates carbendazim-induced endocrine disruption and toxicity in testes and epididymis of rats, *Andrologia*, **2017**, *49*, e12658. [Crossref], [Google Scholar], [Publisher]

[214]. F. Jamal, Q.S. Haque, S. Singh, S. Rastogi, Retracted: the influence of organophosphate and carbamate on sperm chromatin and reproductive hormones among pesticide sprayers, SAGE Publications Sage UK: London, England, Toxicology and Industrial Health, 2016, 32, 1527-1536. [Crossref], [Google Scholar], [Publisher]

[215]. D. Kong, J. Zhang, X. Hou, S. Zhang, J. Tan, Y. Chen, W. Yang, J. Zeng, Y. Han, X. Liu, Acetamiprid inhibits testosterone synthesis by affecting the mitochondrial function and cytoplasmic adenosine triphosphate production in rat Leydig cells, *Biology of Reproduction*, **2017**, *96*, 254-265. [Crossref], [Google Scholar], [Publisher]

[216]. M. Jallouli, I.E.B. Dhouib, H. Dhouib, N. Gharbi, S. El Fazaa, Effects of dimethoate in male mice reproductive parameters, *Regulatory Toxicology and Pharmacology*, **2015**, *73*, 853-858. [Crossref], [Google Scholar], [Publisher]

[217]. A.M. Saillenfait, J.-P. Sabaté, F. Denis, G. Antoine, A. Robert, E. Eljarrat, The pyrethroid insecticides permethrin and esfenvalerate do not disrupt testicular steroidogenesis in the rat fetus, *Toxicology*, **2018**, *410*, 116-124. [Crossref], [Google Scholar], [Publisher]

[218]. J. Yan, W. Zhu, D. Wang, M. Teng, S. Yan, Z. Zhou, Different effects of α-endosulfan, β-endosulfan, and endosulfan sulfate on sex hormone levels, metabolic profile and oxidative stress in adult mice testes, *Environmental Research*, **2019**, *169*, 315-325. [Crossref], [Google Scholar], [Publisher]